Hitachi Zosen Inova Technology

Craig Kedrowski, Peter Chromec
Hitachi Zosen Inova U.S.A. LLC, Norcross, GA, USA

Article Outline

Glossary
Definition of the Subject and Its Importance
Introduction
Description of the Elements of the Hitachi Zosen Inova Energy-from-Waste Technology
Future Directions
Bibliography

Glossary

ACS Auxiliary Control Systems are advanced controls used in addition to the basic CCS in order to better control the combustion, specially with large grates or with inhomogeneous waste.

CEMS Continuous Emission Monitoring System: continuous monitoring of stack emission data, as well storing and transmitting data to environmental authorities.

CFD Computational Fluid Dynamics: mathematical model for calculating velocities, temperatures, concentrations, and properties of fluids flowing for example through a combustion chamber.

CCS Combustion Control System: automated system for controlling the combustion process on the grate including frequency, speed, and stroke of the ram feeder and of each grate module (also called GCS), as well as the flow of underfire air to each grate module, overfire and recirculated airflows.

DCS Distributed control system: automated system for controlling and coordinating all the WTE functions.

ECS Equipment control systems are separate control systems dedicated to control individual equipment functions to assure the desired equipment performance.

EfW Energy from waste (synonym to WTE = Waste to Energy).

FGT Flue Gas Treatment.

HHV Higher heating value or gross calorific value (expressed in kJ/kg or Btu/lb): heat released by a material when completely oxidized (reference temperature: 25°C, approx. 77°F, and assuming that H_2O is in liquid form).

HPS High-Pressure Steam: steam from superheater tubes to steam turbine.

LHV Lower heating value (expressed in kJ/kg or Btu/lb): heat released by a material when completely oxidized (reference temperature: 25°C, approx. 77°F, and assuming that H_2O is in vapor form).

LPS Low-pressure steam: usually from extraction of steam turbine, used for internal or external heating tasks.

LRD Load range diagram (or combustion diagram): shows the operating range of a combustion system in terms of fuel input, on one side, and heat input on the other.

O&M Operation and maintenance.

SCC Secondary combustion chamber: usually the vertical chamber above the grate, where gases and ash released from the fuel are completely combusted. Minimum temperature and residence time requirements often refer to the SCC.

SCR Selective catalytic reduction: process for reducing NO_x (nitrogen oxides) usually by means of reaction with an ammonia-containing reagent and in the presence of a catalyst.

SNCR Selective non-catalytic reduction: process for reducing NO_x (nitrogen oxides) usually by means of reaction with an ammonia-containing in the absence of a catalyst.

TOC Total organic carbon: amount of all non-combusted organic carbon in WTE ash; it is also used to express carbon content in MSW.

VOC Volatile organic carbon: concentration of organic compounds in flue gas.

Definition of the Subject and Its Importance

Traditionally, waste has been landfilled – and still is today, when cost is the main criterion for waste management (Fig. 1). "Out-of-sight, out-of-mind" has been the early concept, before science provided a more complete picture of the effects of landfilling on land, water, and air for a long time after a landfill has been filled [1]. The primary reason for these effects is the continuing decomposition of

M. Kaltschmitt et al. (eds.), *Renewable Energy Systems*, DOI 10.1007/978-1-4614-5820-3,
© Springer Science+Business Media New York 2013

Originally published in
Robert A. Meyers (ed.) Encyclopedia of Sustainability Science and Technology, © 2012, DOI 10.1007/978-1-4419-0851-3

Hitachi Zosen Inova Technology. Figure 1
From landfilling to a modern energy-from-waste plant

organic waste compounds into methane and other gases that escape to the air, or to water-soluble compounds that dissolve in rainwater percolating through the waste and may contaminate surface and groundwater.

This is why today's acknowledged hierarchy of waste treatment options considers landfilling as the least desirable option [2]. As shown in Fig. 2, best options are obviously "avoid" and "reuse," both of which reduce the amount of waste to be treated, and then recycle whatever is reasonably possible from the waste stream. However, the best that has been achieved by recycling and composting is about 70% [3]. This still leaves at least 30% of all waste produced to be treated by waste to energy (also called energy from waste) or landfilling. This entry describes the Hitachi Zosen Inova energy from waste (EfW) technology that recovers the energy contained in the waste and reduces municipal solid waste (MSW) to a maximum 10% of its original volume and to a chemically stable form.

Introduction

The Hitachi Zosen Inova energy-from-waste technology is a mass burn technology which treats post-recycling MSW (i.e., after all reuse and recycling efforts), as collected and without any pretreatment. It consists of a grate-fired steam generator followed by an air pollution control system. Steam is converted to electricity in a conventional steam turbine system. One of the most common configurations is shown in Fig. 3. Collection vehicles dump the waste from the *tipping area* into the *waste pit*. A *waste crane*, manually operated from the *crane control cabin*, or automatically operated by the control system, loads waste from the pit into the *feed hopper*. The waste pit and tipping floor area are ventilated by using the building air as the *primary air intake* for combustion so that no odors can escape to the surroundings. From the *feed hopper*, waste descends through a water-cooled chute and on to the horizontal *feeder table*, over which a hydraulically driven *ram feeder* slides back and forth and pushes waste on to the *reciprocating incineration grate*.

The combustion process is regulated by the combustion control system (CCS). It automatically regulates waste feed, grate movement, and airflow and distribution across the length of the grate to ensure efficient combustion and stable steam generation. Bottom ashes are continuously discharged at the end of the grate, along with siftings falling through the small gaps between the grate blocks, into the *bottom ash discharger* where it is quenched in water. The ash discharger pushes the bottom ash into the bottom ash pit or alternatively (not shown) into a metal separation system that can recover ferrous and nonferrous metals.

Primary air is injected underneath the grate by the *primary air distribution system*. The *secondary air injection* is right above the grate. At about the same location, a part of the cleaned flue gases is recirculated back into the furnace. Both injections create a swirl in the combustion chamber and assure complete combustion with less excess air and thus a higher efficiency. The *start-up*

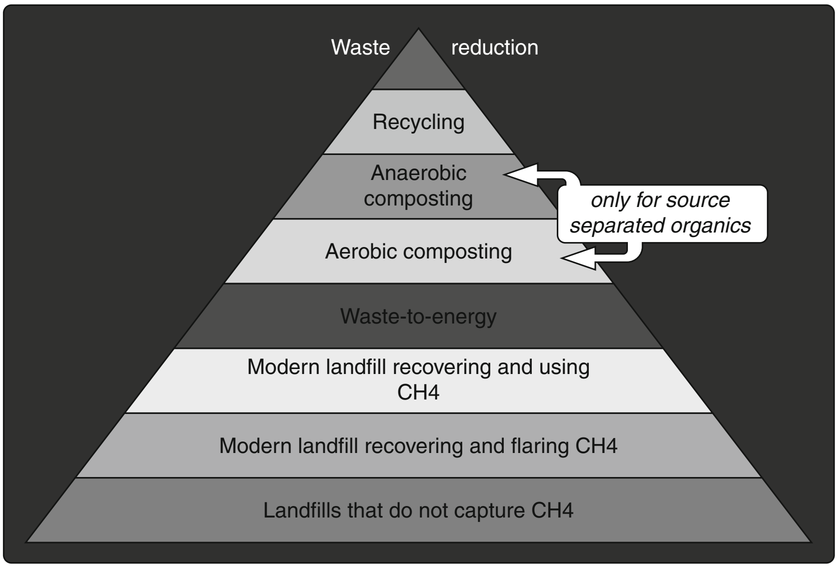
Waste reduction
Recycling
Anaerobic composting
only for source separated organics
Aerobic composting
Waste-to-energy
Modern landfill recovering and using CH4
Modern landfill recovering and flaring CH4
Landfills that do not capture CH4

Hitachi Zosen Inova Technology. Figure 2

Waste treatment hierarchy as per Prof. Themelis [2]

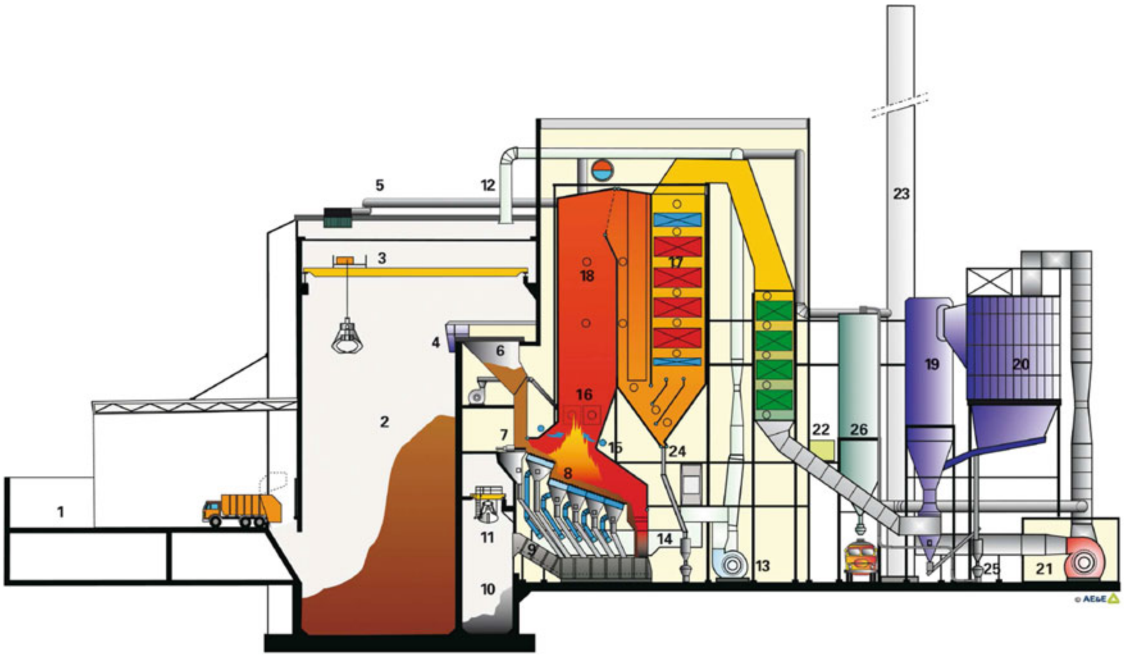

Waste receiving and storage

1 Tripping area
2 Waste pit
3 Waste crane
4 Crane control cabin
5 Waste pit ventilation at plant standstill

Combustion and steam generator

6 Feed hopper
7 Ram feeder
8 Reciprocating incineration grate
9 Bottom ash discharger
10 Bottom ash pit
11 Bottom ash crane
12 Primary air intake
13 Primary air fan
14 Primary air distribution
15 Secondary air injection
16 Start-up burner
17 4-pass steam generator

Flue gas treatment

18 SNCR injection levels
19 Semi-dry reactor
20 Fabric filter
21 Induced draft fan
22 Emission control room
23 Stack

Consumables and residues

24 Ash conveying system
25 Residue conveying system
26 Residue silo

Hitachi Zosen Inova Technology. Figure 3

A typical WTE unit

burner is only needed for start-up and controlled shutdown, as well as to keep temperatures at minimum required levels if wastes with insufficient heat value are treated.

On the way through the *steam generator*, heat from the flue gases is recovered by heat exchangers and used for the production of superheated steam. The heat exchangers consist of membrane walls as well as superheater, evaporator, and economizer tubes. Each of the heat exchangers is designed specifically for the different steam and flue gas temperature ranges and properties. The membrane walls located in the combustion chamber (i.e., first pass) are lined with refractory and/or Inconel cladding to protect against erosion and corrosion. Effective cleaning systems such as sootblowers and water showers are installed to keep fouling of the heat exchanger surfaces within tolerable limits.

The superheated steam produced by the *steam generator* is then piped to a steam turbine / generator which produces electrical energy. A small part of the electricity is used to power the plant. Also, a small part of the low-pressure steam from the turbine is used for heating the plant and preheating combustion air.

The flue gases are cleaned in a multiple-stage flue gas treatment consisting of a selective non-catalytic reduction process (DyNOR®) and a HZ Inova's semidry flue gas treatment process.

The DyNOR® process is based on the principle of selective non-catalytic reduction (SCNR) of nitrogen oxides (NO_x) by injecting ammonia (NH_3) obtained from an aqueous ammonia solution. The *SNCR injection* takes place at the optimum temperature range within the furnace.

After the flue gas has left the boiler, it enters the semidry flue gas treatment process which is designed so that acidic gases are removed by sorption on hydrated lime, while the heavy metal compounds and organic contaminants, such as dioxins and furans, are adsorbed on activated carbon or lignite coke in the same process step. The HZ Inova Semidry FGT process provides intensive contact between the flue gases and the sorbents in a fluidized bed created in the *semidry reactor*. Water is injected to control the temperature in the reactor and to improve the sorption process on the lime. The following *fabric filter* is used for filtering the solid particles from the gases by means of gas-permeable fabric filter bags. A large portion of the filtered solids is recirculated to the semidry reactor in order to improve separation efficiency and sorbent utilization. The rest, generally called fly ash, is transported to the *residue silo* by the *residue conveying system*.

A continuous emission monitoring system (CEMS) is located in the *emissions control room* and monitors continuously the flue gases exiting the air pollution control system. The *induced draft fan* maintains the necessary sub-pressure in the whole plant and assures that the flue gases are conveyed from the furnace to the *stack*.

The above parts of the Hitachi Zosen Inova energy-from-waste technology are described in further detail in the following sections.

Description of the Elements of the Hitachi Zosen Inova Energy-from-Waste Technology

HZ Inova Technology Features

General Grate combustion is the most reliable and proven technology for thermal treatment of municipal and similar wastes. HZ Inova has used this technology for over 70 years and has built over 500 units worldwide. Over this period, the technology has continuously been perfected, supplemented with new developments, and adapted to changing requirements. In the following sections, the HZ Inova EfW technology is presented.

Plant Sizes A single combustion train operates within the range of the load range diagram (LRD) shown in Fig. 4. This diagram shows the waste

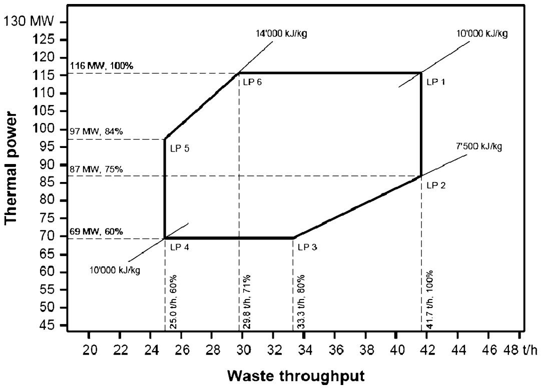

Hitachi Zosen Inova Technology. Figure 4
Typical load range diagram of a 1,000 tpd EfW plant

throughput, in tons per hour (t/h), on the horizontal axis and the thermal load, in megawatts (MW), on the vertical axis for different heating values (here lower heat value LHV, in kJ/kg) of the waste. The LRD of an EfW plant defines, for a given waste LHV, how much of that waste can be treated in this plant and how much energy will be released during combustion within the operating range of the unit.

HZ Inova EfW units (or "trains") are typically built within the following size range:

Waste throughput (metric tons)	t/h	4–42	Per combustion unit
	t/day	100–1,000	Per combustion unit
	kt/year	33–330	Per combustion unit
Waste			
LHV	kJ/kg	4,500–18,000	
HHV	Btu/lb	2,500–8,400	
Thermal capacity	MW	15–120	Per combustion unit

Recently, with the proven reliability of the HZ Inova EfW technology, ever more single train plants are planned and built. The main question related to single train plants is if waste can be stored or otherwise diverted as well as if it is acceptable to have no heat and/or power supply during service outages. For larger plants, or if redundancy is important, multiple trains can be combined in one EfW plant as needed.

Technology Requirements The waste management market requires for EfW solutions with highest possible flexibility regarding calorific values and composition of wastes to be treated. With changing consumer habits and waste management strategies, including various recycling schemes, properties of feed streams available for an EfW plant can significantly change. At the same time, EfW solutions must meet the highest environmental standards, high thermal efficiency, and be cost effective. The main objectives of the thermal treatment of waste can be summarized as follows:

- Complete inertization and volume reduction of waste
- Destruction of organic pollutants
- Recovery of metals and other useful products
- Concentration of inorganic pollutants in a usable or inert form
- Highest recovery of energy contained in waste for substitution of primary energy
- Cleaning of flue gases to very stringent environmental standards

These objectives translate into the following requirements for a grate combustion system:

- Continuous and controlled waste feed to achieve a constant thermal output despite inhomogeneous waste properties
- Closely controlled supply of combustion air to the individual combustion zones (drying, gasification, ignition, primary combustion, post-combustion) and minimization of infiltration air to ensure good and efficient combustion
- Controlled and adapted movement and stoking of the waste on the grate through the above combustion zones to ensure good burnout
- Efficient and reliable boiler system in order to minimize scaling, corrosion, and erosion in a very difficult environment
- Effective and economic air pollution control system that is adaptable to special local requirements, such as non-attainment zones

Specific main components that make up the Hitachi Zosen Inova EfW technology and fulfill the above requirements are described below in detail.

Waste Pit and Crane

General The purpose of the waste pit and crane is to receive the waste as delivered by the collection or transfer vehicles, store the waste, and also blend it and load it into the waste hoppers so that they are always full.

Waste Pit The waste pit is a large concrete bunker for storage of the waste delivered until it is treated. It serves to uncouple the waste delivery from the waste treatment so that the plant can continue to operate during weekends and holidays when waste delivery is interrupted. Also waste delivery can continue while the plant is shutdown for periodic maintenance.

Another important function of the waste pit is to provide the crane operator with the volume needed to mix the waste. To get the highest capacity and to reduce wear and tear of the equipment, the plant should be operated as stably as possible. This can only be done if the incoming waste, where one truckload could contain completely different waste than the next, is mixed within the waste pit.

To prevent the combustible waste from igniting in the pit, infrared cameras are installed. When they detect a hot spot, water cannons are used to cool it down.

To prevent the odors in the waste pit from escaping to the environment, either the entire tipping area is enclosed or the dropshafts are equipped with doors. As noted earlier, air is aspirated from the waste pit and used as primary air for combustion. This assures that when the doors are open, air is drawn into the pit and the odor is contained.

Waste Crane A grapple crane (Fig. 5) is used to move the waste in the waste pit for mixing, stacking, and transferring waste to the feed hopper. A single crane can lift loads of several cubic meters of waste in the grapple.

Scales are integrated into the crane in order to weigh every load which is deposited into the feed hopper. This allows the combustion control system to calculate the operating point, monitor trends of waste composition changes, and adapt operating parameters accordingly.

The crane operation can also be automated for certain periods of time so the operator can follow other duties.

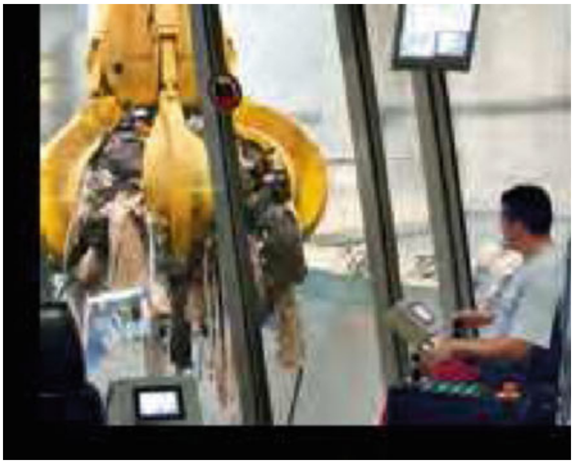

Hitachi Zosen Inova Technology. Figure 5
Crane operator loading waste to feed hopper

Feed Hopper

General The purpose of the feed hopper/feed chute is to receive waste from the waste pit/bunker via the crane and then to convey the waste onto the ram feeder. It also serves the purpose, by means of the compacted waste column in the chute, of forming a seal between the pit bunker and the combustion chamber, which prevents leakage air into the combustion chamber. Alternatively, the feed chute can be shut off by closing its flap gate.

Description Figure 6 shows the complete feed hopper, consisting of hopper, hopper flap gate, feed chute, and support frame. In order to prevent wear, certain key areas are protected with wear-resistant steel sheet. The slope of the hopper walls and the arrangement of

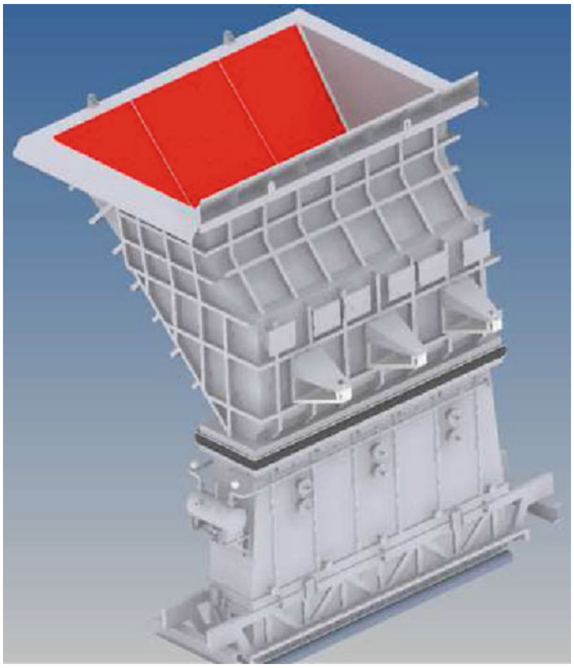

Hitachi Zosen Inova Technology. Figure 6
Feed hopper, chute, and support frame

the hopper flap gate are designed to prevent arch buildup and, thereby, ensure continuous delivery of waste to the ram feeder table. The hopper rests on the concrete loading deck above the bunker pit and a sufficiently high protection barrier is provided for personnel safety.

The height of the feed chute facilitates a sufficiently high waste column that seals the combustion chamber from the waste bunker during combustion. The feed chute and the support frame are water-cooled to resist any thermal stress that may occur during operation.

The feed hopper flap gates (Fig. 7) are installed in the bottom of the hopper, one for each grate lane. These gates are hydraulically operated by cylinders powered by the hydraulic station. The hopper flap gates seal the combustion chamber from the bunker prior to waste charging and during system shutdown. An interlock with the combustion chamber temperature ensures that during system start-up the hopper flap gate cannot be opened and waste cannot be charged until the minimum combustion chamber temperature is reached.

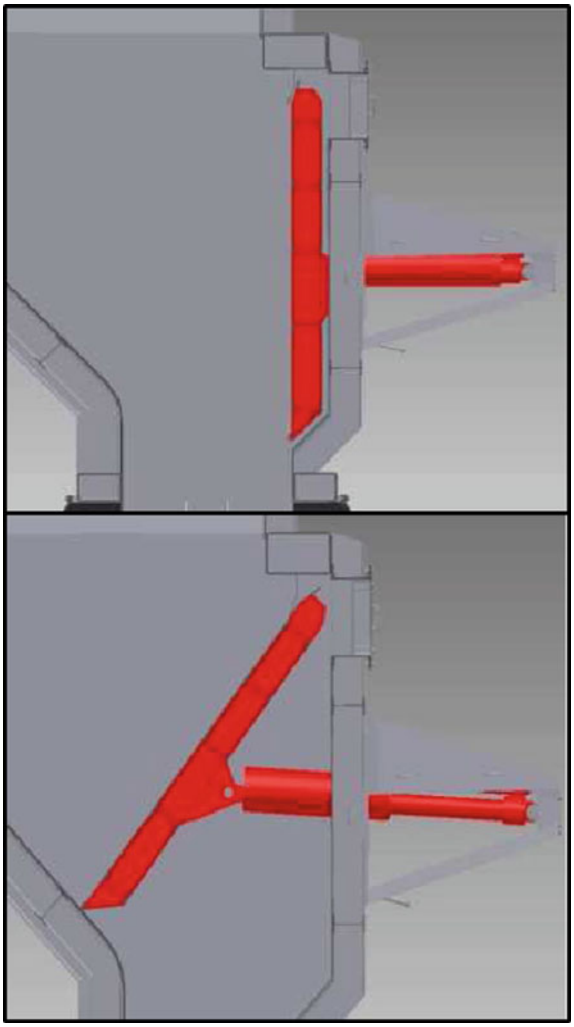

Hitachi Zosen Inova Technology. Figure 7
Feed hopper flap gate

In order to monitor the waste height, a reliable, low-maintenance level monitor is installed on the feed chute to provide a low-level alarm. Depending on the requirements for automated operation, one additional level monitor can be installed in the hopper in order to signal to the crane operator to load additional waste. A third-level detector can be installed in order to signal a possible formation of an arch in the feed hopper.

Ram Feeder

General The purpose of the ram feeder (Fig. 8) is to push the waste from the feed chute and distribute it onto the grate at a controlled rate, as required by the combustion control system.

Description The waste descends in the feed chute and falls on to the horizontal feeder table, over which hydraulically driven ram feeders (one for each grate

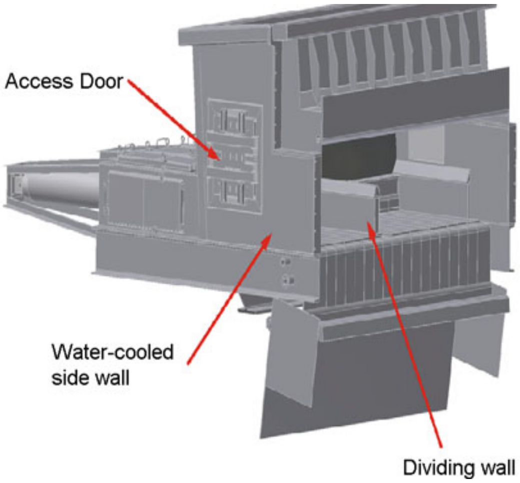

Hitachi Zosen Inova Technology. Figure 8
Ram feeder arrangement

lane) slide. As the feeders slide back, waste falls from the feed chute to the feed table. As the feeders slide forth, waste on the feed table is pushed onto the incineration grate.

The speed and length of the forward stroke can be continuously varied, depending on steam flow demand and waste properties. With each stroke, a defined volumetric quantity of waste is pushed onto the incineration grate. The return stroke is made at full speed. The continuous regulation of the forward stroke allows uniform metering and immediate adjustment of waste required on a specific grate row. The strokes are adjusted by the ram feed controller housed in the grate control cabinet located in the immediate vicinity of the waste-charging area. The ram feeders can also be operated manually from this local control cabinet and monitored by the DCS.

Grate

General The purpose of the grate is to incinerate the waste and to ensure continuous and complete combustion resulting in an adequate burnout of the bottom ash to a level of typically less than 3% TOC (total organic carbon).

Description

Overview The basic component of the combustion grate is the grate module. As can be seen in Fig. 9, the four-grate modules are joined together longitudinally to form one-grate "lane." A grate consists of one to four parallel grate lanes. Figure 10 shows a three-lane grate. The width and the number of grate lanes, and therefore the grate size, are determined by the design throughput and the calorific value of the wastes.

The grate is an inclined forward-feed grate with a slope of 10° to the horizontal. The last grate zone - the burn-out zone - is not inclined, in order to provide for optimal bottom ash quality. The grate, including the riddling hoppers below, is attached to the furnace structure at the feed end by means of a pivot mount which allows it to move. The grate rests on the grate support structure; this allows it to move in response to thermal expansion. The grate cylinders and riddling hoppers move with the grate as it expands and contracts. A boiler-to-grate expansion joint is installed between the grate module and the lower water wall headers.

Each grate module is driven by two hydraulic cylinders. A separate hydraulic control block is provided for each grate element. The stroke acts on the grate carriage located on guide surfaces, thereby cycling the movable grate block rows.

The number, speed, and length of strokes performed by the movable grate block rows can be continuously controlled in response to the process needs and the frequently changing properties of the waste.

Grate Modules Each grate module (Figs. 11 and 12) consists of six grate block rows, alternating between

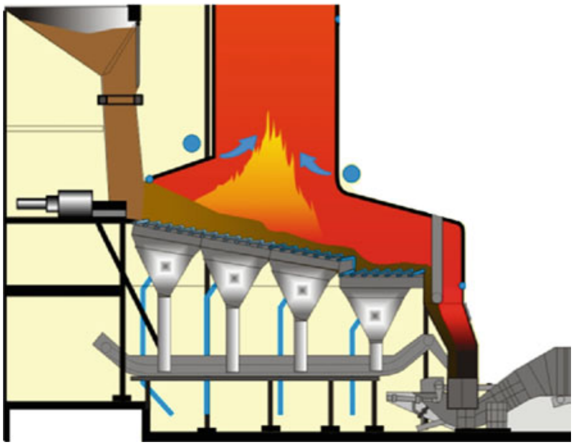

Hitachi Zosen Inova Technology. Figure 9
Four-grate modules in a lane

Hitachi Zosen Inova Technology. Figure 10
Three-lane grate

movable and stationary rows. An end piece is bolted onto the last grate module which forms the transition from the grate end to the bottom ash discharge chute.

With the exception of the side plates, the stationary and movable blocks are identical. The grate blocks are supported and mounted on retaining tubes. The block-retaining tubes for the stationary block rows are supported on brackets which rest on the stationary support structure of the grate module. However, the block-retaining tubes for the movable block rows are connected to brackets, which in turn are secured to the supports of the grate carriage that moves in the direction of the waste. The grate carriage is equipped with rollers and guides the movable grate rows. Dual hydraulic cylinders drive the rows back and forth.

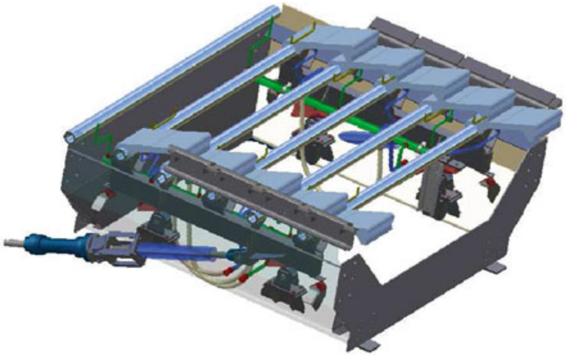

Hitachi Zosen Inova Technology. Figure 11
Grate module

The drive cylinder is attached to the grate carriage and secured to the support structure by means of a universal joint. The piston rod acts on the drive carriage attached to it, and thus to the movable grate block rows. The hydraulic cylinders are powered by a hydraulic station.

Grate Block Rows All of the six grate block rows per module are made up of either air-cooled or water-cooled grate blocks. The grate blocks are supported on the block-retaining tube as shown in Fig. 13. To minimize the gaps between blocks, they are held together by means of a tension rod. The two-part tension rod is inserted into the outermost grate blocks and tightened in the middle with a turnbuckle. This reduces riddlings and prevents undesirable airflow between the grate blocks and maintains a constant pressure drop across the grate.

Air-Cooled Grate Block The grate blocks support and push the waste through the combustion zone, and thus are exposed to extreme thermal, chemical, and mechanical stress. They are made of cast steel and are surface-machined as required.

The grate blocks are also designed to distribute the primary air evenly through the waste bed. This is done by openings at the front of the grate block. These openings are angled downward and protected by a small nose in order to help prevent them from getting fouled or clogged (Fig. 14).

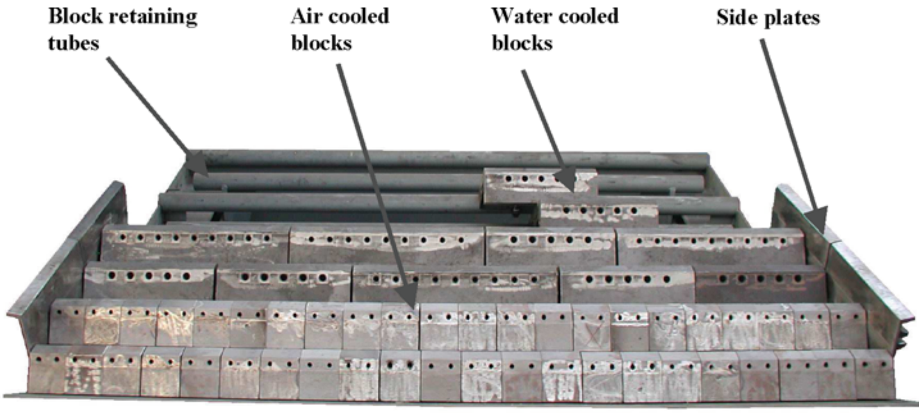

Hitachi Zosen Inova Technology. Figure 12
Rows of grate blocks in a module

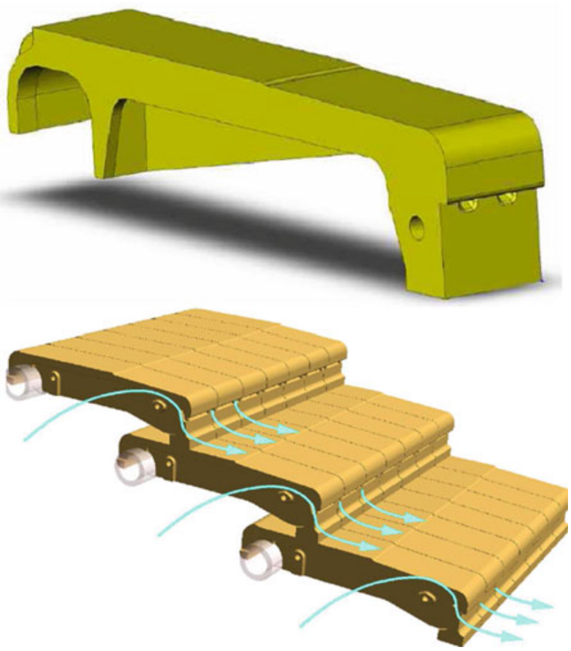

Hitachi Zosen Inova Technology. Figure 13
Air-cooled grate block

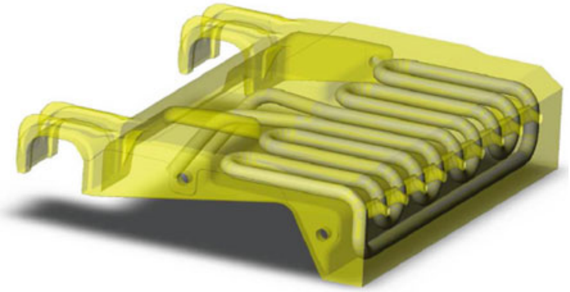

Hitachi Zosen Inova Technology. Figure 14
Aquaroll® water-cooled grate block

To reduce the thermal stress on the grate block, it has to be cooled as uniformly as possible. This is achieved by the air that is guided through the grate block. The total opening of the air path through the grate blocks is designed such that a minimum pressure drop across the grate is maintained at all operation points. This assures an even distribution of the primary air through all grate blocks and reduces the risk of local superheating and associated excessive wear and tear. In addition, good distribution of primary air is essential to prevent excess formation of carbon monoxide and prevents the formation of clinkers on the grate surface.

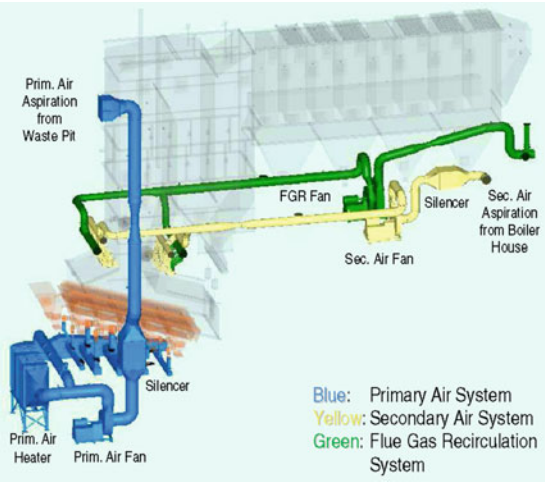
Prim. Air Aspiration from Waste Pit
FGR Fan
Silencer
Sec. Air Aspiration from Boiler House
Sec. Air Fan
Silencer
Prim. Air Heater
Prim. Air Fan
Blue: Primary Air System
Yellow: Secondary Air System
Green: Flue Gas Recirculation System

Hitachi Zosen Inova Technology. Figure 15
Combustion air and flue gas recirculation systems

Water-Cooled Grate Block For high-calorific wastes, the airflow alone does not provide sufficient cooling of the grate blocks. Aquaroll® water-cooled grate blocks as shown in Fig. 14 are used in such applications. Forced water circulation through a cooling tube cast into the grate block assures a low enough surface temperature of the grate block such that wear is drastically reduced.

Combustion Air System

General The main purpose of the primary air system (blue in Fig. 15) is to control and deliver the drying and combustion air to the hoppers underneath the grates at the right flow rate, pressure, and temperature as required for optimum combustion in the individual zones.

The secondary purpose of the primary air system is the ventilation of the tipping and waste pit area such that odors are contained therein.

The purpose of the secondary air system is to control and deliver the secondary combustion air to the combustion chamber above the grate. It creates the turbulence in the combustion chamber, which assures complete burnout of the flue gases.

Primary Air System

Overview The primary air is drawn in from the waste bunker and delivered separately, by the primary air fan, to the underside of the individual grate zones. The air is sucked from the pit in order to maintain a negative pressure and thus control odors. The system comprises the intake filter/screen, the primary air fan, the primary air preheater (if needed), as well as all associated ducts, dampers, and expansion joints. Distribution headers and ducts as shown in Fig. 16 direct the primary air to the respective grate modules and the combustion zones.

The primary air flow is controlled by the variable speed drive of the primary air fan. The distribution of primary air to each of the four zones is controlled by zone dampers. The flow rate of the primary air is measured in total as well as for each of the four zones to provide feedback to the combustion control system.

In areas where the calorific values of the waste are very low, the primary air is preheated using steam. This improves drying of the waste in the first grate zone and ensures proper burnout.

Primary Air Fan The primary air fan is a standard centrifugal, backward inclined blade-type fan with single or double bearing and with direct connection to an electric motor drive. Since the air may contain dust from the waste pit area, the fan is equipped with openings for inspection and cleaning.

Hitachi Zosen Inova Technology. Figure 16
Primary air distribution headers and ducts underneath grate

Primary Air Preheater For waste with low calorific value, a two- or three-stage air preheater is installed on the discharge side (positive pressure) of the primary air fan. The first stage preheats the air by cooling the condensate formed in the subsequent stage(s). The second stage is a low-pressure steam (LPS) and the third stage is a high-pressure steam (HPS) heater. The LPS stage is typically fed off an extraction from the steam turbine, while the HPS stage is feed off the boiler steam drum. This setup uses internal steam sources and therefore increases the plant's overall energy efficiency.

Since the primary air contains dust from the waste pit area, the open cross-sectional area is largely dimensioned, and the tube arrangements used as heat exchanger surfaces are exclusively in-line. A sufficient number of openings are provided for online inspection and cleaning. A bypass is provided for possible cleaning while the heater is off-line.

Secondary Air System

Overview Volatile components of the waste are released on exposure to heat. Some of them do not immediately combust on the grate because they may react more slowly or because oxygen is missing at that particular location in the waste bed on the grate. It is therefore necessary to provide overfire air and thoroughly mix the air with the flue gases above the grate to assure complete combustion of all volatiles released. This air is delivered via the secondary air system (Fig. 17).

Hitachi Zosen Inova Technology. Figure 17
Secondary air and recirculated flue gas headers and injection nozzles

The secondary air is drawn in from the boiler house under the roof in order to recover some energy from the radiant losses of the boiler equipment. It is delivered by the secondary air fan to the secondary air nozzles above the grate (Fig. 18). This system consists of the intake filter/screen, the secondary air fan, the secondary air preheater (if needed), the secondary air nozzles, and associated ducts, dampers, and expansion joints.

The secondary air is injected into the furnace at an angle, so that it causes a swirl flow in the combustion chamber. This swirl assures good mixing of the combustion gases and stabilizes the flue gas flow in the furnace.

The secondary airflow is controlled by the variable speed drive of the secondary air fan. Its flow is controlled by locally adjustable dampers in the distribution lines to the secondary air nozzles. These are preset during initial start-up. The flow rate of the secondary air is monitored and controlled by the CCS.

In case the calorific values of the waste are very low, the secondary air is preheated. This ensures that the combustion products are properly burned out without using auxiliary fuel.

Secondary Air Fan The same type of fan can be used as for the primary air system.

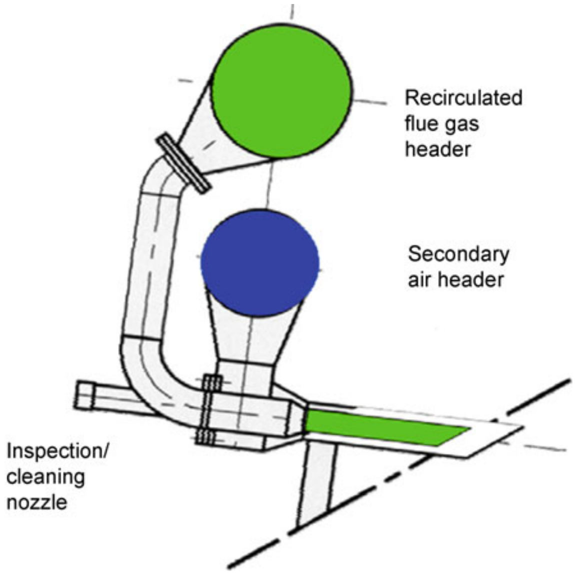

Hitachi Zosen Inova Technology. Figure 18
Secondary air and recirculated flue gas nozzle

Secondary Air Preheater At very low waste heat values, a single-stage air preheater is installed on the discharge side (positive pressure) of the secondary air fan. It uses low-pressure steam. This setup extends the operating range of the furnace without using the auxiliary burners to maintain the furnace temperature. Using internal steam sources increases the plant's overall energy efficiency.

Flue Gas Recirculation System

General The purpose of the flue gas recirculation system (green in Fig. 18) is to supply a portion of the cleaned flue gases back to the combustion chamber, in order to improve mixing and provide additional cooling without the need for more combustion air. This improves the overall energy efficiency of the unit.

Description

Overview Flue gas recirculation reduces the amount of fresh air that has to be injected at the secondary air injection level for cooling and mixing purposes. It controls the combustion chamber temperature without adding air. This reduces the oxygen content in the flue gases as well as carbon monoxide and nitric oxides formation.

The flue gas is diverted downstream of the induced draft fan and is reinjected into the combustion chamber. The system comprises the flue gas recirculation fan as well as all associated ducts, dampers, and expansion joints. The system further has a purge connection for fresh air so the ducts can be purged with ambient air in order to dry them and prevent corrosion during a plant shutdown. The flue gas ducts must be well insulated.

The recirculated flue gases are injected through a central pipe of the secondary air nozzles. The flow rate is controlled by a variable speed drive as calculated by the CCS.

Recirculated Flue Gas Fan The same type of fan can be used as for the primary air system, however, adapted to the higher operating temperature and properly insulated.

Secondary Air/Recirculated Flue Gas Nozzles The nozzles (Fig. 18) are specially designed and placed to provide the impact needed to create a swirl flow pattern in the secondary combustion chamber. The concentric design with the recirculated flue gas in the center tube and clean secondary air in the annular gap minimizes the risk of plugs due to dust possibly present in the flue gases. A poke hole allows cleaning the center tube online.

Flow Optimization with Swirl Injection

General The injection of secondary air and recirculated flue gas as described above has been optimized to achieve best gas burnout. CFD modeling, as shown in Fig. 19, has been used to optimize number, location, and angle of injection points. Tangential injection into the furnace creates a swirl in the combustion chamber. This swirl improves the mixing of the combustion gases and helps maintain a uniform flow pattern.

Description The geometry of the secondary combustion chamber (SCC) is designed for optimal flow conditions. In addition, the arrangement of the secondary air and recirculated flue gas nozzles creates a swirl in the SCC. Due to this swirl, the gas flow is homogenized with respect to temperature, velocity, and concentrations (Fig. 20). This flow configuration results in:

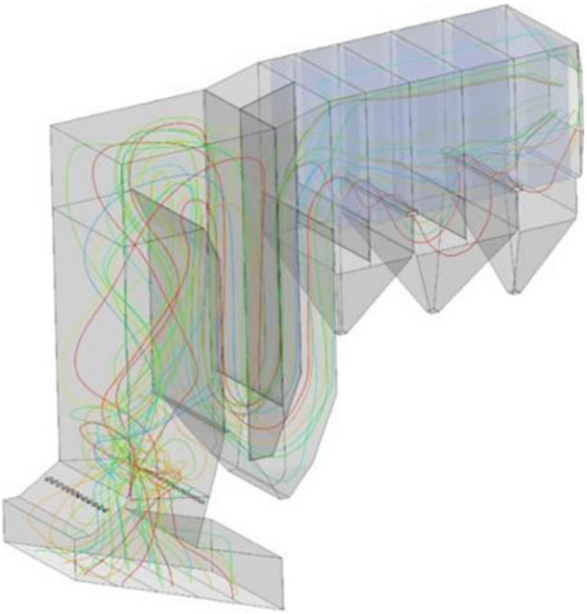

Hitachi Zosen Inova Technology. Figure 19
CFD of swirl injection

- Improved burnout of flue gas
- Uniform temperature profile across the secondary combustion chamber
- Reduction of CO-concentrations by approx. 70% (Fig. 20)
- Minimize risk of corrosion of unprotected heating surfaces
- Improved burnout of fly ash
- Reduced reformation of dioxins

Start-up Burners

General Start-up burners are specially designed for use in waste incinerators. They are located in the lower part of the combustion chamber above the secondary air injection area. Their primary purpose is to heat up the furnace gradually and in line with refractory requirements until the temperature is reached where wastes can be burned. The same applies during a controlled shutdown. During normal operation, the burners are switched off. Very seldom, with very low calorific wastes, the burners have to run to assure the minimum combustion temperature in the furnace.

Description A separate burner fan provides the combustion air needed for the burner. The volume of combustion air is controlled by the burner control system and adjusted by the control damper incorporated into the air manifold. A pressure indicator is located in the duct upstream of the air manifold to monitor the operation of the combustion air fan. Since the burner is normally off during operation, it must be protected from the thermal radiation in the furnace. This can be done by a small, cooling air fan as shown on Fig. 21 together with the burner. Alternatively, a refractory-lined guillotine-type damper can be installed, which isolates the auxiliary burner from the furnace.

The burner control system ensures the burner safety and controls the correct fuel/air ratio. It is installed in a control cabinet located near the burner. All burner-operating commands, and the release signal from the system safety network, come from the plant control system. The local control panel can be used to commission and optimize burner operation as well as to cancel local error messages during operation.

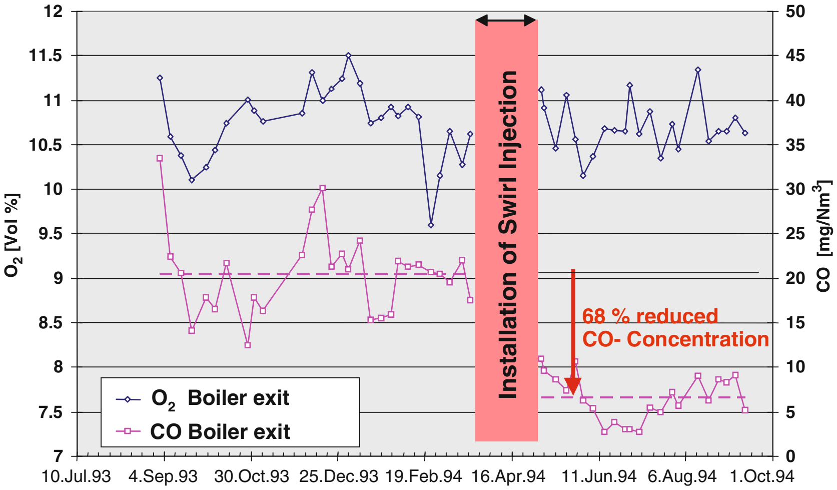

Hitachi Zosen Inova Technology. Figure 20
Average CO levels before and after installation of the swirl injection system

Hitachi Zosen Inova Technology. Figure 21
Typical auxiliary burner with cooling air fan

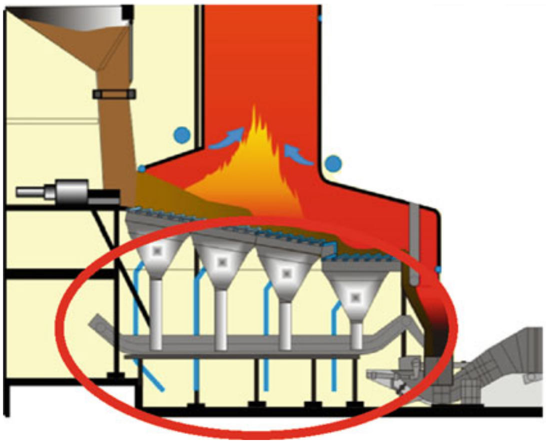

Hitachi Zosen Inova Technology. Figure 22
Riddlings conveyor

Conveyor of Grate Siftings/Riddlings

General While all moving parts of the ram feeder and the grate are designed with minimum gaps, the thermal expansion of the materials between ambient and operating temperatures unavoidably lead to small gaps through which small parts in the waste or the ash can fall through. The purpose of the grate siftings/riddlings conveyor (circled in Fig. 22) is to constantly remove these so-called siftings/riddlings while maintaining the air seal to the environment for the primary air system.

Description A wet drag chain conveyor is used for this application. One conveyor can be used for up to two grate lanes. Riddlings are collected from five locations for each lane: four grate modules and the ram feeder. The siftings/riddlings are collected in hoppers underneath these locations and delivered to the conveyor via chutes. The chutes are immersed under the water level inside the conveyor, thus ensuring an air seal between the furnace enclosure and the environment. The wet drag chain conveyor quenches the grate siftings and transports them toward the bottom ash extractor.

The amount of siftings/riddlings delivered varies and can change over the operating years due to wear and tear of the moving equipment. The drag chain conveyor can be adjusted to these conditions. Appropriate openings are installed at various points of the conveyor for inspection and cleaning as needed. The conveyor is a watertight steel construction. The key areas prone to wear are protected using wear-resistant plates.

The conveyor designed for the case that a heavy piece such as a damaged grate block falls into the conveyor. A shear pin protects the conveyor, and a zero-speed switch alarms the control room. The conveyor's water level is maintained using a float valve.

Bottom Ash Extractor

General The purpose of the bottom ash extractor (Fig. 23) is to cool the bottom ashes from the furnace as well as discharge bottom ashes and riddlings while at the same time maintaining the air seal from the furnace to the environment.

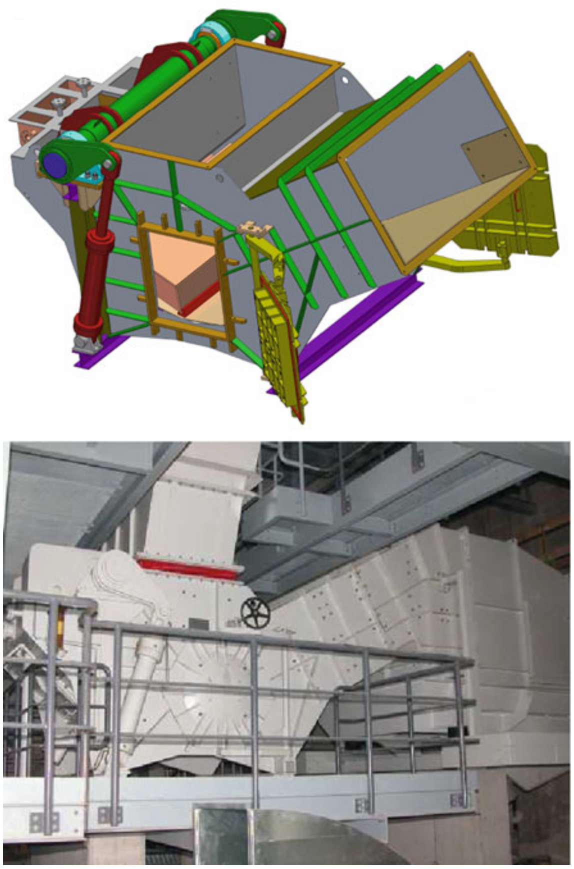

Hitachi Zosen Inova Technology. Figure 23
3D model and picture of bottom ash extractor

Description The bottom ashes remaining at the end of the grate fall into the bottom ash extractor, where they are quenched in a water bath. The grate siftings/riddlings are delivered to the bottom ash extractor via the grate siftings/riddlings conveyor. The bottom ash discharge chute has an airtight connection to the grate, and the water bath in the bottom ash extractor provides an air seal between the furnace and the environment.

The design of the bottom ash chutes and extractor is such that the large pieces of bottom ash can be discharged without difficulty. A hydraulically driven ram pushes the bottom ashes once every few minutes from the bottom of the extractor upward to the sloped chute and toward the outlet. There, the ashes stay until they are further pushed by the next ram stroke. After a few strokes, the ashes reach the edge at the outlet, fall on a belt or vibrating conveyor, and are transported to the ash storage and treatment. During this period, water contained in the ashes drains back to the water bath so that the final moisture content of the bottom ash is typically about 20%.

The hot ashes falling into the water bath cause some of the water to evaporate. This water vapor rises into the combustion chamber through the bottom ash chute. Water vapor is also formed in the outlet chute of the ash expeller since larger ash pieces may still be warm. From there, the vapor is conveyed into the furnace by means of a small fan. A water-level control regulates the feed of water to replace the evaporated water and maintain the water level in the bottom ash extractor.

The bottom ash extractor is made of reinforced steel plates in a completely welded design. In order to reduce wear, the trough is internally lined with wear plates. The bottom ash discharge chute is a double-walled structure made of steel plate.

Hydraulic Station

General The purpose of the hydraulic station is to power the hydraulic cylinders for the feed hopper, the ram feeder, and the grate and the bottom ash extractor.

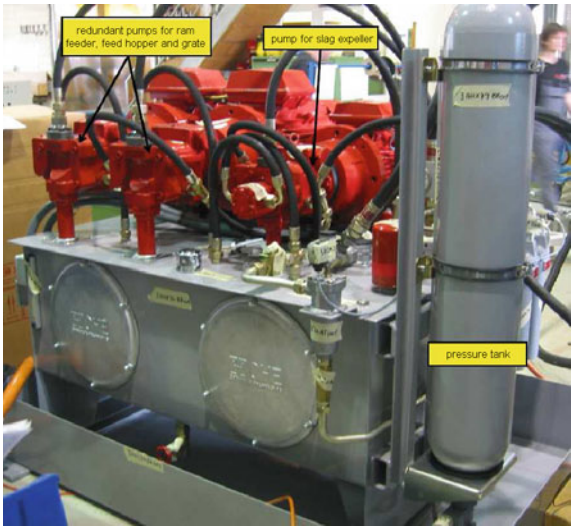

Hitachi Zosen Inova Technology. Figure 24
Typical hydraulic station

Description A single hydraulic station as shown in Fig. 24 is provided for each incineration train. The pumps, tanks, heat exchanger, and valves are all mounted and placed in a secondary containment in an easily accessible location at grade. Hydraulic oil is supplied by a set of hydraulic pumps located on the hydraulic reservoir. Each hydraulic drive has a separate hydraulic control block with electrical control elements.

Two redundant sets are equipped with a pressure-dependent flow rate control system, to perform the respective functions of the feed hopper, the ram feeder and the grate. Each grate module has a separate control block.

A third hydraulic pump is pressure-controlled and is used for the bottom ash extractor. Redundancy is provided by the other two pumps.

A water-cooled heat exchanger is integrated into the return line of the hydraulic circuit.

A pressurized tank is provided for the case of power failure in order to safely close and/or open the necessary cylinders and bring the system into its fail-safe position.

Combustion Control System

General The purpose of the combustion control system (CCS) is to provide a stable steam load in automatic mode. Since waste is a highly variable fuel, this is not a simple task. Various parameters must be monitored and various equipment need to be controlled in a concerted way.

Description

Overview Control Functions Figure 25 shows a typical Hitachi Zosen Inova combustion control system (CCS). It allows for largely automatic and secure operation at the requested load. Even at varying waste qualities, compliance with legal operating conditions such as the combustion chamber temperature and the oxygen content in the flue gas as well as an efficient gas and bottom ash burnout are assured because of the automatic control system. Steady control of the combustion conditions minimizes stress to the equipment and reduces fouling in the combustion chamber. Good combustion control includes:

- Keeping the steam flow constant, as preset by the operator
- Keeping the flue gas flow rate constant
- Ensuring an efficient gas burnout by keeping the oxygen content in the flue gas within the desired limits
- Ensuring the fire is in the right position for an efficient bottom ash burnout

All these aspects are interdependent and are heavily influenced by changing waste properties. Thus, a multivariable control system is required. The following parameters are monitored and controlled:

- Steam flow rate
- Oxygen content at the boiler outlet
- Primary airflow rate
- Primary air temperature
- Secondary airflow rate
- Flue gas recirculation flow rate
- Temperature of ceiling above grate end

Also, the following equipment is controlled:

- Ram feeder
- Grate
- Primary air fan
- Primary air dampers per zone
- Primary air heater
- Secondary air fan
- Flue gas recirculation fan

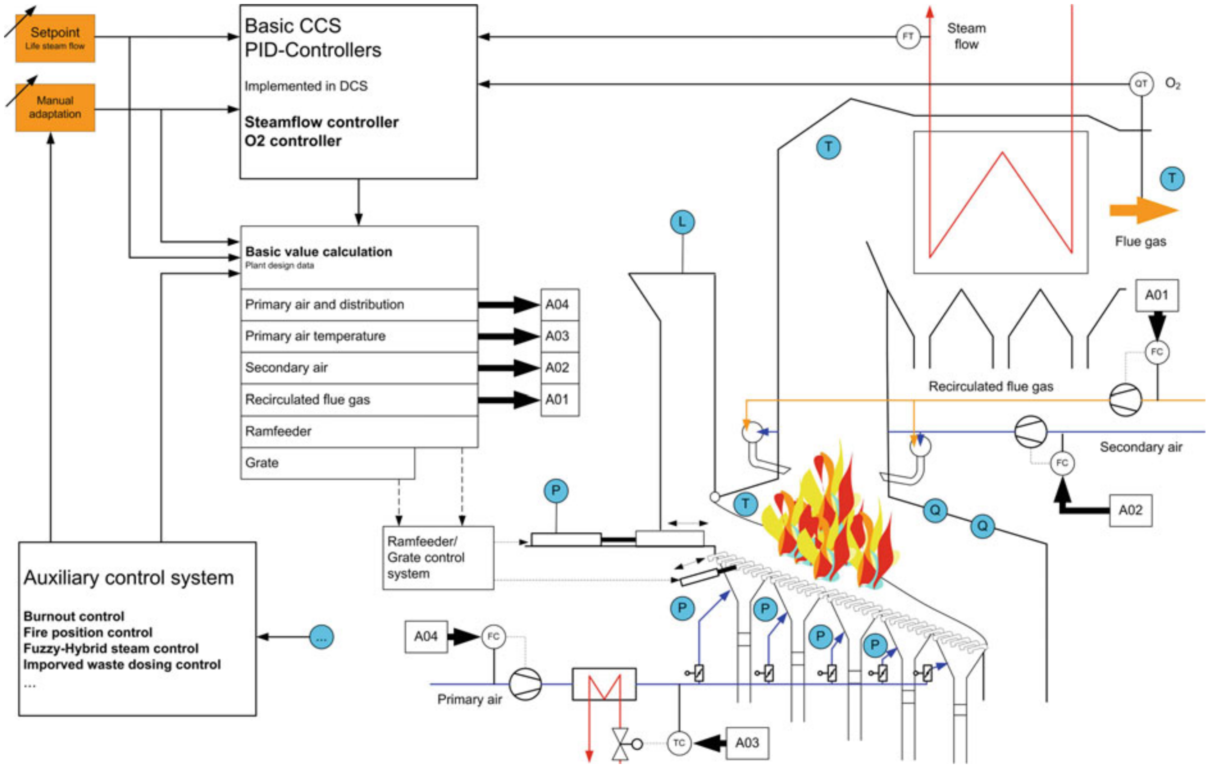

Hitachi Zosen Inova Technology. Figure 25
Overview main combustion control functions

The control structure consists of both parallel connections of different controllers and of serial (cascading) connections of controllers located at various levels in the control system.

Overview Control Systems As shown in Fig. 26, the DCS controls the EfW plant. It contains three main elements: (1) the basic Combustion Control System (CCS) as well as other control systems of the plant such as the controls of the Air Pollution Control System (not shown in the graph). (2) the Sequence Controller, which informs about the state of the plant as well as automatically brings it to the next mode as needed. (3) the Operator Terminals where the plant can be monitored and manually optimized or operated. The DCS receives signals from the plant such equipment status and flowrates or temperatures and it controls the plant through main control variables such as primary air temperatures and flowrates or ram feeder throughput etc. Its parameters and setpoints may not only be determined through the Operator Terminal, but also by Auxiliary Control Systems (ACS) which further improve quality and stability of operation.

The main control variables either directly control certain parameters such as for example the steam flow to the primary air heater such that the correct primary air temperature is reached, or it controls Equipment Control Systems (ECS) which are in turn controlling various individual equipment functions to assure the desired operation. The DCS will for example ask the ECS of the grate and ram feeder to provide more or less waste to keep the steam flow to the turbine constant. But it lets the ECS do the detailed equipment control to feed, move and riddle the waste fuel by setting the stroke of all grate elements in the individual combustion zones. The ideal stroke pattern can be assigned to each individual grate element depending on waste properties and actual combustion profile. The optimum stroke frequency is preset for each grate module.

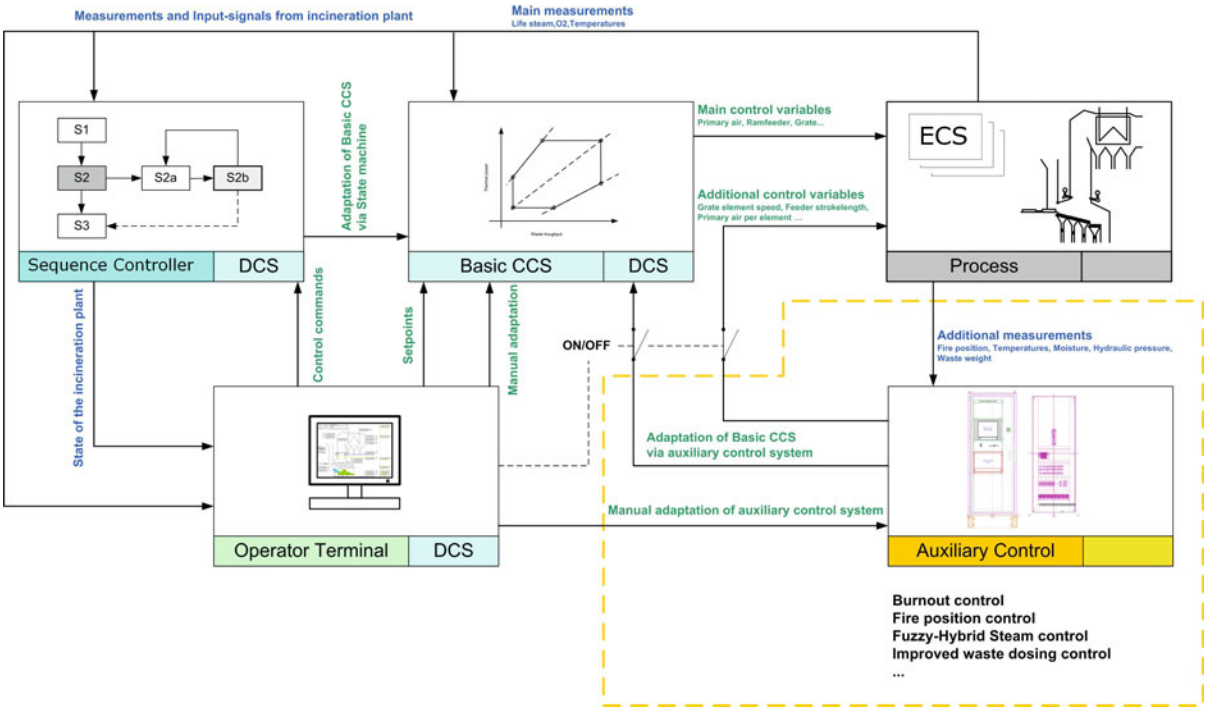
Measurements and Input-signals from incineration plant
Main measurements
Life steam,O2,Temperatures
S1
S2
S2a
S2b
S3
Sequence Controller
DCS
Adaptation of Basic CCS via State machine
Basic CCS
DCS
Main control variables
Primary air, Ramfeeder, Grate...
Additional control variables
Grate element speed, Feeder strokelength, Primary air per element ...
ECS
Process
State of the incineration plant
Control commands
Setpoints
Manual adaptation
ON/OFF
Additional measurements
Fire position, Temperatures, Moisture, Hydraulic pressure, Waste weight
Adaptation of Basic CCS via auxiliary control system
Manual adaptation of auxiliary control system
Operator Terminal
DCS
Auxiliary Control
Burnout control
Fire position control
Fuzzy-Hybrid Steam control
Improved waste dosing control
...

Hitachi Zosen Inova Technology. Figure 26
Main combustion control system architecture

For example, the grate modules in the main combustion zone have a higher stroke rate than those in the burnout zone. For simple changes of the throughput the stroke rates for the entire grate can be uniformly increased or decreased without changing the relationship between the individual grate modules. If there is a change in calorific value and therefore in the combustion profile on the grate, the specific stroke rate for the individual grate zones can be adjusted by changing the frequency or length of strokes. This affects the travelling speed of the waste on the grate, but also the thickness of the waste layer on the grate, the stoking effect and therefore the combustion profile.

For an even more precise and automatic control of the combustion profile, specially for large grates and very inhomogeneous wastes one or more ACS can be installed. The Burnout Control or the Fire Position Control measure the location of the fire by means of pyro-sensors at various locations across the width and along the length of the grate. This allows to automatically adjust the stroke pattern locally on the grate if the waste properties are different on one side of the grate than on the other side. This further improves the burnout of the waste to even lower values. With the basic CCS one typically can only see that the waste properties have changed after the steam flow has already dropped or increased. An improved waste dosing control and fuzzy-hybrid steam control allow to better anticipate possible changes in the waste composition and to proactively change the control settings such that the steam flow to the turbine and therefore the power production constantly remains at the desired value.

Basic Control Functions The basic settings for the controlled equipment are set during design and adjusted during commissioning. These settings are valid for the desired operation point with mean waste properties. During normal operation, there may be two reasons why these settings have to be changed:

The operator needs to operate at a different operation point because he receives more or less waste or because he wants to deliver more or less electricity or steam.

The operator wants to stay at the same operation point, but the properties of the wastes change with time, for example, because the ratio between industrial and residential wastes changes or because the waste is wetter due to heavy rain in the past days or similar.

The main parameter to be controlled is the produced steam flow, while keeping other parameters such as the temperatures and the oxygen content in the flue gases within the desired range. When the steam flow is below the desired value at a given load, the primary airflow below the grate is increased; simultaneously, the secondary airflow above the grate is decreased by the same rate. With this intervention, the combustion load is increased at constant total air supply. At the same time, the ram feeder and the grate stroke frequency are increased. As a result, the fire is intensified and more waste is fed to the grate. If the capacity is increased or if the oxygen concentration in the flue gas drops, the total combustion airflow is increased and the recirculated flue gas flow adjusted. In analogy, when the steam flow is higher than desired, the control interventions are reversed.

Hitachi Zosen Inova Navigator The CCS automates the complete combustion process in such a way that the operator has to select only the set point for the desired steam flow rate and an estimation of the calorific value of the present waste (calorific value adjustment). In case of a change of the waste qualities, all basic set points are simultaneously modified by means of the calorific value adjustment so that favorable combustion conditions are always given.

Using measured data and some minor assumptions, the thermal load from waste in the combustion diagram can be calculated (Fig. 27). The measured waste flow, at the crane, is used to calculate the actual calorific value and set the next operating point (short term, 3 h and 8 h average). The navigator screen is permanently updated.

While this screen allows the operator to see the past operating points, there is also a feature called "calorific value adjustment" in the CCS that allows the operator with one simple adjustment to adjust the system for an anticipated change of the future operating point. The CCS then correctly adjusts the many set points of all the relevant subsystems.

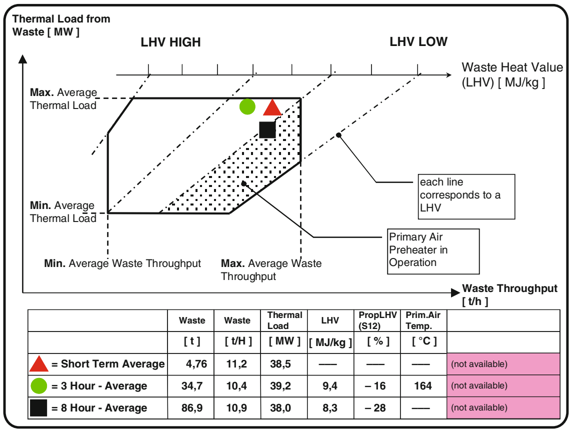
Thermal Load from Waste [MW]
LHV HIGH
LHV LOW
Waste Heat Value (LHV) [MJ/kg]
Max. Average Thermal Load
Min. Average Thermal Load
each line corresponds to a LHV
Primary Air Preheater in Operation
Min. Average Waste Throughput
Max. Average Waste Throughput
Waste Throughput [t/h]

	Waste	Waste	Thermal Load	LHV	PropLHV (S12)	Prim.Air Temp.	
	[t]	[t/H]	[MW]	[MJ/kg]	[%]	[°C]	
▲ = Short Term Average	4,76	11,2	38,5	——	——	——	(not available)
● = 3 Hour - Average	34,7	10,4	39,2	9,4	– 16	164	(not available)
■ = 8 Hour - Average	86,9	10,9	38,0	8,3	– 28	——	(not available)

Hitachi Zosen Inova Technology. Figure 27
Navigator diagram

Additionally, manual intervention is possible allowing the operator to further optimize the combustion process if necessary. However, the Hitachi Zosen Inova CCS is designed so that the plant cannot be continuously operated outside the permissible range as defined by the combustion diagram.

Start-up Sequence Also start-up is automated in the CCS. This includes heating up the post-combustion chamber by means of the start-up burners following a given ramp (Fig. 28) until the temperature in the chamber reaches the required minimal temperature. Once this condition is met, the gate in the feed chute is opened to admit the waste onto the grate where it will start to burn immediately.

Shutdown Sequence After the waste feed is stopped, the temperature of the post-combustion chamber is kept above the minimal required temperature using the burners. When the grate is empty, the temperature in the post-combustion chamber is gradually and steadily decreased as shown in Fig. 29, until it is safe to start maintenance work.

Steam Boiler

General The purpose of the steam boiler is to transfer the heat from the flue gas to water and steam. The most frequent case is to produce superheated steam, as required in a steam turbine / generator to produce electricity. In the case where the recovered energy is

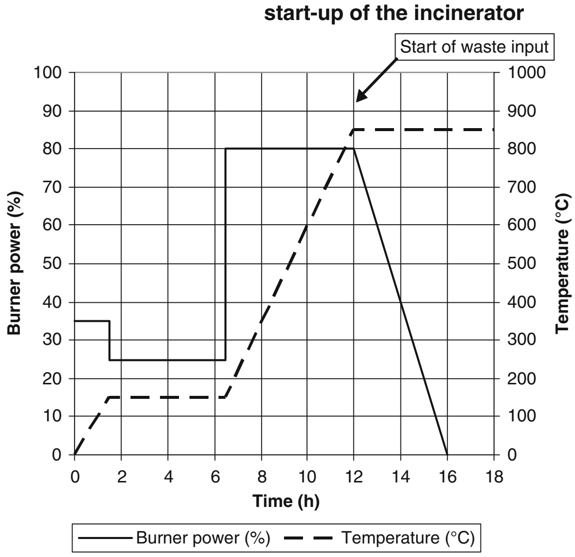

Hitachi Zosen Inova Technology. Figure 28
Typical start-up curve

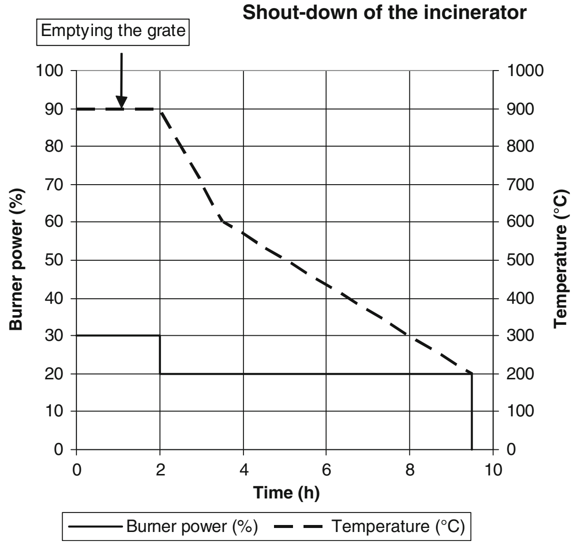

Hitachi Zosen Inova Technology. Figure 29
Typical shutdown curve

used for heating only, a boiler can be designed to produce saturated steam only or heat water to be used in district heating.

Description The Hitachi Zosen Inova steam boiler, in the example of the four-pass vertical boiler shown in

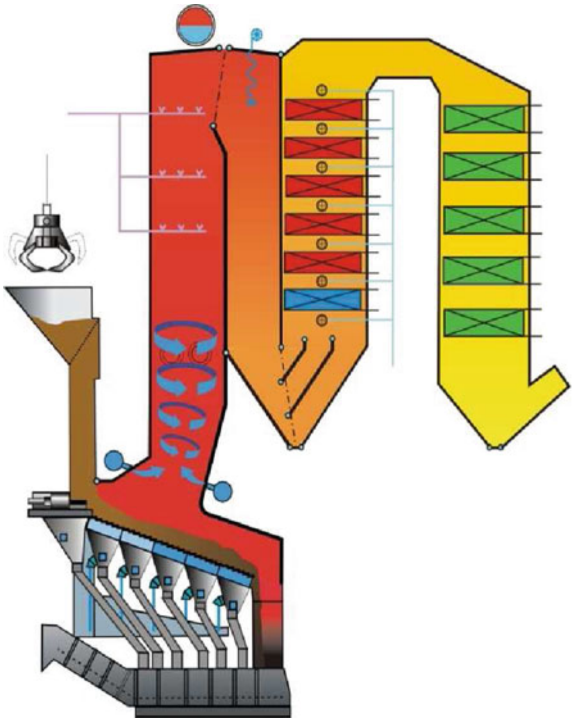

Hitachi Zosen Inova Technology. Figure 30
Typical four-pass steam boiler

Fig. 30, can be described by the following main functions it provides in the water–steam cycle:

- *Economizer* (*green bundles*): In this section, the pressurized feed water is preheated to close to boiling conditions and fed into the steam drum.
- *Evaporator* (*blue bundles and all boiler walls*): In this section, water is recirculated from and to the steam drum. It is heated in the evaporator surfaces such that it partially evaporates. Steam is separated in the steam drum and water is recirculated again.
- *Superheater* (*red bundles*): In this section, the steam separated in the steam drum is further heated to desired conditions.

The steam boiler can also be described by its configuration in terms of the number and arrangement of passes. A pass is a section of the boiler in which the flue gases flow in the same direction. The boiler can be designed in various possible configurations. In the following, a four-pass vertical boiler is described in further detail. It consists of the following passes in which one or more of the above functions are performed:

- *First pass:* Vertical radiation pass made of evaporator membrane walls with refractory lining and/or Inconel cladding on flue gas side.
- *Second pass:* Vertical radiation pass made of evaporator membrane walls and possibly with additional evaporation bundle sections.
- *Third pass:* Vertical convection pass made of evaporator membrane walls as well as with bundles of superheater and evaporator sections.
- *Fourth pass:* Vertical convection pass with steel casing and bundles of economizer sections.

The steam boiler (passes 1–3) can be bottom or mid supported or even suspended. The fourth boiler pass is bottom supported. The steam drum is placed above the first boiler pass on the steel structure.

The first pass is located above the incinerator grate and consists of membrane walls. Since these are exposed to the hottest temperatures and to the fire, they have to be protected by refractory lining or inconel clading. The sidewalls of the boiler extend downward such that the walls on the side of the grate form an integral part of the first pass. The front and back walls of the first pass extend downward to create the sloped roofs above the grate. The differences of thermal expansion between the boiler and the grate as well as between the third and fourth pass are compensated by expansion joints.

Auxiliary Boiler Systems The steam drum is the central part of the steam boiler, where water and steam is separated and the water level and the steam pressure are monitored. It includes a feed water preheater coil as well as separating baffles or cyclones to efficiently separate water from the steam. It is of fusion-welded construction and fabricated from steel plate. It contains a manhole, hinged to open inward, as well as all necessary nozzles, connections, and openings required for operation, maintenance, and testing. All drum nozzles for instruments, valves, fittings, and tubes are welded to the drum.

Since the boiler load may vary and the boiler heating surfaces are subject to scaling, the uncontrolled superheater section may provide more or less superheating depending on load and conditions. To be able to control the superheated steam temperature at all conditions, one or two spray desuperheaters are installed between the various superheater sections. There, feed water is injected in order to accurately adjust the superheater steam temperature.

The superheated steam is collected in an outlet header where a pressure control valve and a stop valve are installed before the live steam pipe is directed toward the steam turbine.

Safety valves are provided on the steam drum and in the live steam pipe to protect the boiler from excessive pressures.

The cleaning of surfaces causes the ash to fall down from refractory, membrane walls or tube bundles. The ash is collected in the ash hoppers below each boiler pass and then removed via double gate or rotary valve to the ash collection system.

All necessary provisions for normal maintenance access are made. Access doors are placed where required on both sides of the boiler. Ample space is provided between each tube bundle for adequate inspection and cleaning. External platforms provide access to each door and all control instruments. Provisions are made so internal platforms can be installed at various boiler levels for inspection, cleaning, and maintenance during outages.

Boiler Cleaning

General A waste incineration boiler is inevitably exposed to high fly ash loads. Hence, the effectiveness of the heat exchanger surface is reduced during the operation time by fouling. The purpose of online cleaning of the heat exchange surfaces is to extend the operating period and reduce maintenance cost. This can be accomplished by various means. The main options are:

- Water shower cleaning
- Sootblowers
- Rappers

Description

Water Shower Cleaning A water shower cleaning system as shown in Fig. 31 can be installed for the online cleaning of the empty boiler pass. It enables an automatic cleaning of the membrane walls by means of water injection. The evaporation of the water on the dust layers results in sudden cooling and contraction of the ash layer which lets the ash layer crack and fall off.

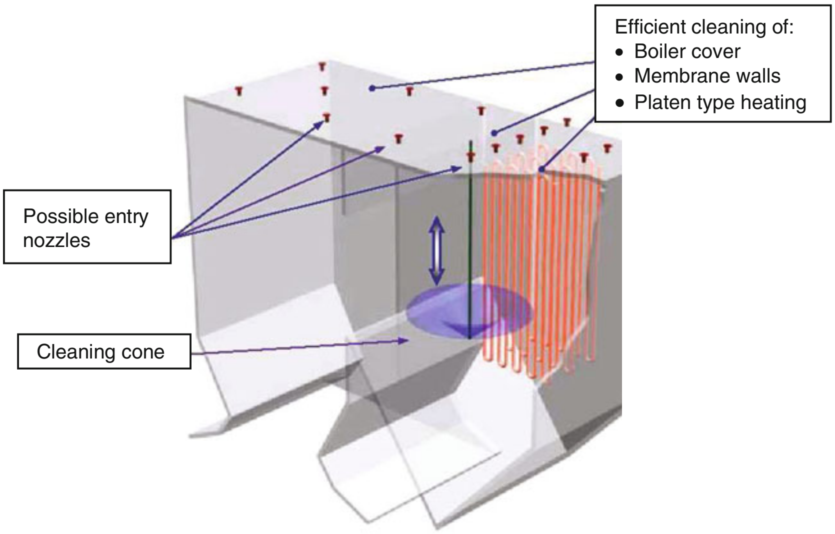

Hitachi Zosen Inova Technology. Figure 31
Typical water shower system

The water shower system is not often used in the beginning of an operation campaign. During that phase, the clean surfaces of the evaporator sections in pass 1 and 2 take more heat out of the flue gases than in the average. So less heat is available in the superheaters in the third pass and they may not reach the required superheated steam temperature at all conditions.

With proceeding of the operation campaign, it is used more and more often to assure that the flue gas temperatures at the inlet to the superheaters do not exceed design temperatures. This is usually about once per week at the end of the operating campaign. And it is used right before shutdown for manual boiler cleaning which makes the cleaning much easier and faster.

Sootblowers Sootblowers as shown in Fig. 32 are installed in before, after, and between bundles in a vertical boiler pass.

The areas of the tube bundles exposed to the direct sootblower spray are protected by stainless steel tube shields. Various types of sootblowers exist. A typical retractable-type sootblower has two opposite high-performance nozzles and is helically moved in and out of the boiler during a cleaning cycle. Between cycles it is located in a cavity of the boiler wall and cooled with a small air stream to avoid prolonged exposure to the high temperatures.

Sootblowers allow an effective online cleaning of tenacious fouling at heating surface banks with high flue gas temperatures. Sootblowers use superheated steam or compressed hot air as blowing agent because wet and moist steam can cause further caking of the fouling and cold air can cause corrosion if surface temperature of the sprayed area falls locally below the acid dewpoint of the flue gases.

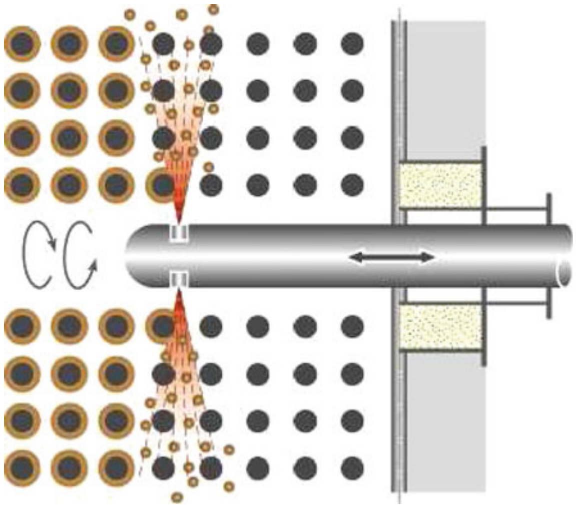

Hitachi Zosen Inova Technology. Figure 32
Retractable sootblower

Rappers Rappers are usually used in vertical tube banks installed in a horizontal boiler pass. One rod connected to each of the vertical tube rows penetrates

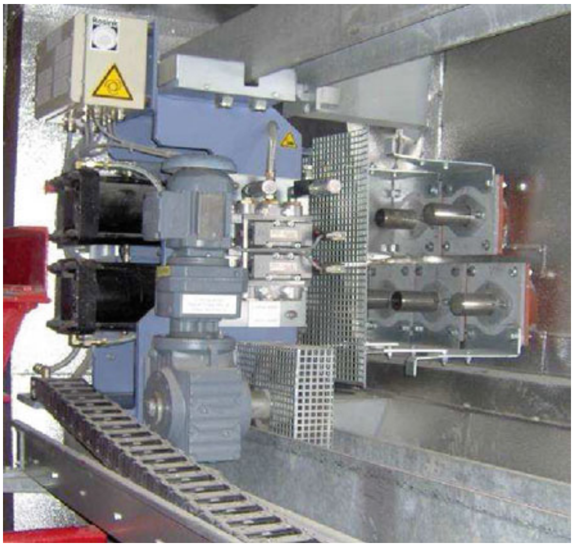

Hitachi Zosen Inova Technology. Figure 33
Automated rapper system

the boiler wall. On the outside of the boiler this rod can be hit with a hammer from time to time. The rod transmits the impact of the hammer to the heat exchanger tubes and creates a vibration such that the accumulated dust and scaling falls off. The key is to hit the bundle at the right place with the right force to achieve ideal vibrations and acceleration.

The hammering of the many heat exchanger tube rows is automated. Figure 33 shows a traveling rapping system which moves along the boiler and strikes each rod at a given interval and with a defined force.

Boiler Surface Protection

General The purpose is to protect the boiler surfaces from flame impingement and aggressive flue gas and boiler ash conditions. Usually, a combination of refractory lining and Inconel cladding is used.

Refractory Lining The refractory is different in various sections of the furnace (Fig. 34) and is optimized for:

- Proper ignition of waste
- Improved burnout of waste on the grate
- Protection of heating surfaces from furnace erosion
- Protect heating surfaces from high flue gas temperatures (corrosion protection)
- Achievement of high residence time of the flue gases at high temperatures for a complete burnout

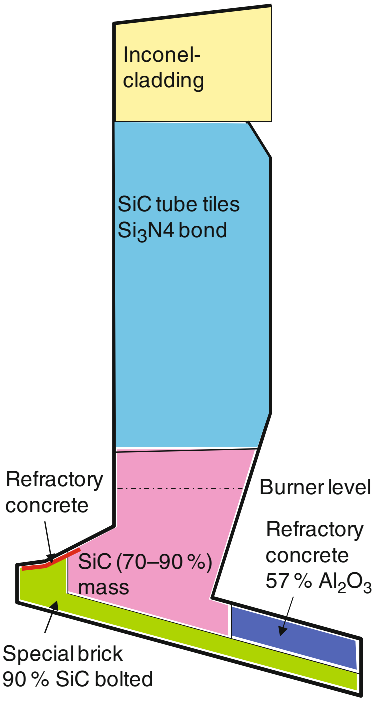
Inconel-cladding
SiC tube tiles Si$_3$N4 bond
Refractory concrete
Burner level
Refractory concrete 57 % Al$_2$O$_3$
SiC (70–90 %) mass
Special brick 90 % SiC bolted

Hitachi Zosen Inova Technology. Figure 34
Surface protection concept in furnace and first boiler pass

These requirements are satisfied by choosing appropriate materials and thickness of refractory in different zones.

Inconel Cladding Inconel cladding is one option to protect the steel surfaces of the boiler from the corrosive atmosphere of the flue gases after waste combustion. Its biggest advantage is that it protects the boiler tubes without reducing the heat transfer. Its main disadvantage is cost. This is why the design of the surface protection concept is always an optimization which has to be done in view of the waste properties and the plant owner's operation and maintenance philosophy. A welding robot applying an Inconel overlay to a boiler membrane wall is shown in Fig. 35.

Sampling Station

General The purpose of the sampling station is to monitor the water and steam quality at various locations in the boiler system (Fig. 36). Correct sampling

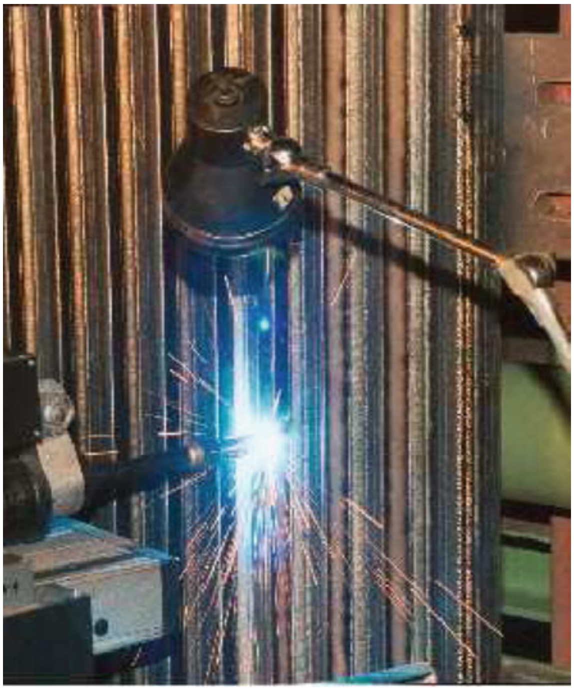

Hitachi Zosen Inova Technology. Figure 35
Welding roboter applying Inconel overlay to boiler tubes

and possible required adjustments prevent corrosion or other serious malfunction of the water side of the boiler or subsequent equipment.

Description The online sampling of a boiler is typically made to analyze the following fluids and parameters:

- Condensate (pH and conductivity)
- Boiler water (pH and conductivity)
- Steam (conductivity)
- Feed water (oxygen, pH, and conductivity)

To simplify analysis, all fluids are piped to an easily accessible location. Therefore, sampling station equipment contains a lot of piping, valves, and instruments, as well as heat exchangers to cool the fluids to temperatures suitable for handling.

Chemical Dosing

General The purpose of the chemical dosing system is to condition the water–steam cycle by the addition of chemicals such that required water and steam properties are maintained.

Hitachi Zosen Inova Technology. Figure 36
Sampling station

Description The water–steam cycle chemistry is controlled in accordance with the requirements in the relevant boiler codes and turbine manufacturers by chemical injection into the feed water, usually of ammonia solution and trisodium phosphate.

Ammonia is fed continuously into the feed water pipe between the feed water tank and the feed water pumps. Trisodium phosphate is fed continuously into the feed water pipe before the economizer of the boiler, but after the connecting pipes for spray water for the cooling of desuperheaters.

Turbine System

General The purpose of the turbine and generator system is to take the superheated steam produced by the boiler and create electrical energy.

Description The turbine system is a standard steam generator turbine package consisting of an extraction turbine, a generator with electrical equipment and

Hitachi Zosen Inova Technology. Figure 37
Typical steam turbine and generator

protection, a lubrication oil system including oil filter and cooler and local control panel (Fig. 37).

The turbine will typically have one or two steam extraction points. The first is typically around 3–5 bars (about 45–75 psi), which will provide steam to various internal, and possibly to external steam consumers via the low-pressure steam (LPS) system. A second extraction point is made if heat is used by a heat consumer at higher temperature. This extraction point is typically around 10–25 bars (150–375 psi), which will provide steam to external and possibly to some internal steam consumers via the medium pressure steam (MPS) system. If there is no second extraction point, any possible internal MPS consumers will be fed with high-pressure steam directly from the boiler. The exhaust steam from the turbine is directed to the condenser at a pressure as low as possible with prevailing ambient conditions.

During normal plant operation, the pressure control in the live-steam header will be performed by the steam turbine's pressure control valve. In case of a trip of the steam turbine, a controlled live-steam release to the condenser via the turbine bypass system will be initiated, in order to prevent the boilers' safety valves from relieving pressure. In the event that the steam turbine's capacity (typically 110% of the nominal load) is exceeded, the turbine bypass system is also activated, which will then take over pressure control in the main steam header. The turbine bypass system is also active during start-up and shutdown of the boiler in order to minimize any water losses. If the controlled live-steam release or the turbine bypass does not work, steam is blown off to the air through safety valves.

Condenser

General The purpose of the condenser is to condense the turbine's exhaust steam during normal operation. However, during start-up, shutdown, and/or upset conditions, the purpose of the condenser is to condensate the entire steam load.

Condenser Types Condensers can typically be one of the following three types:

- Non-evaporative water-cooled condenser
- Evaporative water-cooled condenser
- Air-cooled condenser

The lower the condensation temperature which can be achieved, the higher is the electrical energy efficiency of the turbine and the EfW plant.

A once-through non-evaporative water-cooled condenser will reach the highest efficiency. However, it is rare today to find a large enough body of water which can absorb the cooling needs of a power plant seldom today there is a large enough water carrier close to the EfW plant which is allowed to be heated up for cooling of a power plant. This is why this solution cannot be realized very often.

An evaporative water-cooled condenser reaches average efficiencies of the three proposed solutions. Its downside is the requirement of treated water which is not available everywhere in sufficient amounts and the frequent formation of a vapor plume which is not welcome everywhere.

So an air-cooled condenser as shown in Fig. 38 remains as the least energy-efficient option which however also causes negligible impacts to the environment and the neighborhood.

Description of an Air-Cooled Condenser Large air fans blow ambient air across the steam condenser tubes to cool them.

The condenser is designed both for the maximum steam flow from the turbine in normal operation as well as for the total plant steam flow in the turbine bypass case.

Hitachi Zosen Inova Technology. Figure 38
Air-cooled condenser

Air or other incondensable gases entering the condenser with the steam are extracted from the steam space of the condenser by a two-stage steam jet ejector. The condensed steam is returned to the condensate tank. The air extracted by the ejector is vented to the atmosphere. The driving steam for the ejector is taken from the HPS header.

Cooling System

General The purpose of the cooling system is to adequately cool the turbine and generator's lubrication system.

Description The cooling system is a closed loop cooling system that provides cooling water to the turbine oil cooler, the generator air cooler, the compressor cooling, and the sampling coolers. In an air cooler, the excess heat from the cooling water is transferred to the ambient air supplied by fans. The air cooler consists of different small cooler modules. Each cooler module has a fan with electrical motor.

In case of partial-load operation and/or low ambient air temperatures, the cooling-water outlet temperature can be adjusted by taking some of the cooler modules out of operation. The cooling water is circulated by means of redundant cooling-water circulating pumps. The cooling-water system is filled and/or drained by the cooling-water system filling pump. It is important to keep the pressure constant in the system and this is done by means of a diaphragm pressure-compensating tank equipped with a nitrogen buffer.

Hitachi Zosen Inova Technology. Figure 39
Deaerator and feed water tank

Feed Water System

General The purpose of the feed water system is to provide the boiler and superheaters with the required feed water flow and pressure.

Description The feed water system consists of the deaerator with feed water tank (Fig. 39), the redundant feed water pumps (Fig. 40), and all the associated piping and valves. The feed water tank is sized adequately to provide enough storage volume to provide feed water to the boiler for a defined time.

High-Pressure Steam System

General The purpose of the high-pressure steam (HPS) system is to deliver HPS to the in- and out-of-plant consumers as required.

Description The boiler produces high-pressure superheated steam which is sent to the turbine/generator to create electrical energy during normal operation. In order to compensate for possible variations in load, the steam is first sent to the HPS system. The HPS system typically consists of the live steam piping from the boiler to the HPS header, the HPS

Hitachi Zosen Inova Technology. Figure 40
Feed water pump

Hitachi Zosen Inova Technology. Figure 41
HP steam header

header (Fig. 41), the piping from the HPS header to the turbine, the piping from the HPS header to the air-cooled condenser via steam pressure reduction station of the turbine bypass, the piping from the HPS header to the LPS header via the steam pressure reduction station (HPS/LPS), and the piping from the HPS header to the main and start-up air extraction vacuum pumps. In addition, there may be other HPS consumers as per plant or external steam consumer requirements.

Low-Pressure Steam System

General The purpose of the low-pressure steam (LPS) system is to deliver LPS to the in- and out-of-plant consumers as required.

Hitachi Zosen Inova Technology. Figure 42
LP steam header

Description The LPS system is typically set at approx. 3–5 bars (45–75 psi) pressure. The system supplies steam to the feed water tank with deaerator, to the air preheater and possibly to external LPS consumers, such as a district heating system.

If the turbine is in operation, LP steam is taken from the turbine extraction point to the LPS header. If the turbine is not in operation, the LPS is supplied from the HPS header via the HPS/LPS reduction station. The LPS system consists of an LPS header (Fig. 42), piping from the turbine extraction to the LPS header, piping from the HPS header via the steam pressure reduction station to the LPS header, and piping from the LPS header to the internal users.

Condensate System

General The purpose of the condensate system is to collect and treat all condensates which arise in the plant. The more clean condensates can be recovered, the less demineralized water has to be made up.

Description The condensate system consists of a main condensate tank, the redundant condensate pumps, as well as the connection to all condensate sources. These are typically the main condenser via its condensate pumps, steam ejector condenser, as well as all condensate traps of the internal steam systems and heaters. To recover additional energy contained in the condensate from HPS systems and heaters, high-pressure condensate is first flashed and the generated LPS is utilized in the plant.

Demineralized Water System

General The purpose of the demineralized water system is to clean the available raw water to obtain the required purity and chemistry required for a steam boiler and turbine system in order to prevent corrosion and equipment damage. Additional water purification steps may be needed if the raw water source for the EfW plant is of low quality.

Description A demineralized water system as shown in Fig. 43 is designed for a continuous supply of demineralized water for the boiler. It is designed with sufficient capacity and redundancy. This includes redundancy of all components with the exception of piping and storage tanks.

The typical demineralized water system consists of a raw water tank, a cation exchanger, an anion exchanger, a regeneration unit, a neutralization unit, a demineralized water storage tank, and demineralized water pumps.

Nitrogen Oxides (NO_x) Reduction Measures

General Nitrogen oxides (NO_x, mainly consisting of NO and NO_2) reduction includes multiple measures with the goal to have lowest concentrations of nitrogen oxides in the flue gases leaving the plant. Nitrogen in the combustion air and even more nitrogen chemically bound in the waste will partially react with the oxygen at combustion temperatures and form NO_x.

Hitachi Zosen Inova Technology. Figure 43 Demineralized waste system equipment

Primary measures have the goal to minimize the formation of NO_x. The flue gas recirculation presented above is a powerful means to achieve this goal. Generally the reduction of the oxygen level in the flue gases and in particular the oxygen level achievable using flue gas recirculation has resulted in uncontrolled NO_x level in Hitachi Zosen Inova's latest plants of only about half the levels of plants built in the 1970s.

Secondary measures have the goal to reduce NO_x which has already been formed during combustion. The most known measures include a reaction of ammonia with the NO_x to form nitrogen and water vapor.

$$2NO + 2NH_3 + O_2 \rightarrow 2N_2 + 3H_2O$$

$$2NO_2 + 4NH_3 + O_2 \rightarrow 3N_2 + 6H_2O$$

This reaction can technically occur at different temperature ranges:

- At high temperatures, as a spontaneous and selective reaction, referred to as the selective non-catalytic reduction (SNCR)
- At lower temperatures, only with the aid of a catalyst, referred to as the selective catalytic reduction (SCR)

Selective Non-catalytic Reduction (SNCR)

Overview The SNCR process is based on the principle of injecting an ammonia-containing reagent into the furnace where the temperature range is between 850°C (1,560°F) and 950°C (1,740°F). The reagent is typically an aqueous ammonia or urea solution. The required temperature range exists in the upper part of the furnace (the first pass of the boiler). However, the actual furnace temperature at any given injection point may vary a lot due to typically varying combustion conditions on the grate caused by highly varying waste properties, by load changes, or by fouling of the boiler walls. If actual temperatures become too low, the reaction is not efficient any more and the ammonia slip at the stack is increased. If actual temperatures become too high, the following secondary reactions become significant and actually ammonia is decomposed or burned leading to highly increased reagent consumption and NO_x emissions.

$$4NH_3 + 5O_2 \rightarrow 4NO + 6H_2O \text{ at high temperatures}$$

$$4NH_3 + 3O_2 \rightarrow 2N_2 + 6H_2O$$

The key of a good SNCR process is to inject the reagent at exactly the right temperature level and to mix it evenly into the flue gases.

The Dynamic NO_x Reduction (DyNOR®) System CFD calculations show that flue gases do not mix well perpendicularly to the flow direction [4]. Therefore, the conditions in a vertical segment of the first boiler pass are predominantly defined by what happens on the grate at the bottom of that segment. And since the waste is so inhomogeneous, this can mean that at the same location the short-term temperature changes can be 100°C (180°F) and more.

The main features of the Hitachi Zosen Inova DyNOR® system (Fig. 44) are the following:

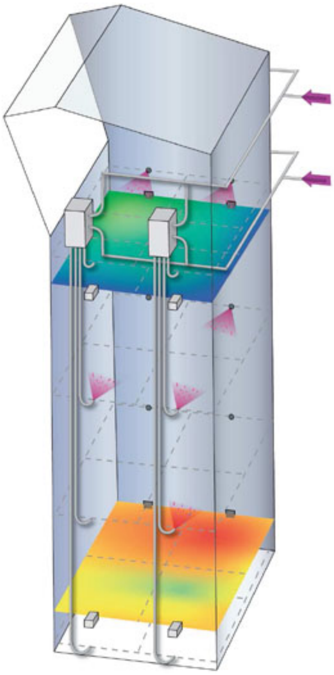

Hitachi Zosen Inova Technology. Figure 44
DyNOR® setup

- The first boiler pass is divided into several vertical segments, depending on the size of the boiler.
- Three or four injection levels are determined and on each level one or more injection nozzles are dedicated to each segment.
- In each vertical segment, a fast infrared temperature sensor measures the instantaneous temperature.
- For each vertical segment, the controller calculates the optimum injection level at each point in time.
- For each vertical segment, a fast distributor directs the reagent and the atomizing medium without time lag to the nozzles closest to the optimum injection level.

As with conventional SNCR systems, the configuration of the nozzles is important to cover the entire cross section of the boiler or segment and assure an even distribution of the reagent across the whole cross section. Other measures that improve the performance of the SNCR system are:

- Keeping steady combustion conditions on the grate with a high-quality combustion control system automatically adjusting to the varying qualities of the waste incinerated (see section "Combustion Control System")
- Good distribution and mixing of secondary air and recirculated flue gases which level out oxygen and temperature profiles as achieved by a swirl flow pattern (see section "Flow Optimization with Swirl Injection")
- No unnecessary internals in the SNCR reaction zone which would disturb the flow pattern and therefore compromise the even distribution of reagent

Selective Catalytic Reduction (SCR)
Overview In the SCR method, the conversion of nitrogen oxides is assisted by a catalyst and can take place at temperatures between about 180–350°C (350–650°F). The reaction is up to typically 90% efficient without stoichiometric overconsumption of ammonia, and thus only with minimum ammonia slip at the stack. As a secondary benefit, dioxins and furans are also oxidized on the catalyst. An undesired secondary reaction is the conversion of SO_2 to SO_3, which can then further react with ammonia to form solid ammonium sulfate salts which deactivate the

catalyst. The reaction will also happen at lower or higher temperatures, but secondary effects such as catalyst deactivation and scaling or energy efficiency considerations have practically led to the mentioned temperature range.

At operating temperatures below about 220°C (430°F), the catalyst needs to be periodically regenerated, during operation. In order to evaporate possible salt deposits from the surface of the catalyst modules, the flue gas entering the catalyst is heated up to about 320°C (610°F) over a period of about 6 h.

To implement an SCR process (Fig. 45) in an EfW plant, the following components are typically needed:

Gas–Gas Heat Exchanger A gas–gas heat exchanger is only needed in tail-end configuration. The flue gases entering the catalyst have to be reheated. The most economic way to reheat flue gases is by cooling down flue gases coming from the catalyst by means of a gas–gas heat exchanger. This can be done by a plate or tube-type steel heat exchanger. An external heat source, preferably a steam preheater, then only has to compensate the gas–gas heat exchanger temperature driving force.

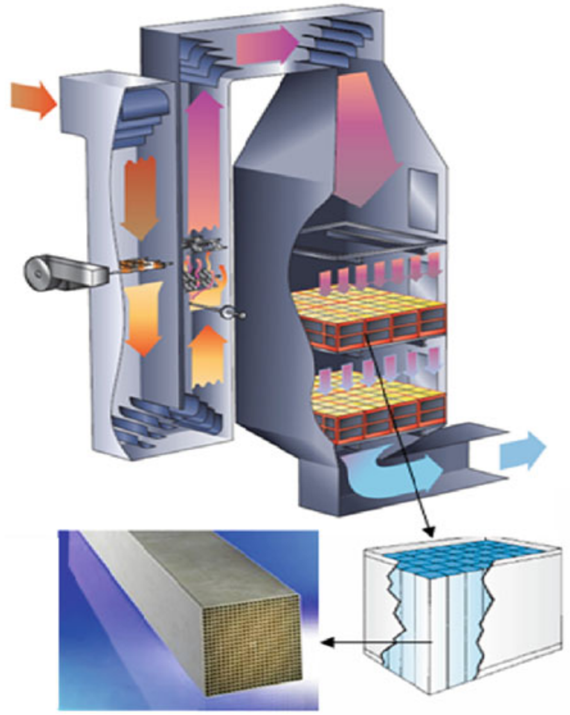

Hitachi Zosen Inova Technology. Figure 45
SCR reactor with layers, catalyst module, and element

If flue gases have to be reheated after a wet scrubber, the cold heat exchanger surfaces have to be protected against corrosion.

Steam Preheater Final preheating can be done with a steam–gas heat exchanger. Steam from the boiler steam drum is typically between 40 and 60 bar (600–900 psi) which allows to heat flue gases to a temperature of about 220–250°C (430–480°F). The steam/gas preheater is a self-supported, flue gas-tight, welded structure made up of sheet-metal sections and equipped with peripheral frame into which the steam bundles can be inserted.

Duct Burner If steam is not available or if the flue gases have to be heated above the temperature range that is practical for a steam preheater, for example, for regeneration, the gas is heated with a duct burner.

Ammonia Injection and Distribution Ammonia-containing gas or solution is injected into flue gas duct upstream of the catalyst. The turbulence generated in a static mixer installed downstream the ammonia injection assures a good distribution of the ammonia in the flue gas and a homogeneous velocity, temperature, and concentration profile. Since in the catalyst there is virtually no further mixing, best reaction efficiency and lowest ammonia slip is heavily dependent on the conditions prior to entering the catalyst.

Catalyst Reactor The reactor is made as a self-supported, flue gas-tight, welded, rectangular steel casing with provisions to hold the catalyst modules. Within the reactor, the catalyst is typically arranged in 1–3 layers and space is provided for a spare layer.

The catalyst modules are ready-to-install steel cases containing the catalyst elements. Depending on the cross section of the reactor, a layer contains several modules. The height of one layer is typically 0.5–1 m (1.5–3 ft). Between the layers there is about 2 m space for access. Depending on the possible dust load in the flue gases, sootblowers are installed upstream of each layer (Fig. 45).

Typically, a plate or honeycomb-type catalyst consisting of TiO_2 (titanium dioxide) support material plus V_2O_5 (vanadium pentoxide) and WO_3 (tungsten trioxide) active substances is used. The channel pitch of a typical SCR catalyst is only a few millimeters and is one of the important design criteria. The smaller the pitch the more surface there is per catalyst volume, however, the bigger is the risk of plugging.

Acid Gas Removal

General Acid gases such as hydrogen chloride, hydrogen fluoride, sulfur dioxide, and sulfur trioxide are formed when wastes containing chlorine, fluorine, and sulfur are burned. Removal of acid gases involves the use of an alkaline reagent, which reacts with the acid and forms a nonvolatile salt, which in most cases has to be disposed of. With the example of hydrated lime as the reagent, the following simplified reactions take place:

$$Ca(OH)_2 + H_2O + SO_2 = CaSO_3 + 2H_2O$$

$$Ca(OH)_2 + H_2O + SO3 = CaSO_3 + 2H_2O$$

$$CaSO_3 + 1/2O_2 = CaSO_4$$

$$Ca(OH)_2 + 2HCl = CaCl_2 + 2H_2O$$

$$Ca(OH)_2 + 2HF = CaF_2 + 2H_2O$$

$$Ca(OH)_2 + 2HF = CaF_2 + 2H_2O$$

$$Ca(OH)_2 + CO_2 = CaCO_3 + H_2O\ (\text{unwanted})$$

Depending on the physical state in which the reaction takes place, three main types of processes are differentiated:

- Wet: The flue gases are cooled down to saturation temperature in the process and the reaction takes place in an aqueous solution or slurry of the reagent.
- Semi-wet or semidry: Semi-wet means the reagent is injected as an aqueous solution or slurry. Semidry means the reagent is injected as a dry powder, but is subsequently conditioned by a separate water injection. However, in both cases, the water evaporates in the process so the reaction products are removed as a dry powder while the water vapor stays in the flue gases. The flue gas temperature is controlled in the process by the amount of water added.
- Dry: The reagent is injected and the reaction products are removed as a dry powder. Temperature control happens upstream of the process.

While Hitachi Zosen Inova offers all the above processes and even combinations of such processes, the following detailed description focuses on the HZ Inova Semidry FGT process, which is one of the most efficient and widely used acid gas removal processes in the EfW sector.

Description of the HZ Inova Semidry FGT Process

Process The flue gases are brought into intensive contact with the reagents in a fluidized bed reactor. Unused reagents and reaction products entained with the flue gases from the reactor and collected in the downstream fabric filter. A large portion of the solids removed in the filter are recirculated and reinjected into the reactor in order to optimize the utilization of the reagents. A small amount is discharged.

The HZ Inova Semidry FGT process (Fig. 46) has the following advantages:

- Highly efficient reaction due to high turbulence and good mixing in the reactor and conditioning water addition to the reaction zone
- High flexibility relative to load changes and contaminant peaks due to the large amount of reagent in contact with the flue gas at any time
- Optimized use of reagent due to solids recirculation
- High availability due to simple construction and no moving parts

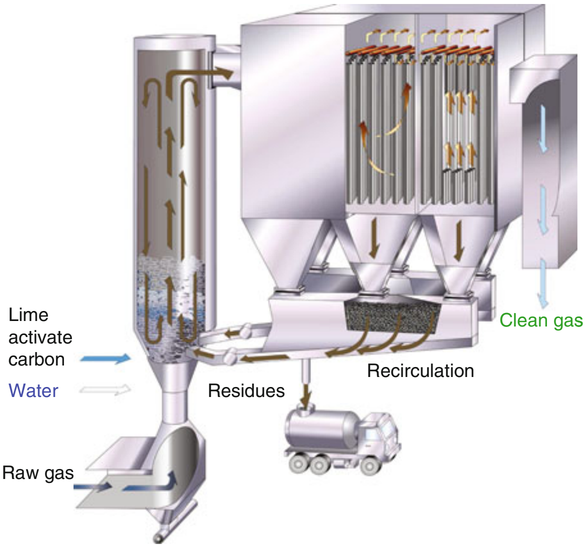

Hitachi Zosen Inova Technology. Figure 46
Hitachi Zosen Semidry FGT process schematic

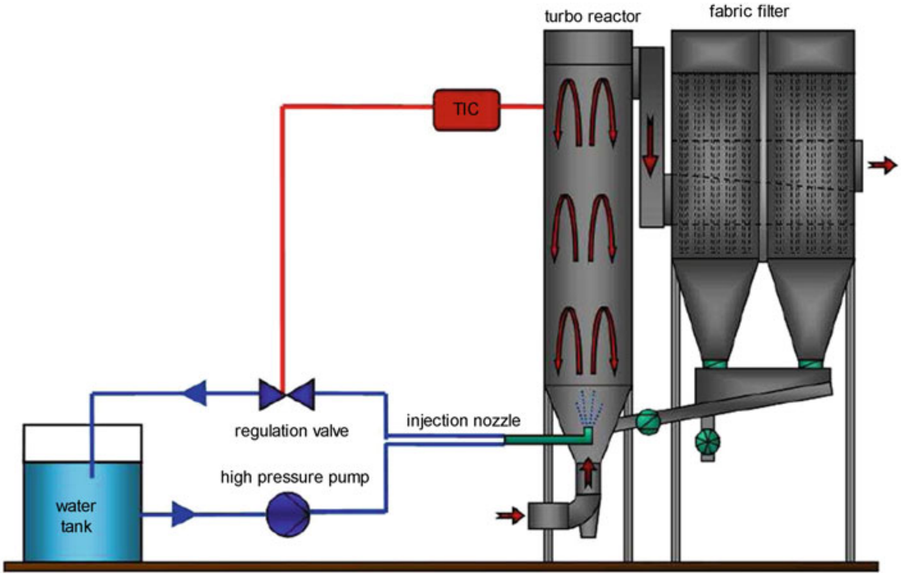

Hitachi Zosen Inova Technology. Figure 47
Temperature control loop

Process Control The HZ Inova Semidry FGT process has three control loops, which regulate the process to achieve low emissions and minimize the consumption of hydrated lime.

The first loop continuously controls the pressure drop across the fluidized bed and maintains fluidized bed level constant by adjusting the flow of recirculated solids.

The second control loop controls the flue gas temperature at the outlet of the reactor by regulating water injection at the bottom of the fluidized bed (Fig. 47).

The third loop controls the acid gas emissions at the stack by regulating the flow of fresh hydrated lime to the reactor (Fig. 48).

The HZ Inova Semidry FGT process is automatically controlled by the plant DCS including sequences for start-up, normal shutdown, and emergency shutdown.

HZ Inova Semidry Reactor The flue gas enters the reactor centrally from below through a venturi-type restriction. Therein, the flue gas velocity is high enough to ensure that all solids are entrained into the reactor or prevented from falling down against the flue gas flow. The fluidized bed is sustained in the reactor by larger particles that are kept in suspension by the upward flowing flue gas. Smaller particles and the flue gases exit the reactor laterally at top of the reactor. Depending on the flow pattern formed at the top of the reactor, a part of the solids will sink back to the bed along the wall where the velocities are lower. The flue gas has a mean residence time of approx. 3 s in the reactor.

The injection ports for hydrated lime, for other reagents, for the recirculated solids, and for the water are located in the conical inlet of the reactor.

Recirculation Conveyor In order to form a fluidized bed and to fully utilize the reagents, the largest part of the solids separated inside the fabric filter is circulated back to the reactor via a moving bed conveyor as shown in Fig. 49. Fluidizing air from special blowers is injected through the bottom of the conveyors. This ensures the steady flux and keeps the solids in a permanent motion thus preventing the formation of deposits.

Water Injection Lance The water is injected through a lance with a specially developed hydraulic nozzle which atomizes the water to the required droplet size of about 30–100 µm. The nozzles are equipped with an automatic cleaning system consisting of a rubber cap

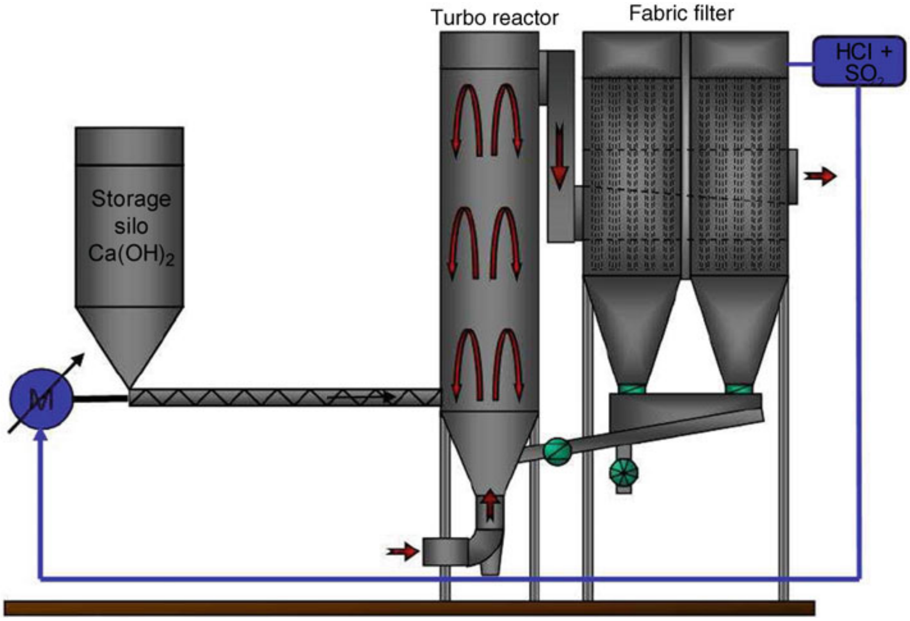

Hitachi Zosen Inova Technology. Figure 48
Emission control loop

Hitachi Zosen Inova Technology. Figure 49
Reagent recirculation conveyor and residue discharge

which can be bloated periodically with pressurized air in order to break off possible deposits (Fig. 50).

High-Pressure Water System Water for injection is supplied from the head tank via a high-pressure pump at about 30–40 bar (450–600 psi). An example of the HP water system equipment is shown in Fig. 51. The amount of injected water is controlled by a valve in the return line to the head tank.

As long as the water does not contain solids incompatible with the injection nozzle, any type of water can be injected. This is often used to safely dispose of contact or wash water collected during such operations. This allows EfW plants to be effluent free.

Volatile Heavy Metal and Organic Component Removal in the HZ Inova Semidry FGT Process

Apart from the chemical reactions between the reagent and the acid gases, the immense surface of the large amount of reagent particles also serves to adsorb other contaminants. In order to enhance the adsorption of volatile heavy metals, predominantly mercury, and volatile organics, such as dioxins and furans, activated carbon or lignite coke is also injected into the reactor. Only small amounts of such an additive assure, due to the good mixing and the high solids recirculation rate in the HZ Inova Semidry reactor, that most such contaminants are safely removed.

Fabric Filter

General The purpose of the fabric filter (Fig. 52) is to separate the ash particles in the flue gas as well as the

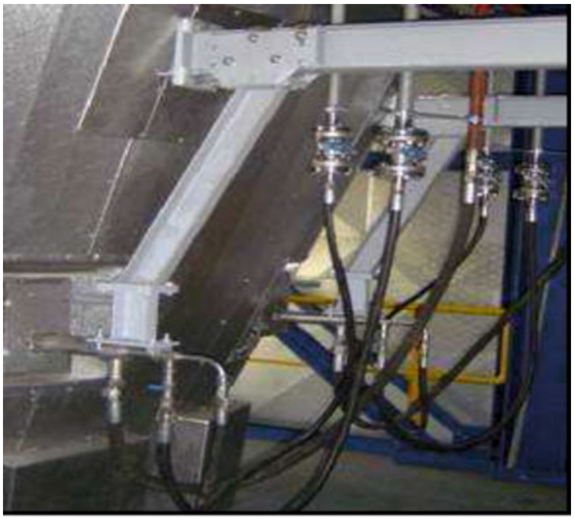

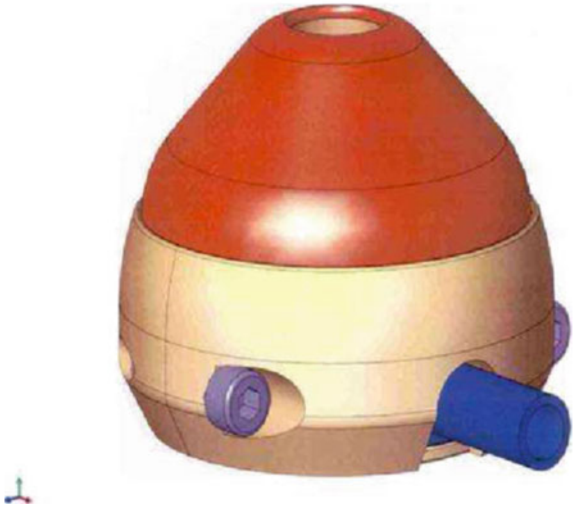

Hitachi Zosen Inova Technology. Figure 50
Water injection lance and nozzle

reaction products from the HZ Inova Semidry reactor from the flue gas.

Description The fabric filters are used for the separation of solids from gases. The separation is a physical process where the solids are filtered on the surface of a gas-permeable fabric. Due to the intensive contact of the flue gas and the adsorbents in the filter layer, the removal of pollutants from the flue gas is also further improved.

Hitachi Zosen Inova Technology. Figure 51
HP water skid

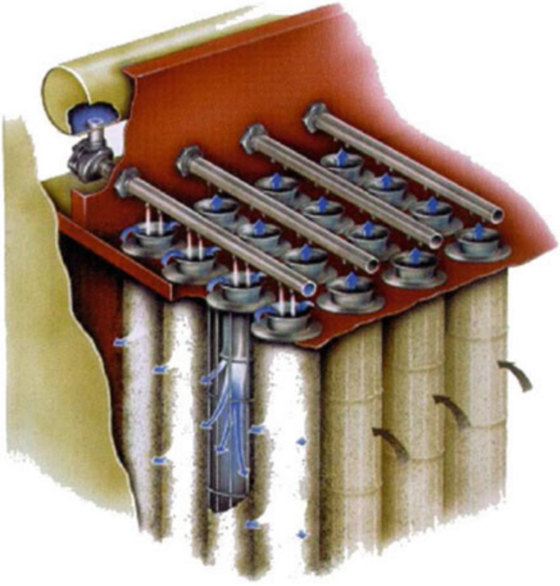

Hitachi Zosen Inova Technology. Figure 52
Filter chamber

The fabric filter consists of several filter chambers into which the total flue gas stream is divided up. Each chamber can be isolated from the flue gas stream in case of a leakage in the filter material. The flue gases enter into the respective filter chamber and are deflected by a distributor panel to assure a uniform distribution of the gases through the filter and separate a large part of the solids carried with the flue gas. The gases flow around the outside of an array of the filter bags suspended in the chamber. Then they pass through the filter media, which are supported on a wire cage, and are collected from the inside of the filter bags through the top of the filter chamber into a common clean gas duct.

Due to the flow characteristics induced by the chamber geometry as well as the pressure drop, the flue gas passes uniformly through the filter bags. This causes a uniform deposition of the solids on the outside of each individual filter bag. These need to be cleaned when solids layer on the bags becomes too thick and the pressure drop across the filter becomes too large (Fig. 53). This happens in an automated process. The solids are purged by suddenly inflating the bags with pulses of compressed air from the clean gas side. The filter bags are inflated for a short time which breaks off the solid layer on the outside. These fall down into the hoppers below the filter bags, from where they are transported away by the recirculation conveyor. The hoppers of the fabric filter can be isolated from the pneumatic conveyors by means of manually operated slide gate valves.

The cleaning air is supplied via compressed air reservoirs (one per filter chamber). From there it is distributed by a series of nozzle lances to each row of filter bags.

The fabric filter is equipped with differential pressure, temperature, and level-measuring instruments. The devices assure the supervision of the filter operation and the detection of possible malfunctions.

On top of the clean gas chamber, there is an accessible platform with complete enclosure – the filter penthouse. It is dimensioned such that there is enough room to install and remove bags from the fabric filter via walk-in plenum to the clean gas chamber.

In order to prevent deposits of and corrosion by the hygroscopic and corrosive reaction products at cold temperatures, the fabric filter hoppers are heated with electric heaters during start-up and shutdown.

Additive Systems

General The purpose of the additive feed system as shown in Fig. 54 is to store and transport additive (reagents and sorbents) to the HZ Inova Semidry reactor.

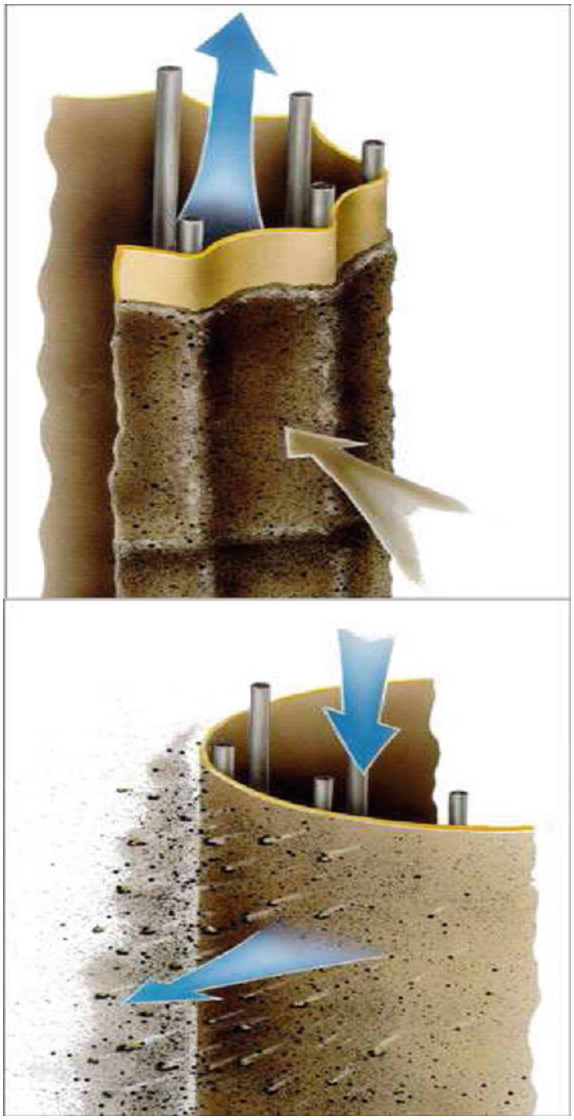

Hitachi Zosen Inova Technology. Figure 53
Filter bag during operation and cleaning

Reagent System (Hydrated Lime) The reagent silo typically contains a few days' to a weeks' supply. The discharge from the silo is ensured by a mechanical discharge and dosing system. Then the hydrated lime is conveyed to the reactor pneumatically and injected as dry powder together with the transport air directly into the HZ Inova Semidry reactor. Solids dosing and transport systems are preferably designed redundant since they assure compliance with the plant's emission limits.

Hitachi Zosen Inova Technology. Figure 54
Reagent and residue silos

The concentrations before and after the flue gas treatment system of the lead acid gas component are used to control the flow of hydrated lime. The hydrated lime dosing and transport system is dimensioned such that also expected peaks of pollutants can be safely treated.

Sorbent System (Activated Carbon) The sorbent storage can be a silo or a big bag, depending on the size of the plant. It typically contains a few days' to a weeks' supply. The discharge from the storage is ensured by a mechanical discharge and dosing system. Then the activated carbon is conveyed to the reactor pneumatically and injected as dry powder together with the transport air directly into the HZ Inova Semi-dry reactor. Solids dosing and transport systems are preferably designed redundant since they assure compliance with the plant's emission limits.

Hitachi Zosen Inova Technology. Figure 55
ID-fan with thermal and noise insulation

The amount of activated carbon to be injected into the reactor depends on the expected concentrations of volatile organics (dioxins/furans) as well as volatile heavy metals (mercury). The quantity of activated carbon per volume of flue gas is set during commissioning and annual emission testing.

Induced Draft Fan

General The purpose of the induced draft fan (ID-fan, Fig. 55) is to maintain a negative draft in the combustion chamber and flue gas cleaning system and then to push the flue gas through the stack.

Description The ID-fan is controlled to keep the furnace pressure constantly a little below atmospheric. Since the ID-fan is the largest electrical consumer in the plant, this is done by means of a variable speed drive which gives the best energy efficiency for this task.

The fan is equipped with openings for inspection and cleaning purposes. The fan and its drive are mounted on a common concrete frame structure designed to absorb and dampen vibrations. Bearing temperature and vibrations are constantly monitored.

Emissions: Continuous Emission Monitoring System

General The purpose of the continuous emission monitoring system (CEMS) is to monitor purity of the flue gas exiting the stack and to provide signals to the various control loops of the air pollution control systems.

Flue Gas Quality The following table shows European and US standard emission limits as well as a range of typical values achieved in various Hitachi Zosen Inova plants (Table 1).

While all legal emission limits can be safely kept, it is also possible to design plants which lead to substantially lower emissions as required by the referenced

Hitachi Zosen Inova Technology. Table 1 Typical Emission Limits and Hitachi Zosen Inova EfW Plant emission data

	EU		USA		Hitachi Zosen INOVA	
	(1) (3)	(2)	(1)	(2) (4)	(1) (13)	(2) (13)
CO	50 mg/Nm^3	56 ppmv	89 mg/Nm^3	100 ppmv	10–50	11–56
TOC (5)	10 mg/Nm^3	13 mg/scm	–	–	1–10	1.3–13
Particulate	10 mg/Nm^3	13 mg/scm	15 mg/Nm^3	20 mg/scm	1–10	1.3–13
HCl (6)	10 mg/Nm^3	8.6 ppmv	29 mg/Nm^3	25 ppmv	1–10	1.3–13
HF	1 mg/Nm^3	0.9 ppmv	–	–	0.1–1	0.09–0.9
SO_2 (7)	50 mg/Nm^3	24.5 ppmv	61 mg/Nm^3	30 ppmv	5–50	2.5–24.5
NO_x as NO_2 (8)	200 mg/Nm^3	136 ppmv	220 mg/Nm^3	150 ppmv	40–200	27–136
NH_3 (8)	10 mg/Nm^3	18.5 ppmv	–	–	1–10	1.8–18
Hg (9)	0.05 mg/Nm^3	0.065 mg/scm	0.038 mg/Nm^3	0.05 mg/scm	<0.038	<0.05
Cd (+Tl) (10)	0.05 mg/Nm^3	0.065 mg/scm	0.008 mg/Nm^3	0.01 mg/scm	<0.008	<0.01
Pb (+HM) (11)	0.5 mg/Nm^3	0.65 mg/scm	0.107 mg/Nm^3	0.14 mg/scm	<0.1	<0.14
PCDD + PCDF	0.1 ng/Nm^3 TEQ		0.1 ng/Nm^3 TEQ	13 ng/scm 12	0.01–0.1	1–10

(1) European emission values are daily average values or average values over a sampling period based on 11% O_2 in dry flue gas standardized at 273K and 101.3 kPa
(2) US emission values are based on 7% O_2 in dry flue gas standardized at
(3) As per EU Directive 2000/76/EC [5]
(4) As per EPA Title 40 Part 60, Subpart Eb [6]
(5) Total organic carbon (TOC)
(6) While the EU value is absolute, the US value can be exceeded if the removal efficiency is at least 95%
(7) While the EU value is absolute, the US value can be exceeded if the removal efficiency is at least 80%
(8) Local air permits in the USA often reduce NO_x and introduce NH_3 emission limits, specially in non-attainment zones
(9) While the EU value is absolute, the US value can be exceeded if the removal efficiency is at least 85%
(10) The EU value includes the sum of Cd + Tl, the US value only Cd, which is however by far the largest portion of the sum
(11) The EU value includes the sum of the following heavy metals Sb + As + Pb + Cr + Co + Cu + Mn + Ni + V, the US value is only for Pb, which is one of the larger portions of the sum
(12) The EU value is based on a toxic equivalence concept which calculates a weighted sum of all different PCDD and PDCF isomers is calculated. The US value uses the sum of all isomers without weighing. For typical mixtures of PCDD and PCDF isomers present in flue gases of EfW plants, these emission limits are similar
(13) Same units as used in preceding columns

national limits. However, this is often a factor of the waste composition and of the complexity of the air pollution control equipment – thus of the cost which a region is ready to spend for responsible waste treatment.

Description of the CEMS A separate CEMS monitors the flue gas properties and composition at the stack for each incineration line. Each system mainly consists of:

- Temperature, pressure, and flow rate measurement
- Particulate measurement
- Complete extractive gas analyzer for concentration measurement of typically the following flue gas components: H_2O, O_2, CO, HCl, SO_2, NO_x, NH_3, VOC.
- Computer-based data evaluation and storage system

The instruments are directly installed on either the discharge ductwork between the ID-fan and stack or the stack. The flue gas is extracted through a heated extraction line and conveyed to the analytical instruments installed in the CEMS container.

The emission measurement system is designed to meet the particular requirements of the operating permit for the plant. It complies with the applicable directives for installation and quality assurance and has the possibility to generate direct reports for the supervising Environmental Protection Agency.

Stack

General The purpose of the stack is to expel the clean flue gases to the atmosphere at a high enough point to ensure adequate dispersion (Fig. 56).

Description The cleaned flue gases enter the stack with a temperature of about 150°C (300°F). In multiple train plants, all flues can be integrated into the same stack structure. The internal flues are made of steel for flue gases above typically 130°C (270°F) or of fiber-reinforced plastic below. The flues are thermally insulated to avoid excessive condensation along the walls. The stack support structure can be steel or concrete.

Underneath the flue gas inlet to the stack, condensed water vapor or rain water is collected on an inclined stack base plate and discharged via a condensate discharge line. The condensate discharge is drained into the contact water storage.

Hitachi Zosen Inova Technology. Figure 56
Stack with individual support of single flues (Moerdijk, the Netherlands)

The stack includes a safety ladder to a maintenance and work platform at the top of the stack from where the flues can be monitored and the lightning protection and air traffic lighting systems can be maintained. Depending on the location of emission monitoring nozzles an additional platform may be located in the middle of the stack.

Since the stack is normally the most visible part of an EfW plant, there are ideas how a stack could be converted to a landmark, for example in Fig. 57.

Future Directions

The EfW (or WTE) technology described above has been shown to be reliable, efficient, and proven:

- Reliable means that a large number of plant owners operate their Hitachi Zosen Inova plants in the range of 7,900–8,300 h per year, which corresponds to 90–95% availability.
- Efficient means that all national emission limits can be met, sometimes with a considerable margin. It also means that energy can be efficiently recovered in the form of electricity and/or heat meeting or exceeding the relevant energy efficiency standards [7].

Hitachi Zosen Inova Technology. Figure 57
Stack with combined support of flues and architectural treatment (Osaka, Japan)

- Proven means that this technology has been developed and has matured with the over 500 reference plants built worldwide since the 1930s.

It is evident that the Hitachi Zosen Inova technology is mature. Technical developments concentrate mainly on the following areas:

- Increase energy efficiency and electricity production og EfW plants
- Improve the automated control of the EfW plants in order to further increase average plant capacity and availability.
- Improve monitoring of plant components in order to allow operators to track the plant efficiency and better plan preventive maintenance actions.
- Further improve stack emission limits.
- Further improve bottom ash quality and recycling options for bottom ash (recovery of valuable resources such as copper, aluminium, brass and other metals).

However, since EfW technology in many areas still commercially competes with relatively cheap landfilling or is not available for large economic areas, one goal of development is always concentrated on plant economics:

- Achieve the same performance with less and simpler equipment
- Find less-expensive materials of construction, in terms of investment and maintenance cost
- Further improve the operation flexibility and availability of the plant thus reducing O&M cost

Last but not least, the goal must be to do all that is necessary to make EfW plants politically acceptable and a part of the infrastructure in the densely populated areas. Wastes are created and energy is needed where the people live. EfW plants are an essential part needed to close the loop of the material cycle [3]. Whatever cannot be reused or recycled can be efficiently treated for energy recovery in an EfW plant. An excellent example is the Isséane EfW plant that started operations in 2008 in France:

- It is located in the middle of the Paris metropolitan area about 5 km (3 miles) from the Eiffel Tower along the river Seine.
- It is an integrated part of the city's recycling activities and contains a plastics sorting and recycling facility.
- It serves a population of about one million people all living within a short distance from the plant.
- It provides electricity to the national electrical grid.
- It provides heat to the city's district heating system.
- However, both electricity and heat are consumed in the vicinity of the plant. This concept helps reduce the need for long-distant transport of energy and the associated complexity of energy distribution.
- The EfW plant was designed to fit architecturally into the neighborhood and, in fact, may not even be recognized as an EfW plant.

Although the total cost of the Isséane EfW plant (Fig. 58) is on the high side compared to other modern EfW plants, it is an excellent example of sustainability within the material and energy cycles. Research and

Hitachi Zosen Inova Technology. Figure 58
Isséane energy-from-waste plant, Paris, France

development is focusing on all aspects needed to make such a concept available to more and more highly populated areas. This includes emissions and architecture to increase acceptability to the public as well as efficiency, reliability, and total cost in order to increase its affordability to communities in developing nations.

Bibliography

1. Kjeldsen P, Barlaz MA, Rooker AP, Baun A, Ledin A, Christensen TH (2002) Present and long-term composition of MSW landfill leachate: a review. Critical Reviews in Environmental Science and Technology 32(4):297–336
2. Kaufman SM, Themelis NJ (2009) Using a direct method to characterize and measure flows of municipal solid waste in the United States. J Air Waste Manage Assoc 59:1386–1390. doi:10.3155/1047-3289.59.12.1386, ISSN:1047-3289; Copyright 2009 Air & Waste Management Association, Earth Engineering Center, Columbia University, New York
3. European Environment Agency (2007) Sustainable consumption and production. In: State of the environment report no 1/2007 (Chap 6). Office for Official Publications of the European Communities, Luxembourg. http://www.eea.europa.eu/publications/state_of_environment_report_2007_1
4. Sigg F, Halter R, Chromec P (2010) DyNOR® DeNOx performance confirmed in further MSW plants, NAWTEC18-3504. In: Proceedings of the 18th annual North American waste-to-energy conference, Orlando. Copyright 2010 by ASME
5. Directive 2000/76/EC of the European Parliament and of the Council of 4 December 2000 on the Incineration of Waste, 28.12.2000, Official Journal of the European Communities, L 332/91
6. US Electronic Code of Federal Regulations (Title 40, Part 60, Subpart Eb) current as of 29 July 2010
7. Reimann DO (2004–2007) Results of specific data for energy, R1 plant efficiency factor and net calorific value (NCV) of 231 European WtE plants. In: CEWEP Energy Report II (Status 2004–2007). http://www.cewep.eu/studies/climate-protection/index.html

Hydrogen from Biomass

Ralf Schmersahl[1,2], Marco Klemm[3],
Ruth Brunstermann[4], Renatus Widmann[4]
[1]Deutsches BiomasseForschungsZentrum GmbH, German Biomass Research Centre (DBFZ), Leipzig, Germany
[2]Institute of Agricultural Engineering Bornim e.V. (ATB), Potsdam, Germany
[3]German Biomass Research Centre (DBFZ), Leipzig, Germany
[4]Department of Urban Water and Waste Management, University of Duisburg-Essen, Essen, Germany

Article Outline

Glossary
Definition of the Subject and Its Importance
Introduction
Biological Hydrogen Production
Hydrogen Production by Solid Biomass Gasification
Future Directions
Bibliography

Glossary

Biohydrogen Hydrogen derived from biomass.

Biological biohydrogen generation Production of hydrogen based on a biological resp. biochemical conversion of biomass.

Biomass From a scientific and technical point of view, biomass is defined as material of biological origin excluding material embedded in geological formations and/or transformed to fossil.

Thermochemical biohydrogen generation Production of hydrogen based on a heat-induced resp. thermochemical conversion of biomass.

Definition of the Subject and Its Importance

Today, there is no disputing that the use of renewable energy has to be increased in order to reduce anthropogenic CO_2 emission as well as the dependence on the fossil fuels. Approximately 95% of the hydrogen produced today comes from carbonaceous raw material, but primarily with a fossil resource as original energy source. Only a fraction of this hydrogen is currently used for energy purposes; the bulk serves as feedstock for manifold purposes, e.g., in the petrochemical industry as well as for food, electronics, and metallurgical processing. However, the share of hydrogen in the energy market is increasing, and hydrogen production will need to keep pace with this growing market [1]. In this sense, this paper summarizes the state of the art of the most important processes, techniques, and research activities in the field of hydrogen production using biomass resources.

Introduction

Hydrogen (H_2) is a secondary energy carrier that has to be produced from other energy carriers. A more and more discussed option for H_2 production is the use of biomass. It may be carried out either by biological or thermochemical processes. The characteristics of thermochemical H_2 production differ significantly from those of biological processes. The differences cover the feedstock basis as well as the reaction chemistry, the plant design, and the plant scales.

In the case of biological H_2 production, H_2 may be produced as a photosynthesis product (e.g., by microalgae). A second option is the use of fermentative microbiological degradation pathways, where H_2 occurs as metabolism product. Both pathways are still in the research scale.

Thermochemical biomass processes, such as combustion, pyrolysis, and gasification, are applied to produce different forms of energy carriers and chemicals. From those basic processes, gasification complies best with the requirements for the production of H_2. However, none of the present biomass gasifier designs is a genuine H_2 supplier: the product gas needs sophisticated posttreatment techniques to achieve both high H_2 yield and a sufficient H_2 purity.

Within the following explanations, these two hydrogen provision routes are discussed in detail.

Biological Hydrogen Production

Biological hydrogen production can be carried out by a wide variety of different organisms [2]. The biological

M. Kaltschmitt et al. (eds.), *Renewable Energy Systems*, DOI 10.1007/978-1-4614-5820-3,
© Springer Science+Business Media New York 2013
Originally published in
Robert A. Meyers (ed.) Encyclopedia of Sustainability Science and Technology, © 2012, DOI 10.1007/978-1-4419-0851-3

processes differ according to the essential boundary conditions. Below, the process principles as well as some examples are discussed.

Process Principles

An overview about different biohydrogen production methods is given in Table 1. Biohydrogen production by photolysis and dark fermentation and photofermentation are described and discussed below.

Photolysis Hydrogen production by the microalgae (i.e., *Chlamydomonas reinhardtii*) has been studied intensively in the recent years. This algae use the direct photolysis pathway to produce hydrogen out of water, if the microorganisms are stressed by lack of sulfur. Under these conditions, the algae produce hydrogen and oxygen but cannot grow. By this reason, a second stage with optimal conditions for the growth of the algae is necessary. Therefore, carbon dioxide is needed to build organic compounds like carbohydrates by photosynthesis. Additionally, by this pathway, hydrogen and oxygen are produced simultaneously, and the produced oxygen inhibits the enzyme hydrogenase, which is involved in the process. The color of the photosystems of the algae and phototrophic bacteria limits the dimension of the reactor because the penetration of light is reduced by the microorganisms itself [12]. For this reason, different reactor types are designed, for example, tubular or flat panels with a diameter or depth respectively of 10 cm at maximum [5]. Most of the experiments are done in lab scale by using artificial light. An advantage of this process is the clean energy production, because only hydrogen and oxygen are produced by this process.

However, the development of photobiological algae systems for biohydrogen production is still fundamental research. Due to the fact that the produced hydrogen yield per lightened area is very low – 1.5% based on a full solar spectrum [4] – further investigations are necessary to develop economic, viable, large-scale applications. Via genetic modification and cloning of the microorganisms, higher yields may be achieved [5]. Apart from that, H_2 and O_2 are produced simultaneously, which requires careful handling.

In contrast to the direct photolysis, it is possible during indirect photolysis to separate the oxygen formation by photosynthesis from hydrogen production in either time or space; this process is divided in three steps (Table 1). First, the photosynthesis takes place. In this step, CO_2 is needed, and oxygen is produced. Biochemical reaction of dark fermentation and photofermentation takes place in the second and third steps. This avoids the inhibition of the enzyme by oxygen. Still, the overall efficiency of the process is low like direct photolysis [4].

Dark Fermentation Dark fermentation is based on anaerobic degradation pathway, which is currently used for methane production with different biomass

Hydrogen from Biomass. Table 1 Possible biochemical reactions of biological hydrogen production processes [3]

Process	Biochemical reaction	Boundary conditions
Direct photolysis	$2H_2O$ + light → $2H_2 + O_2$	E.g., green algae in pure cultures, sterile conditions, lack of sulfur inhibition of the enzyme Fe-hydrogenase by oxygen
Indirect photolysis	$12H_2O + 6CO_2$ + light → $C_6H_{12}O_6 + 6O_2$	Photoautotrophic bacteria, e. g., Cyanobacteria in pure culture, sterile conditions, enzymes: hydrogenase
	$C_6H_{12}O_6 + 2H_2O \rightarrow 4H_2 + 2CH_3COOH + 2CO_2$	
	$2CH_3COOH + 4H_2O$ + light → $8H_2 + 4CO_2$	
Dark fermentation	Biomass + $H_2O \rightarrow H_2 + CO_2$ + VFA (e.g., acetic acid)	Exclusion of methane-producing bacteria, mixed culture generated from different origin
Photofermentation	$CH_3COOH + 2H_2O$ + light → $4H_2 + 2CO_2$	Photoheterotrophic bacteria (e.g., purple bacteria), enzyme nitrogenase, lack of nitrogen

as feedstock. The biological process is divided in four steps. Depending on the composition of the biomass, different degradation pathways are used, and different microorganisms are involved. In steps 2 and 3, hydrogen is produced as an intermediate in several degradation pathways by a variety of microbes. In a conventional anaerobic digestion, this hydrogen is transformed into methane by methanogenic bacteria in the fourth step. The degradation pathways during anaerobic digestion depending on the composition of feedstock are shown schematically in Fig. 1. There, the biomass is divided in fats, carbohydrates, and proteins because the anaerobic degradation pathway depends on the structure of molecules.

If the hydrogen consumption is stopped by elimination of the hydrogen-consuming microorganisms (i.e., the methanogenic bacteria), hydrolysis gas accrue, which consist mainly of hydrogen and carbon dioxide. The methanogenic microorganisms might be eliminated by heat treatment of the start culture, for example, digested sludge [6, 7], or by using a seed material without strict anaerobic hydrogen-consuming bacterial-like compost or soil [3, 8] or pure stains of hydrogen-producing bacteria [4].

An opportunity to prohibit the hydrogen consumption by using a mixed culture out of digested sludge is to optimize the applied condition for hydrogen production and suppress hydrogen consumption. This is possible because methane is generated at a pH value between 6.0 and 8.0, whereas the hydrolytic and acidogenic bacteria prefer pH value between 4.5 and 6.0 for the degradation of carbohydrates. Nevertheless, the generation time of the methane-producing bacteria is within 2–7 days, much higher than the generation time of hydrogen-producing bacteria. Due to the fact that the generation time of carbohydrate-degrading acidogenic bacteria is only 30 min at optimal conditions, the hydraulic retention time (HRT) might be shorter. In contrast to the hydrogen-producing bacteria, the methane bacteria cannot accumulate in the reactor at a hydraulic retention time less than 48 h. These facts indicate as well that carbohydrates are most suitable for the dark fermentation process by using mixed cultures, which are generated out of digested sludge.

The process might be driven in the mesophilic [3, 7], thermophilic [6], or hyperthermophilic temperature range. Every temperature has its own advantages and disadvantages.

The extreme thermophilic anaerobic bacteria provide the highest hydrogen yields, reaching almost a maximum of 4.0 mol H_2/mol of glucose by using pure stains. Using pure cultures implicates that the feedstock has to be sterilized to avoid an accumulation of other microorganisms in the reactor. Additionally, the energy demand of the process is higher than at lower temperatures. The above-mentioned hydrogen yield of 4.0 mol H_2/mol glucose (this corresponds with 498.38 Nl H_2/kg glucose) is only reached if the combination of feed (different kinds of sugar) and microorganisms is optimal [4, 10, 11]. That implicates that a small change of feedstock (e.g., hexose instead of glucose) results in less efficiency of the plant. For this reason, a pretreatment step for the conversion of more complex biomass to simple sugars is necessary, which reduce the efficiency of the plant as well.

Hence, with the diversity in a mixed culture of strict anaerobic bacteria like Clostridia and facultative anaerobic hydrogen-producing bacteria, a variety of biomass can be converted to hydrogen. This process may be realized in the mesophilic or thermophilic temperature range. Due to the less energy demand, better stability of the process and approximately the same hydrogen yields [3], the mesophilic temperature range seems to be most promising for a technical application with a mixed bacteria culture as seed material and biowaste as feedstock in short term.

Beside the hydrogen yield (given in Nl hydrogen per kg of substrate), the gas and especially the hydrogen production rate is important for a technical application. Due to the fact that the bacteria density has to be low as well as the organic concentration in the influent, only the reduction of hydraulic retention times (HRT) provides an increase of hydrogen production rate. Hence, different reactor types were used. Continuous stirred-tank reactor (CSTR) is the easiest technique, which is similar to the used technique in wet anaerobic digestion. But the hydraulic retention has to be higher than the generation time of the microorganisms to provide an accumulation of these bacteria. Therefore, the hydraulic retention time has to be higher than 12 h.

A disadvantage of dark fermentation is the inhibition by its end product hydrogen. This is caused by biochemical equilibrium and thermodynamics of reactions. Figure 2 shows the energy yield of different reactions based on the hydrogen partial pressure, which affects the

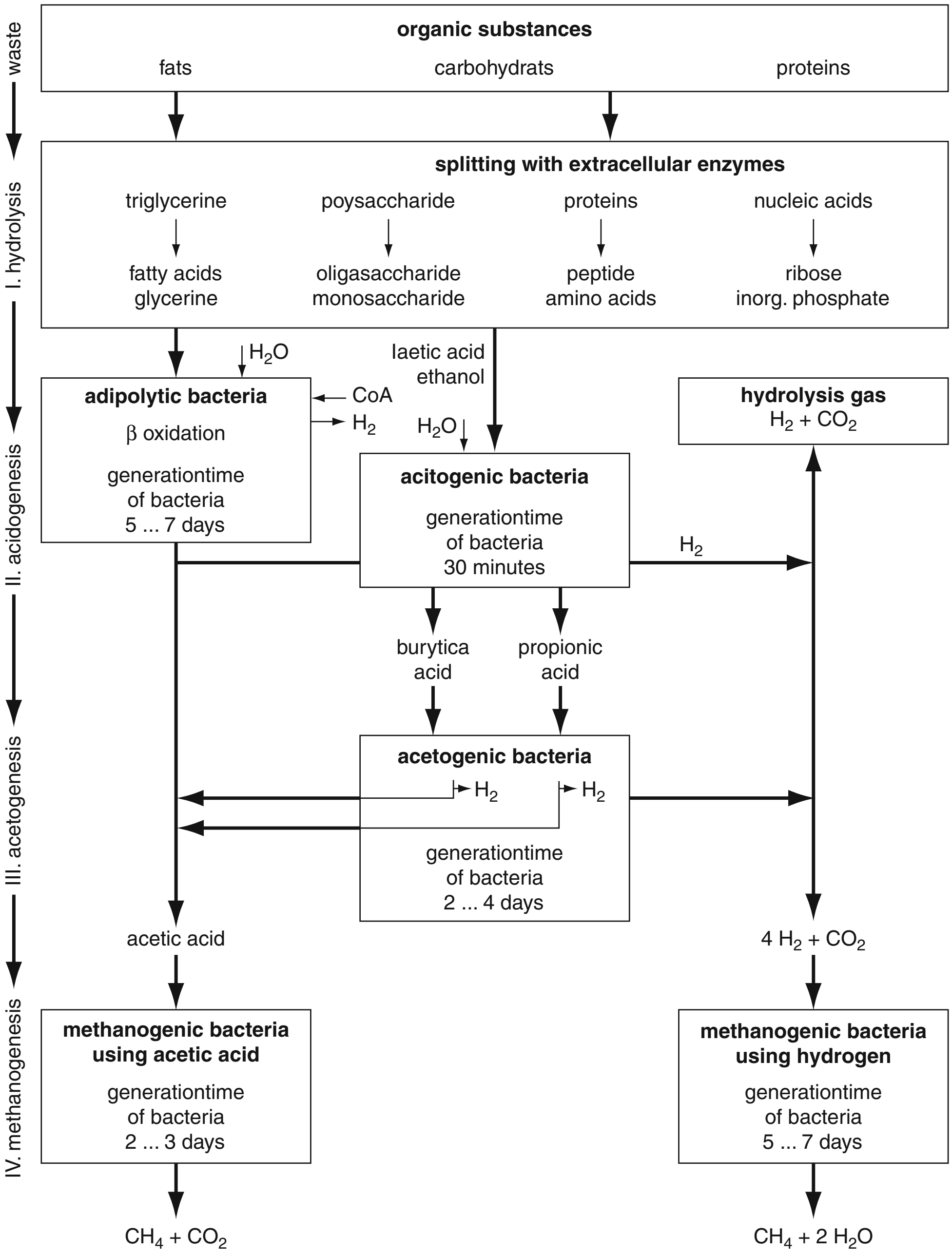

Hydrogen from Biomass. Figure 1

Degradation pathway during anaerobic digestion

solubility of hydrogen in the liquids. Only if the hydrogen partial pressure is less than 0.1 bar will the conversion of organic acids to hydrogen become exothermic.

To provide these conditions, the produced hydrogen has to be removed from the system continuously. This can be done by:

- Purging with nitrogen or another inert gas
- Stirring with a high frequency

The purging with inert gas results in an increase of gas production. In parallel, the hydrogen concentration within the produced gas is decreasing, and therefore, an

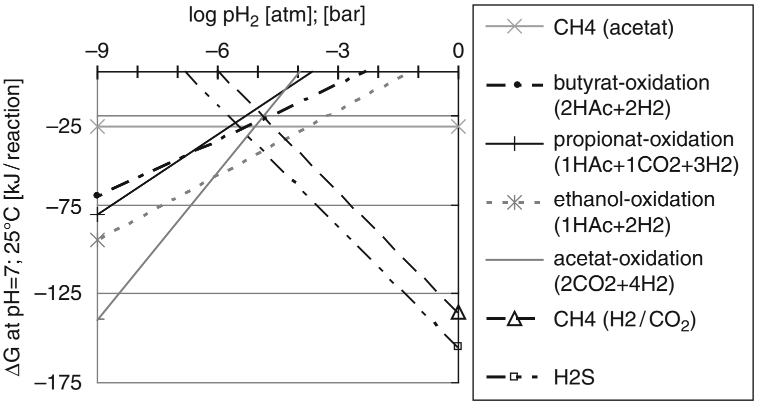

Hydrogen from Biomass. Figure 2

Energy yield of reactions dependent on hydrogen partial pressure

upgrading before the use (e.g., in a fuel cell) is necessary.

In general, hydrogen production by dark fermentation is restricted by the incomplete degradation of organic matter into volatile fatty acids, hydrogen, and carbon dioxide. Consequently, a further conversion of the liquid residues into an energy carrier is necessary.

Photofermentation Photofermentation is driven by photoheterotrophic microorganisms, like purple bacteria (i.e., different strains of *Rhodobacter*). These bacteria are unable to split water. However, under anaerobic condition, these bacteria are able to degrade simple organic components like volatile fatty acids and alcohols into hydrogen and carbon dioxide under nitrogen-limited circumstances. The catalyst of the process is nitrogenase, which is sensitive to oxygen like hydrogenase. There are certainly no problems because no oxygen is produced. Normally, this enzyme catalyzed the fixation of molecular nitrogen (N_2) to ammonia NH_3, which is needed by the bacteria to grow. In absence of nitrogen, the enzyme is able to catalyze the evolution of hydrogen. The produced gas consists of hydrogen (80–90% (v/v)) and carbon dioxide (10–20% (v/v)) [4, 5].

The process depends on light. So, the reactor needs a high surface-to-volume ratio like the direct and indirect photolysis. By using sunlight, the increase of temperature has to be taken into account to prevent the system from damage by high temperature.

The above-mentioned limitation to convert only organic acids and alcohols by using of light as an energy source makes it a possible second treatment step after dark fermentation.

Comparison So far, all biohydrogen production technologies have been tested in lab scale. The feasibility of a technical implementation for hydrogen-producing photosystems is currently restricted by space requirements [12]. Additionally, the surface-to-volume ratio is restricted by the penetration of light into the reactor. Table 2 shows a comparison of required dimensions of bioreactors to produce enough gas to power a PEM fuel cell.

Up to now, very few technical and economic studies for biological hydrogen production systems have been carried out [4, 5, 13].

Regarding space requirements, no algae photosystem provides a sufficient amount of hydrogen in relation to the necessary reactor size. Without intensive further research and development of the methods, a technical realization in the large scale seems to be impossible within the next decade. Additionally, most of the photosystems work with pure strains of microorganisms and lack of nutrients (sulfur or nitrogen). Therefore, antiseptic techniques are needed to avoid an accumulation of other bacteria or yeast. Furthermore, circumstances in respect to nutrient limitations have to be taken into account.

Although the process of biohydrogen production by dark fermentation has been investigated very intensively during the last decade, there are still a lot of open

Hydrogen from Biomass. Table 2 Size of bioreactor required to power PEM fuel cells 0

System	Size of bioreactor (m^3) required to power a PEM fuel cell of			
	1.0 kW	1.5 kW	2.5 kW	5.0 kW
Direct photolysis	341	512	856	1,710
Indirect photolysis	67.3	101	169	337
Photofermentation	149	224	374	758
Dark fermentation min.	0.198	0.297	0.495	0.989
Dark fermentation max.	2.91	4.38	7.31	14.62

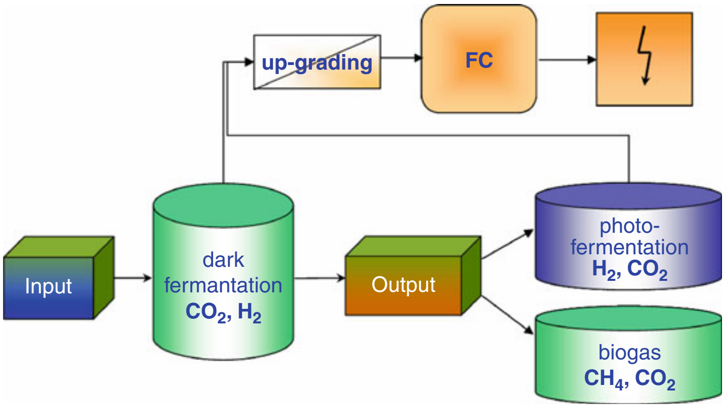
up-grading
FC
ϟ
Input
dark fermantation CO_2, H_2
Output
photo-fermentation H_2, CO_2
biogas CH_4, CO_2

Hydrogen from Biomass. Figure 3
Biological-based biomass to hydrogen concepts

questions. Most of the research has been carried out in batch test systems, just small continuous systems have been operated yet. The reactor dimensions usually do not exceed a working volume of a few liters. Additionally, the dark fermentation is an incomplete degradation of organic matter with volatile fatty acids in the liquid phase. Consequently, the dark and photofermentation are promising processes. In case of dark fermentation, a second treatment step is necessary. In case of photofermentation, a pretreatment step is required.

Biomass to Hydrogen Systems

A complete biological conversion into hydrogen and carbon can only be realized by a combined multistage treatment (e.g., dark fermentation as the first stage and conversion of the produced volatile fatty acids into hydrogen by photofermentative microorganisms as the second stage [4]). For implementation, even combined dark fermentation/methane fermentation plants or a material utilization of the reactor effluent is conceivable.

With conventional anaerobic digestion, an energy carrier in form of biomethane is already established. Therefore, methane fermentation combined with steam reforming will lead to energy losses by the hydrogen production step. Hence, it should be carefully considered whether methane could be used directly for energy generation, e.g., in a suitable fuel cell (MCFC, SOFC) or in the mobility sector (gas upgrading to natural gas quality).

Below, some examples of combined systems are discussed in detail (Fig. 3).

Combination of Dark Fermentation and Photofermentation The combined dark fermentation and photofermentation process connects two new

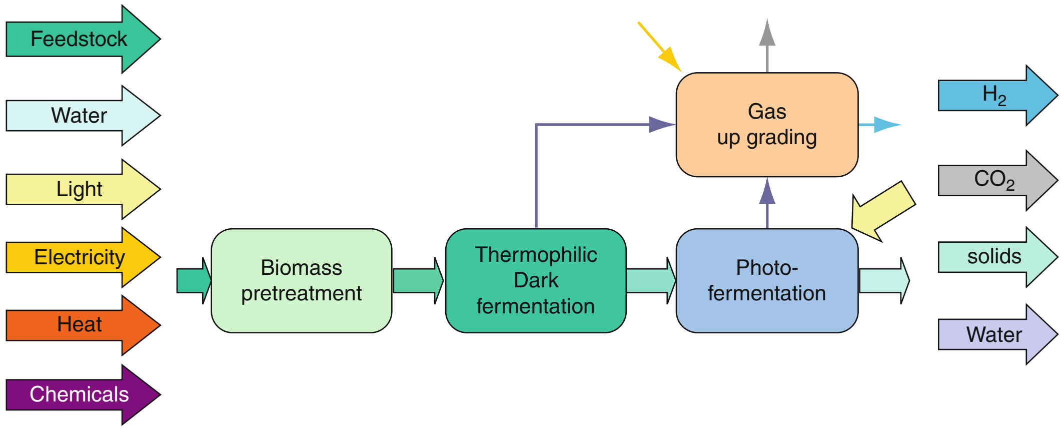

Hydrogen from Biomass. Figure 4
Scheme of combined dark and photofermentation [9] (simplified)

technologies with high research requirements because they have only been realized in lab scale and not in pilot or technical scale yet. This will cause additional problems for technical implementation [9]. Figure 4 shows a scheme of the combined dark and photofermentation system.

Caused by the specific microorganisms and to increase the conversion of biomass to hydrogen during dark fermentation with pure bacteria strains, a pretreatment step is used. Here, hydrolytic bacteria and/or addition of chemicals should degrade a variety of biomass (especially carbohydrates) to simple molecules. The thermophilic temperature range is supplied by heating the system. This process operates with specific anaerobic bacteria specialized to degrade only different kinds of sugar or starch to H_2, CO_2, and organic acids. The thermophilic temperature in this stage provides sanitation and decreases the competition with other microorganisms. Additionally, chemicals are used in this stage for nutrient supply and pH stabilization. The effluent contains mainly volatile fatty acids and alcohols dissolved in water. This effluent is pumped in photobioreactor. Here, the light-dependent photofermentation takes place. The biochemical reactions in this combined system, except the biomass pretreatment, are shown in Table 3.

Hydrogen from Biomass. Table 3 Biochemical reactions for the combination of dark and photofermentation with glucose as substrate

Substrate	First reactor (dark fermentation)	Second reactor (photofermentation)
$C_6H_{12}O_6$ + 2 H_2O→	$2CH_3COOH$ + **$2CO_2 + 4H_2$** [3, 4]	**$8\ H_2 + 4\ CO_2$** [14]
	$2CH_3COOH$ + $4H_2O$ + Light→	

Combined Dark and Methane Fermentation

Hydrogen yields of 4 mol/mol glucose (Eq. 1) at maximum are possible by dark fermentation with only 2 mol acetates as by-product [2, 15]. If only butyric acid occurs as by-product, the hydrogen yield decreases to 2 mol/mol glucose (Eq. 2) [15]. Typically, the end product of dark fermentation by using mixed microflora is a mix of different volatile fatty acids like acetic and butyric acid [7, 16]. Accordingly, the biochemical possible hydrogen yield is 2.5 mol/mol glucose (Eq. 3).

If the liquid effluent of the H_2 reactor is used as carbon source in a methane reactor, the organic acids become degraded to CO_2 and CH_4. The theoretical methane yield that can be generated depends on the liquid products of the hydrogen stage. If the acidogenesis takes place in the first reactor, only acetic acids would be transferred into the methane reactor, and only these acids would be converted

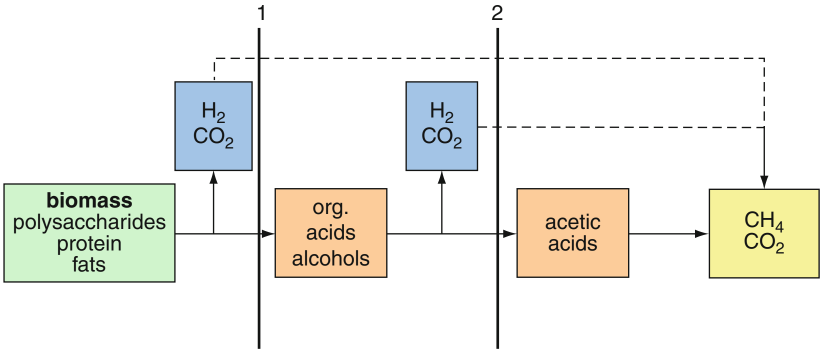

Hydrogen from Biomass. Figure 5
Combined biological hydrogen and methane production out of biomass

Hydrogen from Biomass. Table 4 Biochemical equation for the combined biological hydrogen and methane production with glucose as energy source

	Substrate	First reactor (H_2)	Second reactor (CH_4)
Eq. 1	$C_6H_{12}O_6 + 2\ H_2O \rightarrow$	$2CH_3COOH + \mathbf{2CO_2 + 4H_2}$ [2, 15]	
		$2CH_3COOH \rightarrow$	$\mathbf{2CH_4 + 2CO_2}$
Eq. 2	$2\ C_6H_{12}O_6 \rightarrow$	$2C_3H_7COOH + \mathbf{4CO_2 + 4H_2}$ [17]	
		$2C_3H_7COOH + 2H_2O \rightarrow$	$\mathbf{5CH_4 + 3CO_2}$
Eq. 3	$8\ C_6H_{12}O_6 + 4\ H_2O \rightarrow$	$4CH_3COOH + 6C_3H_7COOH + \mathbf{16CO_2 + 20H_2}$ [7, 16]	
		$4CH_3COOH + 6C_3H_7COOH + 6H_2O \rightarrow$	$\mathbf{19CH_4 + 13CO_2}$
Eq. 4	$C_6H_{12}O_6 \rightarrow$		$\mathbf{3CH_4 + 3CO_2}$

into CH_4 and CO_2. This case is signed by line 2 in Fig. 5. Line 1 indicates that only the hydrolysis and acetogenesis take place in the first reactor. If so, the hydrogen yield decreases, and the methane yield increases according to Eq. 2 and Eq. 3. The stoichiometries of some possible biochemical reactions for the combined hydrogen and methane production with glucose as carbon source are given in Table 4. The chemical equation for the optimal degradation of glucose by a conventional fermentation (Eq. 4) is also given in this table.

An engineered approach towards a technical system has not been made yet. However, up to now, the combined hydrogen/methane fermentation system offers the highest realization potential regarding the biological hydrogen production methods. This is due to the fact that only one pretreatment module has to be implemented in a proved technology.

Hydrogen Production by Solid Biomass Gasification

Thermochemical hydrogen production can be carried out by a wide variety of different processes. Below, the basic principles as well as some examples are discussed.

Process Principles

Generally, gasification is a thermochemical process that converts a carbon-containing substance, here lignocellulosic biomass, by partial oxidation into a fuel gas. A gasification agent (i.e., air, oxygen, or steam) provides the required oxygen. While air gasification generates a low-calorific-value gas suitable for power generation, oxygen and steam gasification lead to a medium-calorific-value gas, referred to as syngas.

Syngas is suitable for the production of energy carrier such as H_2, methane, and liquid hydrocarbons.

The overall gasification reaction for biomass may be expressed after Eq. 5.

$$\begin{aligned}\text{Biomass} + H_2O + O_2 &\rightarrow H_2 + CO + CO_2 \\ &+ CH_4 + \text{hydrocarbons} + \text{char}\end{aligned} \tag{5}$$

The heat of reaction (ΔH_R) is positive for steam gasification (endothermic reaction) and negative for oxygen gasification (exothermic reaction). Reaction stoichiometry favors steam as gasification agent for a maximum H_2 output, but pure steam gasification requires an external heat supply adding up to a concept called allothermal steam gasification. At first glance, oxygen gasification is comparatively less attractive for H_2 production since less H (in form of steam) enters the gasifier. But other aspects have to be considered that prohibit such a simple conclusion:

- Oxygen gasification achieves higher temperatures enabling higher carbon-to-gas ratios.
- Autothermal operation is advantageous for overall process efficiency since heat transfer losses are smaller.
- Steam addition in downstream processing may balance the initial lower H content.

Biomass gasification typically operates under thermodynamic conditions that imply an almost complete carbon conversion into gaseous species (i.e., CO, CO_2, and CH_4). Assuming carbon conversion is complete, the equilibrium gas composition is given by two homogenous gas reactions, methane steam reforming (Eq. 6) and water–gas shift (Eq. 7).

$$CH_4 + H_2O \leftrightarrow CO + 3H_2 \quad \Delta H_R = +206\ \text{KJ/mol} \tag{6}$$

$$CO + H_2O \leftrightarrow CO_2 + H_2 \quad \Delta H_R = -41\ \text{KJ/mol} \tag{7}$$

In practice, carbon conversion is restricted due to mass transfer limitations and reaction kinetics. The raw syngas often contains light and heavy hydrocarbons being intermediates in terms of volatilization of the biomass organics. Especially aromatic compounds, known as tars, require a sophisticated conversion process or in depth removal before downstream gas processing.

Biomass gasification for fuel production relies on different gasification concepts, namely entrained flow, fluidized bed, and dual fluidized bed steam gasification:

- Fluidized bed gasification is realized by a bed of fine, inert or catalytic active, material that is fluidized by blowing oxygen upwards through the bed. In contrast to power and heat applications, air is an improper gasification agent as nitrogen dilutes the syngas, boosting the downstream gas treatment effort. Depending on the gas velocity, the bed material is agitated (bubbling fluidized bed, BFB) or suspended throughout the gasifier (circulating fluidized bed, CFB). The syngas leaves the reactor at the top. In case of CFB, it has to be separated from the bed material with a cyclone. Fluidized bed gasifiers allow for pressurized operation. Typical gasification temperatures are in the range of 850–950 C. Compared to other gasification options, the main advantages of CFB gasifiers are high cold gas efficiencies, low investment costs, and a wide applicable power range of some tens to some hundreds of megawatts. Major drawbacks are related to comparatively low H_2 content in syngas and limited operating pressure because of feeding and fluidization issues.
- Entrained flow gasification takes on a special position in biomass gasification. In contrast to fluidized bed gasifier designs, it refers to established fossil fuel technologies for large-scale implementation. The key measure to enable entrained flow gasification for biomass is to manipulate the biomass properties by pyrolysis processes, such as torrefaction and carbonization, in a way that they become more similar to coal. The resulting bio-oil, char, or slurry are pressurized and then atomized with pure oxygen in a burner at the top of the gasifier. Gasification temperatures are in a range of 1,300–1,600°C, high enough to convert ash into slag. Entrained flow biomass gasification has some advantages compared to other gasification processes: (1) the high syngas pressure is favorable for H_2 purification and distribution, (2) the raw gas is tar-free and therefore requires only modest gas cleaning efforts, and (3) the possibility to combine decentralized, small-scale biomass pretreatment

with centralized, large-scale gasification avoids the long-distance transport of raw biomass with a low energy density while still profiting from economy of scales. On the other hand, there are some major drawbacks: (1) the overall concept implies an efficiency penalty due to losses during thermochemical pretreatment, (2) formation and discharge of slag is difficult to handle since biomass feedstock provides a wide range of ash properties, and (3) the H_2 content in syngas is low, providing a heavy duty for downstream gas conditioning.

- Dual fluidized bed steam gasification provides a major advantage for H_2 production by increasing the amount of H entering the process. But because the gasification process is endothermic, an external heat source and a heat transfer medium are required. Therefore, steam gasification concepts usually work with two fluidized beds, one for the gasification process and a second one for combustion. As an example, the process principle of the Fast Internally Circulating Fluidized Bed (FICFB) technology is shown in Fig. 6 0. Here, biomass is fed into the gasification chamber where it is converted into nitrogen-free syngas and char using steam as gasification agent. Char, recycled syngas, and recycled tars are burnt with air in the combustion chamber, heating the accompanying catalytic bed particles. The hot bed material is then fed back into the gasification chamber, providing the required reaction heat. Dual fluidized bed gasifiers operate at ambient pressure with a gasification temperature of 800–870°C [18].

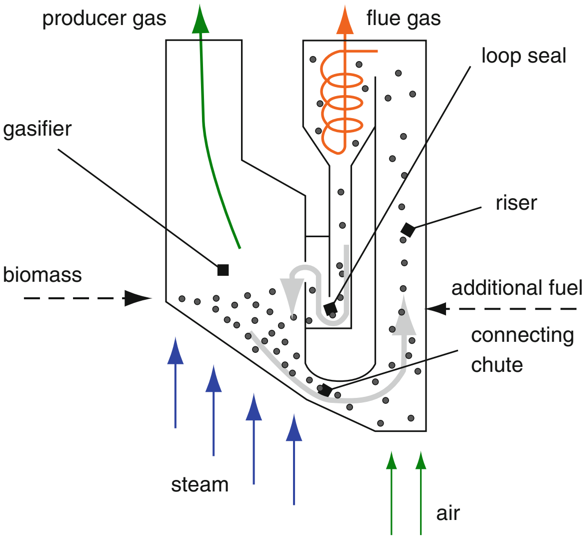

Hydrogen from Biomass. Figure 6
Fast Internally circulating fluidized bed (FICFB) gasification 0

In case of H_2 production, all presented biomass gasifiers require further downstream gas processing to achieve better H_2 yield und purity. Gas conditioning by steam reforming (Eq. 6) and water–gas shift (Eq. 7) utilize steam to generate additional H_2:

- Steam reforming is the process where methane and other hydrocarbons are converted into carbon dioxide, carbon monoxide, and H_2 in the presence of steam. In technical applications, reforming is performed utilizing a catalyst, which is usually nickel-based. Steam reforming should be performed at high temperatures to shift the equilibrium to the right side of Eq. 6. There should be an excess of steam to prevent coking. At temperatures below 900°C, most of the nickel catalysts are sensitive to sulfur poisoning. Methane steam reforming is strongly endothermic. As for the gasification process itself, the question arises, whether the heat is provided autothermal by oxygen supply or allothermal from an external source. Low pressure is favorable since it shifts the reaction equilibrium towards H_2.
- In contrast, the water–gas shift reaction is exothermic. Unfortunately, the excess heat is not suitable to support steam reforming because the temperature level is too low. Water–gas shift is often performed in two steps: a high temperature shift and a low temperature shift. The high temperature shift usually is performed at 300–400°C using iron–chrome catalysts, and the low temperature shift operates below 250°C utilizing copper and zinc oxide catalysts. The amount of carbon monoxide can be lowered to less than 1%. The equilibrium is not sensitive to pressure.

Biomass gasification with downstream gas conditioning results in an H_2-rich gas that typically contains a significant amount of accompanying gas species (e.g., carbon dioxide, carbon monoxide, nitrogen, and a variety of trace components). Physical or chemical scrubbers for acid gas removal (AGR) permit a comparatively cheap and efficient bulk CO_2 removal, but high purity H_2 output requires (additional) pressure swing adsorption, membrane separation, or preferential CO oxidation upstream of the acid gas removal.

Pressure swing adsorption works on the principle of molecular sieving. Molecular sieves are zeolites or activated carbon with a defined pore structure allowing for the separation of molecules according to size and polarity. The gas is fed to a system of packed beds. Frequent pressurization of the beds leads to, alternately, adsorption and release of the unwanted gas species. After desorption, the bed is purged. In the time, the first bed is regenerated; the second bed is pressurized, after which the gas feed is switched back to the first bed.

Biomass to Hydrogen Systems

The basic concept of biomass gasification plants for H_2 production is presented in Fig. 7. It involves several main process steps: (1) biomass pretreatment, mainly drying and sizing, but in case of entrained flow gasification also thermochemical treatment such as fast pyrolysis or torrefaction; (2) the gasification process itself, performed either allothermal with a dual fluidized bed design or autothermal with fluidized bed or entrained flow gasifiers; and (3) downstream gas processing that covers gas cleaning for the removal of impurities, gas conditioning by reforming and water–gas shift reaction, and H_2 purification.

A biomass gasification plant is not energy autonomous. Most of the processes require a significant amount of electrical energy. Steam generation is also an issue. Depending on infrastructural and business conditions, it could be a favorable option to integrate power and heat generation. If so, some of the syngas is used to fire an engine or a gas turbine for the simultaneous generation of electricity, heat, and fuel. Another option is the conversion of surplus heat with a steam turbine. In the future, the operation of a fuel cell feed with H_2 is another possibility. If power and heat generation exceeds the demand of the plant, surpluses can be sold in addition to the H_2 product. This approach is referred to as polygeneration concept [19].

Present biomass gasification plants are originally designed for the production of biofuels other than H_2. But a proper downstream process design allows for H_2 production as well. If designed for H_2 output, the fuel synthesis island has to be replaced by H_2 purification processes.

In case of entrained flow gasification concepts, biomass pretreatment and the gasification process itself will be the same for all biofuel output option. Gasification parameters do not allow for further optimization of the H_2 yield because there is a trade-off between efficiency and H_2 yield: a higher steam input requires more oxygen to achieve the necessary operating temperatures. Carbon conversion in entrained flow gasifiers is almost complete. The hot raw gas consists of H_2, CO, and CO_2. It is cooled by a water quench using the sensible heat of the gas stream for water vaporization. The amount of water fed into the gas stream lowers the demand for additional steam during the water–gas shift.

H_2 production asks for an as high as possible CO conversion since the energy content of unconverted

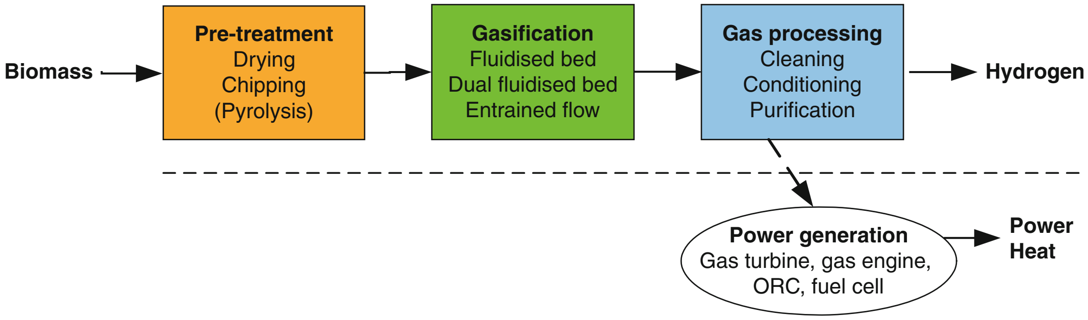

Hydrogen from Biomass. Figure 7

Concept of biomass gasification plants for H_2 production

CO is lost for H_2 output. Therefore, a staged water–gas shift layout is essential. Available catalysts are sensitive to sulfur poisoning so that sulfur components have to be removed upstream. Depending on the requested H_2 quality, different H_2 purification processes have to be applied. Figure 8 provides at the left side a basic scheme of a process chain for H_2 production based on entrained flow gasification.

Recently, several large-scale biofuel production concepts based on entrained flow gasification were developed:

- The production of FT-Diesel from wood on a 45-MW scale with a staged gasification process has been demonstrated. The Carbo-V® process operates at 5 bar pressure. First, biomass is converted into tar-containing gas and charcoal by autothermal pyrolysis at 400–500°C. Second, the pyrolysis gas is fed to an entrained flow gasifier operating at about 1,500°C. Third, charcoal is used for cooling the hot gas down to 900°C by a chemical quench process. The tar-free raw gas contains 30–40% of both H_2 and CO, balanced by CO_2 and H_2O 0.
- The bioliq® concept couples decentralized fast pyrolysis of straw with centralized entrained flow gasification of the resulting bioslurry. The fast pyrolysis is performed at ambient pressure and 500°C. The resulting char and pyrolysis oil are mixed to form slurry, which is transported to the gasification plant. There, it is fed to an entrained low gasifier operating at 30 bar and 1,200°C. The raw gas contains 30–40% CO and 20–30% H_2, balanced by N_2, CO_2, and H_2O. Favored product outputs are FT-Diesel and dimethyl ether, but H_2 production is considered as an option [20].

Fluidized bed gasification concepts, as shown in the middle part of Fig. 8, avoid the need for thermochemical biomass pretreatment. They have milder requirements regarding feedstock drying and sizing.

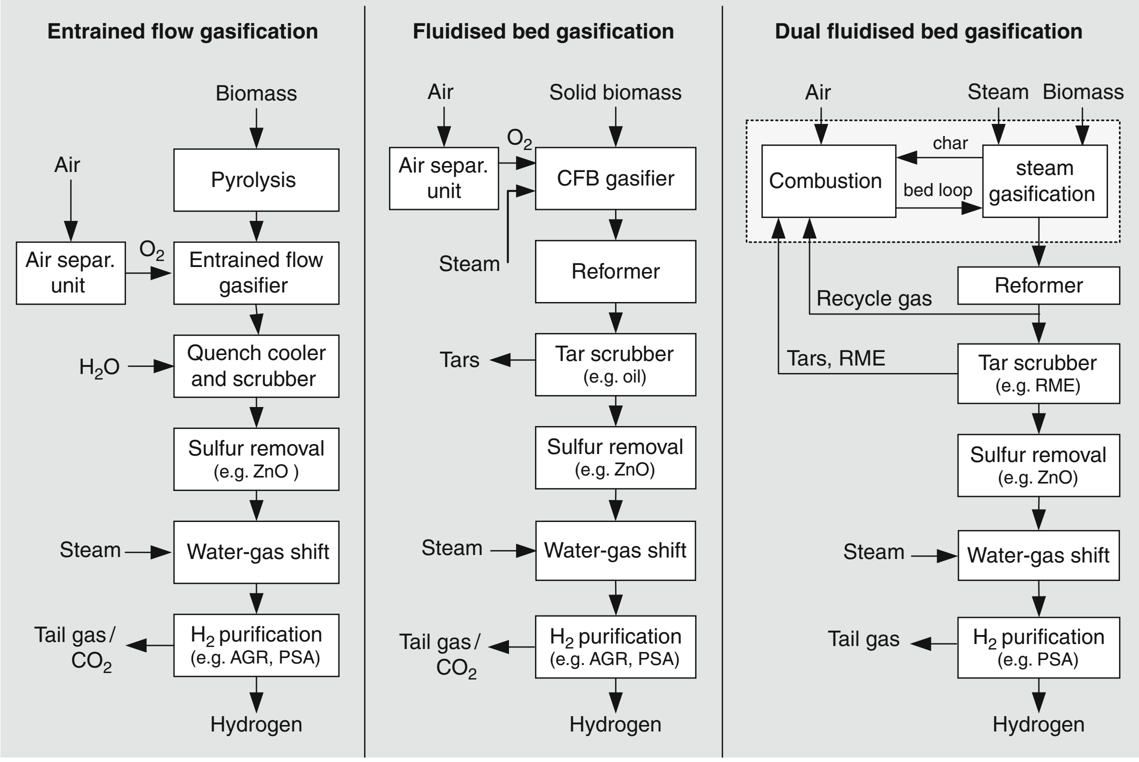

Hydrogen from Biomass. Figure 8

Biomass gasification process chains for H_2 production

Wood chips are a common fuel. Circulating fluidized bed (CFB) gasifiers are in some major aspects similar to entrained flow gasifiers. They use the same gasification agent – oxygen – and may operate pressurized.

An important difference compared to entrained flow gasifiers is related to ash. Because sintering and slag formation would create problems in terms of bed fluidization, the operating temperature is limited to roughly 1,000°C. At this operating condition, carbon conversion is around 95%. The limited carbon conversion is linked to a major problem of fluidized bed gasifiers: syngas quality suffers from tars. Since tars are not only impurities but also carry a significant amount of the chemical bound energy, tar treatment is crucial for the overall efficiency. A preliminary reforming of tars – and other hydrocarbons including methane, which is a major component in CFB raw gas – recovers the chemical energy to a large extent in form of CO and H_2 before a secondary tar removal process purifies the syngas. Further downstream processes are similar to those of entrained flow gasification based H_2 concepts. Differences in syngas composition and pressure level decide over the choice of the most suitable H_2 purification steps.

At present, CFB biomass gasification for H_2 is still under development. In Scandinavia, different demonstration projects deal with a slipstream H_2 train:

- In Värnamo (Sweden), the VVBGC demonstration project rebuilds a biomass-fueled IGCC plant into a synthesis gas producing unit with research and development [21].
- In Varkaus (Finland), a consortium is demonstrating a 12-MW syngas atmospheric oxygen/steam–blown CFB gasifier. The ultra clean gas (UCG) project focuses on syngas treatment to provide a reliable interface for different production targets, including H_2 [22, 23].

Dual fluidized bed gasification concepts, as shown in the right part of Fig. 8, cover process steps similar to those of CFB-based process chains. The major differences are: (1) the carbon conversion in the gasification chamber of roughly 75% leads to a smaller amount of syngas containing a higher percentage of H_2, (2) the duty of the water–gas shift is lower because the raw syngas composition provides a higher H_2/CO ratio due to the utilization of steam as gasification agent, and (3) tars are recycled to the combustion chamber because the segregation of gasification and combustion permits an easy handling of additional fuel.

Dual fluidized bed gasification concepts for the production of fuels and chemicals are mainly designed for methane output, often as a part of a polygeneration concept. But some concepts are as well optimized for H_2 production:

- A biomass gasification concept for the production of gaseous and liquid fuels has been introduced. A dual fluidized bed gasifier integrates a tar reformer utilizing the heat of the flue gases to boost the syngas H_2 content from 20% up to more than 45% [24, 25].
- The so-called Güssing model follows the strategy of decentralized, local energy production from all available renewable resources in a region. Here, an 8-MW_{th} FICFB gasifier (Fig. 6) is operated in CHP mode [26]. Additionally, the gasifier provides opportunities for testing different bed materials and for the use of a syngas side stream for process development purposes, for example, the development of methane and BtL fuel production downstream equipment.

Table 5 summarizes the characteristics of the presented biomass gasification process chains regarding H_2 production. Those process chains provide a basis for additional or pure H_2 output but rely on an initial design for other output options. H_2 production is specified as a potential output stream but has not been demonstrated on an industrial scale. From the view of process economics, a major drawback of current gasifier designs is the initial low H_2 content of the syngas. Recently, new processes with higher H_2 concentrations have gained interest. Particularly, a process called adsorption enhanced reforming (AER) provides good opportunities for commercial H_2 production from wood and herbaceous biomass [27] 0.

Case Study: The AER Process

The AER process is a new approach to improve dual fluidized bed gasification. Figure 9 describes the process principle. By using a bed material such as mineral calcite ($CaCO_3$) in a dual fluidized bed gasifier, a chemical loop is established where the bed material

Hydrogen from Biomass. Table 5 Main characteristics of biomass gasification process chains for fuels and chemicals

	Dual fluidized bed	Circulating fluidized bed	Entrained flow
Gasification characteristics			
Reactor type	Dual fluidized bed	Fluidized bed	Entrained flow
Gasification agent	Steam	Oxygen (+steam)	Oxygen (+steam)
Heat supply	Bed loop	Autothermal	Autothermal
Temperature level (°C)	800–870	900–1,000	1,300–1,600
Pressure level (bar)	1	1–20	5–80
Residues	Ash	Ash	Slag
H_2 at outlet (vol%)	30–40	20–30	25–35
CH_4 at outlet (vol%)	9–12	10–15	<1
Required downstream processes for H_2 production			
Tar removal/conversion	Yes	Yes	No
Steam reforming	Yes	Yes	No
CO shift	Yes	Yes	Yes
H_2 purification	Yes	Yes	Yes
Plant characteristics			
Conversion efficiency[a]	50–60	50–60	45–55
Target scale (MW_{th})	10–100	30–200	250–1,000
Drawbacks	Tar load	Feeding system (pressurization), tar load	Biomass pretreatment, process control
Announced products	CH_4, BtL, polygeneration	BtL, CH_4, H_2, IGCC	BtL, CH_4, H_2

[a] Biomass to H_2 on LHV basis, estimation

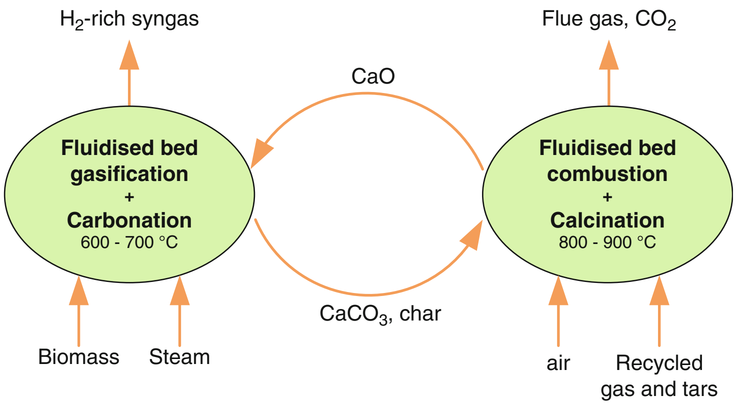
H2-rich syngas
Flue gas, CO2
CaO
Fluidised bed gasification + Carbonation 600 - 700 °C
Fluidised bed combustion + Calcination 800 - 900 °C
CaCO3, char
Biomass
Steam
air
Recycled gas and tars

Hydrogen from Biomass. Figure 9
Principle of AER gasification process

not only acts as a heat carrier but also adsorbs CO_2 and transports it from the gasification reactor to the combustion chamber where it is released.

CO_2 absorption in the gasifier part shifts the equilibrium of the water–gas shift reaction towards H_2 (Eq. 7). Hence, an H_2-rich product gas results with reduced CO_2 and CO concentration. The idealized sum reaction of the AER gasification – without considering the formation of methane and other secondary products – is given by Eq. 8 [28].

$$CH_xO_y + (2 - y)H_2O + CaO \rightarrow CaCO_3 + (0.5x + 2 - y)H_2 \quad (8)$$

$$CaO + CO_2 \leftrightarrow CaCO_3 \quad \Delta H_R = -181.4\ \mathrm{kJ/mol} \quad (9)$$

The operating temperature of the gasification reactor is 600–700°C. According to Eq. 9, CO_2 adsorption (carbonation) is highly exothermal so that the heat demand of the gasifier part is lower as compared to FICFB steam gasification. The fluidized bed material – calcite ($CaCO_3$) and char at this moment – is directed to the combustion chamber where char and additional fuel are burned to provide the calcination temperature well above 800°C. The heated bed material – now quicklime (CaO) – is recycled to the gasification chamber. Because the temperature difference of more than 200°C between gasifier and combustor is much higher than those 50°C of the FICFB process, it is necessary to reduce the bed material circulation rate. In order to do so, the particle size of the bed material is increased, and the primary fluidization in the combustor is decreased [29].

The desired properties on the bed material for AER gasification are:

- High mechanical stability to avoid dust problems in downstream equipment
- High CO_2 capacity and sufficient reaction rate of carbonation and calcination
- High catalytic activity towards tar conversion and CO shift reaction

Different limestones as a bed material have been tested with two biomass fuels, wood pellets, and straw pellets in a 100-kW_{th} process development unit [29]. The tested bed material consisted mainly of calcite coming from different mining companies. Clear variations in overall performance of wood gasification regarding gas composition and dust load have been observed:

- The H_2 concentration varies in a range from 59% to 70%.
- The tar content in raw syngas varies from 0.4 to 2.8 g/Nm^3 with most of the values lower than 1 g/Nm^3.
- The dust content is between 12 and 42 g/Nm^3.

In contrast to conventional dual fluidized bed steam gasification, the AER process provides favorable conditions for straw gasification. Straw is a difficult fuel for biomass gasification because of its low sintering point at 700–750°C, causing bed agglomeration in reactors operating at the temperatures above. The lower gasification temperature and the positive influence of CaO on the melting behavior of straw enable this widely available biomass resource for H_2 production. Compared to wood pellets, drawbacks are a higher dust load (~80 g/Nm^3) due to the high ash content, a higher tar content of 2–3 g/Nm^3, and a lower H_2 concentration of 52% [29].

The same 100-kW_{th} apparatus have been used to perform a comparison between FICFB and AER gasification regarding mass and energy balances [30]. The bed materials were olivine in case of FICFB gasification and calcite for the AER process. Oil was used as additional fuel. Table 6 provides an overview of the main results of those test runs. In contrast to conventional steam gasification, syngas properties of the AER process are more advantageous for H_2 production since the effort for downstream processing is much lower, but the conversion efficiency is comparatively low.

Future Directions

The market implementation of hydrogen from biomass is strongly influenced by the aimed utilization. The fields of use are significant:

- Chemical industry, replacing hydrogen from fossil fuel
- Transportation fuel
- Energy carrier for the storage and dissemination to decentralized applicants

The barrier for market access will be the lowest one in the first case because the market is established, the

Hydrogen from Biomass. Table 6 Comparison of wood gasification with conventional FICFB and AER process [30]

	FICFB	AER
Operating parameter		
Bed material	100 kg olivine	100 kg calcite
Steam/fuel ratio (kg/kg)	0.63	0.79
Gasification temperature (°C)	841	645
Combustion temperature (°C)	920	894
Syngas properties		
H_2 (vol%, dry)	39.1	73.9
CO (vol%, dry)	29.1	6.1
CO_2 (vol%, dry)	17.5	6.0
CH_4 (vol%, dry)	11.4	11.7
Hydrocarbons C2–C6 (vol%, dry)	2.9	2.3
Dust (g/Nm^3)	5.9	22.8
Char (g/Nm^3)	35.2	28.8
Tar (g/Nm^3)	3.5	1.4
H_2O (vol%)	33.2	51.4
Energy balance		
Fuel, wood pellets (kW)	123.5	123.5
Additional fuel, oil (kW)	26.6	9.6
Auxiliaries and steam (kW)	11.4	12.0
Syngas chemical power (kW)	105.6	66.5
Conversion efficiency[a] (%)	70.4	50.0
H_2 yield (l_{H2}/kg_{wood})	280	580

[a] Fuels to syngas, LHV

infrastructure is still available, and there is hardly any alternative to hydrogen as a raw material for processes realized within the chemical industry. The replacement of fossil fuel in the hydrogen production can generate an important environmental benefit. This can be done step by step if the production plants based on fossil fuels reached their end of the lifetime.

In the other market mentioned above (use as a transportation fuel and/or storage medium), a new infrastructure has to be installed before a hydrogen use in the large scale is possible. The creation of such a new infrastructure may be much more expensive than exclusive erection of the production plants. In addition, for these fields of application, renewable alternatives such as biomethane and liquid fuels still exist. It cannot be foreseen which position hydrogen will achieve within this competition field with the given fuel alternatives in years to come.

Some H_2 production methods from biomass are well developed, and several processes are demonstrated. Nevertheless, a commercial status could not be reached until now, neither based on the thermochemical nor on the biochemical or biological route:

- The process steps for the thermochemical hydrogen production based on biomass are well known and scientifically analyzed. Demonstration of the whole provision pathway in a near commercial size has to be the next implementation step. Basically, these processes have to show their economic performance.
- Biochemical pathways for the generation of hydrogen are still in the status of basic research. Therefore, these pathways might have the potential for an important contribution to bioenergy supply only if basic questions are solved based on increased research activities.

The viability of a future biomass to H_2 technology critically depends on the development of efficient, large-scale, cost-effective, and sustainable H_2 production systems. There are lots of activities ongoing, but so far, an economic breakthrough on the market cannot be seen. The years to come will show if this option has a realistic chance to contribute with a considerable share within the overall energy system [1, 31].

Bibliography

Primary Literature

1. Milne TA, Elam CC, Evans RJ (2001) H_2 from biomass – state of the art and research challenges. A report for the international energy agency agreement on the production and utilization of H_2; Task 16, H2 from carbon-containing materials. National

Renewable Energy Laboratory, Golden. http://ieahia.org/pdfs/H2_biomass.pdf. Accessed July 2010

2. Hallenbeck PC, Benemann JR (2002) Biological hydrogen production; fundamentals and limiting processes. Int J Hydrogen Energy 27(11):1185–1193
3. Brunstermann R (2010) Entwicklung eines zweistufigen anaeroben Verfahrens zur kontinuierlichen Wasserstoff- und Methanerzeugung aus organischen Abfällen und Abwässer. Forum Siedlungswasserwirtschaft und Abfallwirtschaft, Universität Duisburg-Essen. Shaker, Aachen
4. Reith JH, Wijffels RH, Barten H (2003) Bio-methane and bio-hydrogen status and perspectives of biological methane and hydrogen production. Dutch Biological Hydrogen Foundation, The Hague. ISBN 9090171657
5. Petrovic T, Wagner HJ, Lente A, Widmann R (2005) Photobiologische Wasserstofferzeugung durch Mikroalgen – Beschreibung konkurierender Systeme zur H_2-Erzeugung. Stärkung der technologischen Position an den Ruhruniversitäten Teilprojekt 8 ef. Ruhr Förderkennzeichen 856569-T-170
6. Rechtenbach D (2009) Fermentative Erzeugung von Biowasserstoff aus biogenen Roh- und Reststoffen. Dissertation am Institut für Abfallressourcenwirtschaft, Technische Universität Hamburg-Harburg. In: Stegmann R (ed) Hamburger Berichte 34. Verlag Abfall aktuell, Stuttgart
7. Krupp M (2007) Bio hydrogen production from organic waste and waste water by dark fermentation – a promising module for renewable energy production. Forum Siedlungswasserwirtschaft und Abfallwirtschaft, Universität Duisburg-Essen. Shaker, Aachen
8. Van Ginkel SW, Logan B (2005) Increased hydrogen production with reduced organic loading. Water Res 39:3819–3826
9. Hyvolution. http://www.fch-ju.eu/sites/default/files/documents/ga2010/pieternel_claassen.pdf
10. Modigell M, Schumacher M, Claassen PAM, Friedl A, Wukovits W (2006) Entwicklung eines zweistufigen Bioprozesses zur Produktion von Wasserstoff aus Biomasse. GVC IT, Wiesbaden
11. Zeidan AA, van Niel EWJ (2007) Developing a thermopilic hydrogen-producing co-culture for efficient utilization of mixed sugars. WHTC, Montecationi Terme
12. Levin DB, Pitt L, Love M (2004) Biohydrogen production: prospects and limitations to practical applications. Int J Hydrogen Energy 29(2):173–185
13. Hemmes K, de Groot A, den Uil H (2003) Bio-H2 Application potential of biomass related hydrogen production technologies to the Dutch energy infrastructure of 2020–2050. ECN-C-03-028. Energy Research Center, Petten
14. Schlegel HG (1997) Allgemeine Mikrobiologie, 1st edn. Thieme, Stuttgart. ISBN 3-13-444607-3
15. Hawkes FR, Dinsdale RM, Hawkes DL, Huss I (2002) Sustainable fermentative H_2 production: challenges for process optimization. Int J Hydrogen Energy 27:1339–1347
16. Benemann JR (2004) Biological production of hydrogen-methane mixtures for clean electricity production. In: 15th hydrogen energy conference, Japan
17. IHS (2005) CEN/TS 14961 Solid biofuels – fuel specification and classes. IHS, Englewood Cliffs
18. Hofbauer H, Veronik G, Fleck T, Rauch R (1997) The FICFB gasification process. In: Bridgwater AV, Boocock D (eds) Developments in thermochemical biomass conversion, vol 2. Blackie Academic & Professional, Glasgow, pp 1016–1025
19. Thrän D, Seidenberger T, Zeddies J, Offermann R (2010) Global biomass potentials – resources, drivers and scenarios. Energy Sustain Dev 14(3):200–205
20. Dinjus E, Kolb T, Dahmen N (2009) State of the art of the bioliq BTL process. In: European biomass conference and exhibition 2009, Hamburg
21. Albertazzi S, Basile F, Brandin J, Einvall J, Hulteberg C, Fornasari G et al (2005) The technical feasibility of biomass gasification for H_2 production. Catal Today 106:297–300. doi:10.1016/j.catted.2005.07.160
22. McKeough P, Kurkela E (2008) Process evaluations and design studies in the UCG project 2004–2007. VTT Research Notes 2434. http://www.vtt.fi/publications/index.jsp
23. Harju-Jeanty T, Nuortimo K, Hotta A, Coda-Zabetta E, Palonen J, Kokki S et al (2009) Innovative utilization of renewable energy sources to combat climate change. In: Fourth international bioenergy conference 2009, Jyväskylä
24. Paisley MA, Overend RP (2002) Verification of the performance of future energy resources' SilvaGas ® biomass gasifier – operating experience in the Vermont gasifier. Paper presented at the Pittsburgh coal conference, 24–26 September 2002, Pittsburgh
25. Paisley M (2007) Advanced biomass gasification for the production of biopower, fuels, and chemicals. AIChE, Salt Lake City
26. Hofbauer H, Rauch R, Loeffler G, Kaiser S, Fercher E, Tremmel H, et al (1998) Six years experience with the FICFB-gasification process. In: Twelfth European conference and technology exhibition on biomass for energy, industry and climate protection, Amsterdam
27. Koppatz S, Pfeifer C, Rauch R, Hofbauer H, Marquard-Moellenstedt T, Specht M et al (2009) H_2 rich product gas by steam gasification of biomass with in situ CO_2 absorption in a dual fluidized bed system of 8 MW fuel input. Fuel Process Technol 90(7–8):914–921. doi:10.1016/j.fuproc.2009.03.016
28. Marquard-Möllenstedt T, Sichler P, Specht M, Michel M, Berger R, Hein K et al (2004) New approach for biomass gasification to H_2. In: Proceedings of the second world conference and technology exhibition on biomass for energy, industry and climate protection, Rome, pp 10–14
29. Soukup G, Pfeifer C, Kreuzeder A, Hofbauer H (2009) In situ CO_2 capture in a dual fluidized bed biomass steam gasifier – bed material and fuel variation. Chem Eng Technol 32(3):348–354. doi:10.1002/ceat.200800559
30. Pfeifer C, Puchner B, Hofbauer H (2009) Comparison of dual fluidized bed steam gasification of biomass with and without selective transport of CO_2. Chem Eng Sci 64(23):5073–5083. doi:10.1016/j.ces.2009.08.014
31. IEA Hydrogen Implementing Agreement (2006) Prospects for hydrogen from biomass, Annex 16 Subtask B, Final report

Books and Reviews

Bienert K (2009) Commercial scale BTL production on the verge of becoming reality. Biomass gasification seminar, Stockholm, 22–23 Oct 2009

Crotogino F, Hamelmann R (2007) Wasserstoff-speicherung in Salzkavernen. In: Tagungsband "14. symposium zur nutzung regenerativer energiequellen und wasserstofftechnik", Stralsund

Droste-Franke B, Bert H, Kötter A et al (2009) Brennstoffzellen und virtuelle kraftwerke. In: Gethmann CF (ed) Ethics of science and technology assessment, vol 36. Springer, Berlin, pp 43–131. http://www.springerlink.com/content/vu43p4/

DWV (2005) Deutscher Wasserstoff- und Brennstoffzellen-Verband e.V.; Press Release No. 5/05: Wasserstoff Spiegel 5/2005

DWV (2007) Deutschland schließt wieder zur Weltspitze auf–aber die Konkurrenz schläft nicht. Deutscher Wasserstoff- und Brennstoffzellen-Verband e.V.; Press Release No. 1/07 (22 Feb 2007)

Erdle EK (2001) Grundlagen, stand und perspektiven der brennstoffzellen-technik. In: VDI-Gesellschaft Energietechnik (ed) Stationäre brennstoffzellenanlagen: markteinführung Tagungsband. VDI, Düsseldorf, pp 3–14

FNR (ed) (2006) Wasserstoff aus biomasse, vol 25. Gülzower Fachgespräche, Gülzow

Gao M, Krishnamurthy R (2009) Hydrogen transmission in pipelines and storage in pressurized and cryogenic tanks. In: Gupta RB (ed) Hydrogen fuel – production, transport and storage. CRC-Press, Boca Raton, pp 341–379

Hoogwijk M, Faaji A, van Den Broek R, Berndes G, Gielen D, Turkenburg W et al (2003) Exploration of the ranges of the global potential of biomass for energy. Biomass Bioenerg 25:119–133. doi:10.1016/S0961-9534(02)00191-5

Jorde F (2006) Laboruntersuchungen zur fermentativen erzeugung von Biowasserstoff in den testsystemen sensomat und ATS unter Einsatz von Rein- und Mischkulturen. Diploma Thesis at the Institute of WasteRessourceManagement, TUHH, unpublished

Jurschik E-M (2007) Optimierung diskontinuierlicher versuche zur fermentativen bio-wasserstoffproduktion, sowie aufbau und inbetriebnahme eines bio-methanreaktors. Diploma Thesis at the Institute of WasteRessourceManagement TUHH, unpublished

Maddy J, Cherryman S, Hawkes FR, Hawkes DL, Dinsdale RM, Guwy AJ, Premier GC, Cole S (2003) Hydrogen 2003. Report Number 1, ERDF part-funded project entitled "A sustainable energy supply for Wales: towards the hydrogen economy." University of Glamorgan, Pontypridd, Mid Glamorgan, Wales, ISBN 1-840540-90-7

Meyer M, Rechtenbach D, Stegmann R (2007) Biological production of H2 from organic raw and waste materials by fermentation with pure and mixed cultures. In: 15th European biomass conference, Berlin, 05 July–05 Nov 2007 (Proceedings CD)

Nandi R, Sengupta S (1998) Microbial production of hydrogen: an overview. Crit Rev Microbiol 24(1):61–84

Noike T, Takabatake H, Mizuno O, Ohba M (2002) Inhibition of hydrogen fermentation of organic wastes by lactic acid bacteria. Int J Hydrogen Energy 27:1367–1371

Pehnt M, Höpfner U (2009) Wasserstoff- und stoffspeicher in einem energiesystem mit hohen anteilen erneuerbarer energien: analyse der kurz- und mittelfristigen perspektiven. Kurzgutachten. IFEU -Institut für Energie und Umweltforschung, Heidelberg. http://www.bmu.de/files/pdfs/allgemein/application/pdf/ifeu_kurzstudie_elektromobilitaet_wasserstoff.pdf. Accessed 22 Feb 2010

Plath M (2006) Untersuchung und Optimierung der diskontinuierlichen erzeugung von biowasserstoff in dem testsystem ATS unter einsatz von klärschlamm und glukose. Project work at the Institute of WasteRessourceManagement, TUHH, unpublished

Rechtenbach D (2009) Fermentative erzeugung von biowasserstoff aus biogenen roh-und reststoffen. Hamburger Berichte 34, Abfallwirtschaft, T.U.Hamburg- Harburg, Germany, Verlag Abfall aktuell

Rechtenbach D, Meyer M, Stegmann R (2006) Fermentative production of bioH2 from organic raw and waste materials. In: Proceedings of the international conference ORBIT 2006 – biological waste management from local to global, 13–15 Sept 2006, Weimar; Kraft E, Bidlingmaier W, de Bertoldi M, Diaz LF, Barth J (Hrsg) Lombego systems & goldwiege. Visualle Projekte, Weimar, pp 869–877, ISBN 3-935974-09-4

Reiß T, Hüsing B (1993) Biologische wasserstoffgewinnung – forschungsperspektiven und technikfolgen. Verlag TÜV Rheinland, Köln. ISBN 3-8249-0150-1

Tanksale A, Beltramini JN, Lu GM (2010) A review of catalytic H_2 production processes from biomass. Renew Sustain Energy Rev 14(1):166–182. doi:10.1016/j.rser.2009.08.010

van Ginkel S, Sung S, Lay J-J (2001) BioH_2 as a function of pH and substrate concentration. Eviron Sci Technol 35:4726–4730

Zurawski D, Susanto AL, Stegmann R (2004a) Fermentative erzeugung von bio-wasserstoff aus biogenen roh- und reststoffen. In: Proceedings (CD-ROM) des 10. Internationalen kongresses für nachwachsende rohstoffe und pflanzenbiotechnologie NAROSSA, Magdeburg, 07–08 June 2004

Zurawski D, Susanto AL, Stegmann R (2004b) Sind bioabfälle und energiepflanzen zur biologischen wasserstofferzeugung geeignet? In: Fricke K, Kosak G, Wallmann R, Fischer J, Vogtmann H (eds) Schriftenreihe des ANS, 65. Informationsgesprächs des ANS e.V. "EEG und Emissionshandel – Neue Chancen für Biomassenutzung und Abfallwirtschaft", 06–07 Dec 2004, Braunschweig, pp 189–200. ISBN 3-935974-06-X

Zurawski D, Meyer M, Stegmann R (2005) Fermentative production of bioH_2 from biowaste using digested sewage sludge as inoculum. In: Cossu R, Stegmann R (eds) Proceedings of Sardinia 2005 – tenth international waste management and landfill symposium. CISA Environmental Sanitary Engineering Centre, Santa Margerita di Pula, Cagliari, 03–07 Oct 2005

Hydrothermal Systems, Geochemistry of

David Nieva, Rosa María Barragán,
Víctor Arellano
Instituto de Investigaciones Eléctricas, Cuernavac,
Morelos, Mexico

Article Outline

Glossary
Definition of the Subject
Introduction
Geothermometry
Geochemical Modeling of Hydrothermal Fluids
Future Directions
Bibliography

Glossary

Adiabatic process A process undergone by a system during which there is no heat exchange between the system and its surroundings.

Enthalpy Thermodynamic potential (akin to the internal energy) of a system that remains constant when the system undergoes an adiabatic process at constant pressure and composition.

Geothermal reservoir engineering Branch of engineering that applies scientific principles to the problems arising during the extraction of mass and heat from a geothermal resource.

Geothermal resource, Unless otherwise specified, in this article the meaning is restricted to a hydrothermal system selected for exploitation with the purpose of extracting usable heat.

Magma chamber Large accumulation of molten rock found beneath the surface of the Earth.

Definition of the Subject

In its most ample definition, geochemistry involves the study of the abundance, distribution, transformation, and transport of the elements, and their isotopes and compounds in the Earth and other planets. In this entry, this extremely ample subject is drastically reduced by two constraints. In the first instance, it is restricted to the discussion of hydrothermal systems, the only type of high-temperature geothermal resource that is exploitable with current conventional technology for the production of electricity and process heat. The second constraint consists of the pragmatic approach to the subject. Indeed, the entry refers to the interplay between science and technology, which has led to the development of techniques based on geochemical considerations that have proven useful for the characterization and exploitation of hydrothermal systems.

Early studies of hydrothermal systems were concerned with the underground flow of heat and water [1–4]. Soon afterward, the systematic study of geochemical features of these systems started [5–7]. Since then, geochemistry has accompanied the development of technology for the exploration and exploitation of geothermal resources. Geochemical techniques provide information on the structure and the distribution of temperature and other physicochemical parameters in a hydrothermal system. When combined with reservoir engineering considerations, geochemistry provides information on processes induced in the geothermal reservoir by the continuous extraction of mass and heat.

Introduction

A hydrothermal system is a volume of rock which is permeated by water or steam and heated to a temperature higher than normal for the particular depth. The source of heat is usually a magma chamber lying a few kilometers underneath; less frequently, the source of heat is a crustal site with an abnormally high concentration of radioisotopes, mainly potassium (^{40}K), thorium (^{232}Th), and uranium (^{235}U and ^{238}U). The origin of the fluid is meteoric, that is, rain water that infiltrates the ground to depths of up to a few kilometers, frequently mixed with fluids and solutes of magmatic origin. The essential features of a hydrothermal system are shown in Fig. 1, which is similar to an early sketch by White [8]. A third feature is the so-called cap rock, which is a layer of less permeable rock overlying the volume of permeated rock (i.e., the “reservoir”). The permeability and degree of fracturing of this cap rock varies from site to site and so do the intensity and the abundance of the surface manifestations of hydrothermal systems (boiling springs, steam vents, hot ponds, geysers).

M. Kaltschmitt et al. (eds.), *Renewable Energy Systems*, DOI 10.1007/978-1-4614-5820-3,
© Springer Science+Business Media New York 2013

Originally published in
Robert A. Meyers (ed.) Encyclopedia of Sustainability Science and Technology, © 2012, DOI 10.1007/978-1-4419-0851-3

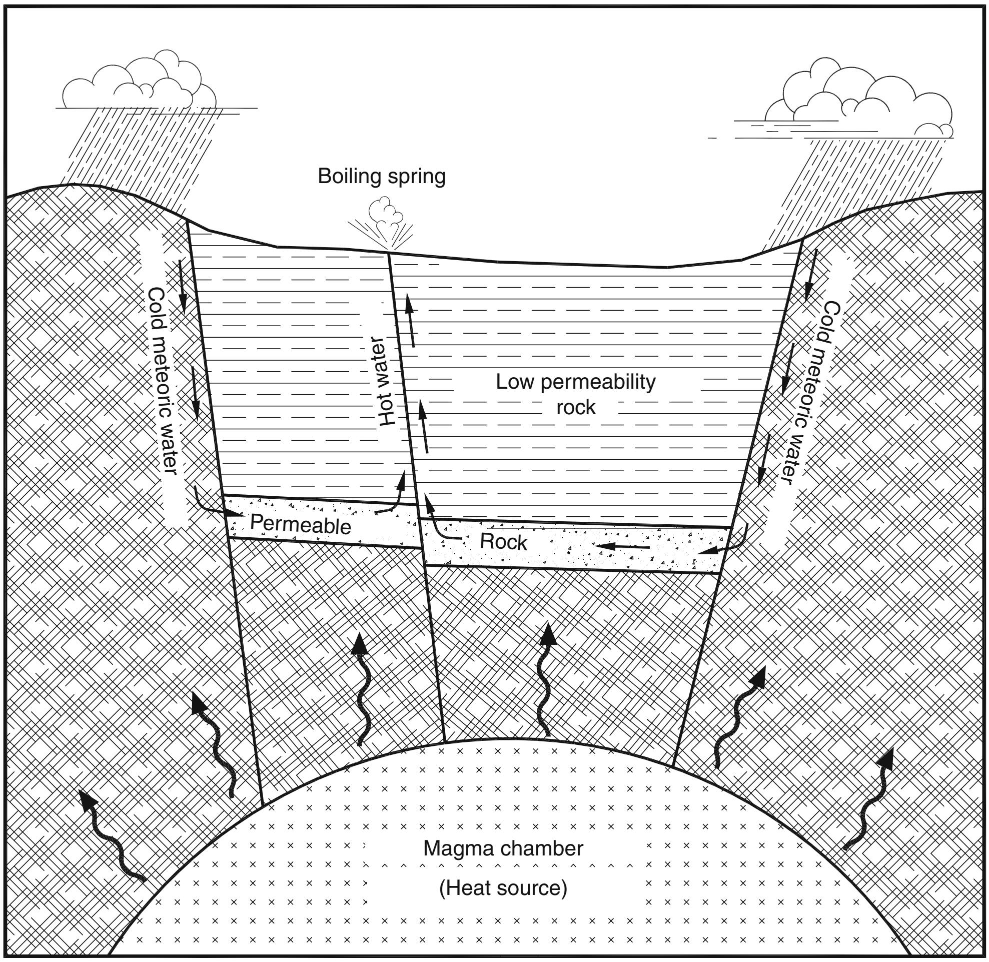

Hydrothermal Systems, Geochemistry of. Figure 1
Schematic model of a hydrothermal system

A more detailed model from a geochemical perspective is that shown in Fig. 2 [9]. Degassing of magma produces a fluid that, on the basis of the analysis of high-temperature gases released from basaltic [10] and andesitic magmas [11] is estimated to consist of water vapor with 20–40% by weight of CO_2, 5% of sulfur (SO_2/H_2S), and 1–2% HCl. As this fluid ascends, mixes with deeply circulating ground water and experiences a reduction in temperature, it forms a highly acidic fluid which interacts with the wall rock in a process called "primary neutralization." The result of this process is postulated to be a virtually complete cation leaching of the rock, forming close to neutral solutions with cation contents similar to the composition of the original rock, and with chloride and sulfate as the main anions. It is postulated further that magnesium and calcium are rapidly redeposited in the form of Mg- and Ca- rich minerals and sulfate is also deposited in the form of pyrite, alunite, or anhydrite. The result of this "primary neutralization" process is the production of the typical brine encountered in geothermal reservoirs, that is, a neutral or close to neutral aqueous solution with chloride as the main anion and sodium and potassium as the main cations. This brine, which contains much of the magmatic CO_2 and some of the sulfur as H_2S [9], may reach the surface mixed with varying proportions of meteoric water in natural hot springs or could be brought to the surface by man-made wells. The natural upward migration of this NaCl/KCl brine through the main upflow zone

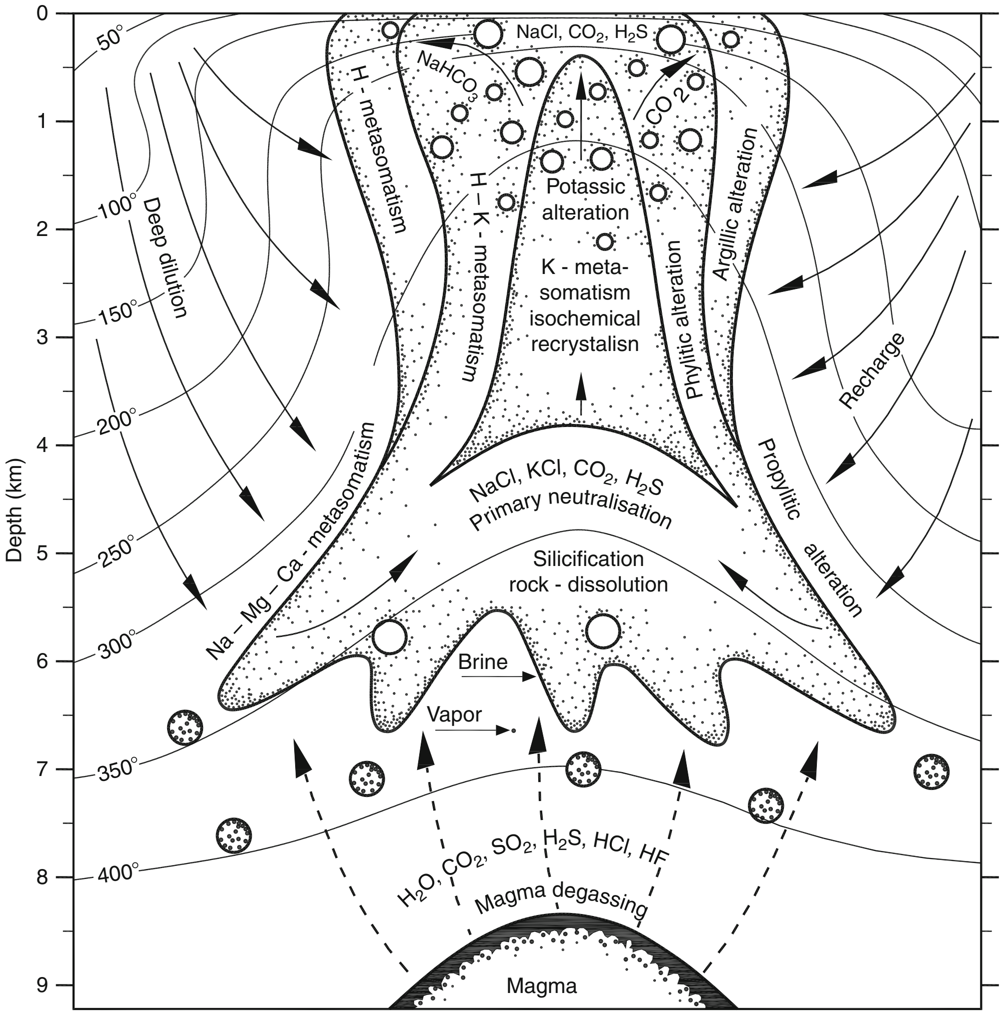

Hydrothermal Systems, Geochemistry of. Figure 2
Schematic cross section of a hydrothermal system with details of fluid genesis and fluid-rock interaction, as drawn by Giggenbach [9]

(i.e., the "geothermal reservoir") causes some characteristic alteration of the rock which leads to its enrichment in potassium (K-metasomatism).

In some hydrothermal systems, the deep, preneutralized liquid phase, finds its way to the surface, mixed with meteoric waters. The oxidation by atmospheric oxygen of the H_2S to produce H_2SO_4 gives rise to surface discharges with very low pH and high concentrations of chloride and sulfate ions; the cation composition of these waters may approach the composition of the original (dissolved) rock [12].

A third type of surface discharge originates from CO_2-rich steam separation from the rising brine, its interaction with the rock at shallower levels to produce calcite, and its mixture with oxygen-rich meteoric waters, which produce surface discharges with bicarbonate as the dominant ion, close to neutral pH, and varying concentrations of sulfate and chloride ions. The mineralogical consequences of this acid-induced alteration (H-metasomatism) of the rock are observable in the periphery of the main upflow zone.

A hydrothermal system is clearly not in equilibrium; there are thermal, mechanical, chemical, and nuclear processes that lead to conductive, convective, and radiative transport of energy, and to mass transport in and out of the system as well as between parts of the system (fluid flow, dissolution and precipitation of material, chemical reactions in liquid, gaseous, and solid phases). However, in certain stages of development, and certain parts of the system, where temperature and pressure vary only very slowly, fast chemical reactions adjust to the conditions prevailing at any given time and may be said to be at equilibrium. Many of the useful geochemical inferences that may be made on the prevailing physicochemical conditions in a hydrothermal system depend on these partial equilibrium states, which may be best referred to as *steady states*.

In the early stages of exploration of a hydrothermal system, when only evidence available from the surface is at hand, the aim of a geochemical survey is the generation of a model that would assess the temperature and chemical conditions of the fluid at depth. Naturally, the confidence that may be placed on this assessment increases with the ability of the model to accommodate as much of the available evidence as possible, and to explain the composition of all surface discharges [13–16].

Geothermometry

Perhaps the single most important hydrothermal reservoir parameter that could be estimated with geochemical techniques is the temperature. Indeed, there are algorithms, called geothermometers, which relate the geothermal reservoir temperature to mathematical expressions involving the concentrations of ionic and neutral species in the hydrothermal fluid. In this section, a general discussion of the bases and application of geothermometers is provided.

Cation Geothermometry

Geothermometers based on the ionic composition of hydrothermal fluids explicitly or implicitly refer to mineral–solution reactions of the following type:

$$\begin{aligned}&\text{Mineral assemblage 1} + a\text{A}^{w+} + b\text{B}^{x+}\\&\quad = \text{Mineral assemblage 2} + c\text{C}^{y+} + d\text{D}^{z+}\end{aligned} \tag{1}$$

where A, B, C, and D stand for cations in solution; a, b, c, and d are stoichiometric coefficients, and the charge conservation condition: $aw + bx = cy + dz$ is obeyed.

To a first approximation, the activities of minerals in contact with hydrothermal solutions may be taken as constant and equal to unity. Also, many hydrothermal aqueous solutions are only moderately concentrated, so the activity coefficients of ionic species in solution approach unity. With these simplifications, the equilibrium constant for reaction 1 is given by

$$Keq = \frac{[C^{y+}]^c [D^{z+}]^d}{[A^{w+}]^a [B^{x+}]^b} \tag{2}$$

where the quantities in brackets refer to molal concentrations.

The natural logarithm of the equilibrium constant is related to the reaction changes in standard enthalpy and entropy by the following expression:

$$\ln Keq = -\frac{\Delta \text{H}^0}{\text{RT}} + \frac{\Delta \text{S}^0}{\text{R}} \tag{3}$$

where ΔH^0 and ΔS^0 are the reaction change in standard molal enthalpy and entropy, respectively, T stands for the absolute temperature and R is the gas constant. For many reactions, ΔH^0 and ΔS^0 vary only slightly with temperature and pressure in the range of interest (25–300°C; 1–200 bar), so one would expect to find an approximately linear relationship between the logarithm of the equilibrium constant and the reciprocal of the absolute temperature.

The first indicator of this sort that was identified is the ratio of the concentrations of sodium and potassium ions in the hydrothermal fluid, as it was observed that the ratio K/Na increases with temperature [5, 6]. Mercado [17] generated a model of natural flow in the Cerro Prieto geothermal field (Mexico) based on this indicator.

Several relations of the type:

$$\ln \frac{[\text{K}^+]}{[\text{Na}^+]} = -\text{A}\left(\frac{1}{\text{T}}\right) + \text{B} \tag{4}$$

where A and B are constants, have been fitted to data on fluid chemical composition and measured underground temperature from geothermal wells, oil field brines, and natural hot springs [5, 18–24]. Those relations which were fitted to sufficiently ample data bases from geothermal wells and oil field brines [22–24] approach the expression that would be obtained for Eq. 3 from modern thermodynamic data [25] for the reaction:

$$\text{albite} + \text{K}^+ = \text{K} - \text{feldspar} + \text{Na}^+ \tag{5}$$

Fournier and Truesdell [19] developed a geothermometer based on two hypothetical mineral–solution reactions represented by the single expression:

$$\text{Mineral assemblage 1} + \mathrm{K}^+ = \text{Mineral assemblage 2} + (\beta/2)\mathrm{Ca}^{2+} + (1-\beta)\mathrm{Na}^+ \quad (6)$$

where β could take one of two possible values, namely, 1/3 and 4/3. Those authors proposed a graphical method to estimate reservoir temperatures in a plot of the type of Eq. 3 for the above reactions. An analytical expression for this geothermometer, provided by Fournier [26], is as follows:

$$\log_{10}\frac{(\mathrm{Na}^+)^{1-\beta}(\mathrm{Ca}^{2+})^{\frac{\beta}{2}}}{\mathrm{K}^+} = 1647\left(\frac{1}{T}\right) - 2.47 - 2.06\beta \quad (7)$$

where the parentheses on the left-hand term refer to concentrations in mg/kg. The procedure proposed by the authors is to apply Eq. 7, on a first trial, utilizing a value of 1/3 for the parameter β. In case the result obtained is a temperature greater than 100°C, one is to consider it the final value; otherwise, one should utilize the value of 4/3 for β. As pointed out by Giggenbach [9], the fact that a single value for the coefficient of (1/T) is utilized implies that β is to be considered a statistical weighing factor rather than a stoichiometric coefficient in reaction 6.

This Na–K–Ca geothermometer has been applied extensively in the exploration of hydrothermal resources. Several authors have identified systematic errors in its application which seem to be associated with high contents of CO_2 in the hydrothermal fluid [9, 27, 28], and a modified expression has been proposed [27]. In addition, Fournier and Potter [29] have proposed a correction term to be used when this geothermometer is applied to Mg-rich thermal waters.

Geothermometers based on the concentration of the four main cations (Na^+, K^+, Ca^{2+}, Mg^{2+}) have been developed. Nieva and Nieva [24] developed a procedure that leads to the utilization of one of four possible equations with a given sample, depending on its chemical characteristics. This geothermometer, called the Cationic Composition Geothermometer (CCG), is designed to ensure that the equation:

$$\log_{10}\frac{[\mathrm{K}^+]}{[\mathrm{Na}^+]} = -1178\left(\frac{1}{\mathrm{T}}\right) + 1.239 \quad (8)$$

similar to the expression developed by Fournier [22], is applied only to waters showing preliminary signs of having a high-temperature origin, thus adopting a conservative approach which avoids overestimation of temperatures at depth. Application of this geothermometer to a hot-spring NaCl/KCl brine with close to neutral pH is safe and the resulting estimated temperature should be considered a lower bound for the reservoir temperature. In Eq. 8 brackets indicate molal concentrations.

Giggenbach [9] also developed a procedure to estimate temperatures at depth based on the consideration of chemical equilibria involving the four main cations. This author concluded that the mineral assembly muscovite, clinochlore, silica, albite, and K-feldspar is at chemical equilibrium in the deep parts of the main upflow zone of the hydrothermal system according to the following reactions:

$$0.8\,\text{muscovite} + 0.2\,\text{clinochlore} + 5.4\,\text{silica} + 2\,\mathrm{Na}^+ = 2\,\text{albite} + 0.8\,\mathrm{K} - \text{feldspar} + 1.6\,\text{water} + \mathrm{Mg}^{2+} \quad (9)$$

and

$$0.8\,\text{muscovite} + 0.2\,\text{clinochlore} + 5.4\,\text{silica} + 2\,\mathrm{K}^+ = 2.8\,\mathrm{K} - \text{feldspar} + 1.6\,\text{water} + \mathrm{Mg}^{2+} \quad (10)$$

The above reaction system includes, of course, reaction 5. From these considerations, and taking as a reference modern thermodynamic data, Giggenbach [9] proposed the use of a K-Na geothermometer and a K-Mg geothermometer, as given respectively by the following expressions:

$$\log_{10}\frac{[\mathrm{K}^+]}{[\mathrm{Na}^+]} = -1390\left(\frac{1}{\mathrm{T}}\right) + 1.75 \quad (11)$$

and

$$\log_{10}\frac{[\mathrm{K}^+]^2}{[\mathrm{Mg}^{2+}]} = -4410\left(\frac{1}{\mathrm{T}}\right) + 14 \quad (12)$$

In Eqs. 11 and 12 concentrations are in mg/kg. Reaction 5 seems to re-equilibrate very slowly as the fluid ascends and encounters strata with lower temperatures. Thus, as mentioned above, K-Na geothermometers applied to waters from hot springs provide a reasonable lower bound for reservoir temperature at depth. On the other hand, the proportion of magnesium and potassium ions readjusts more rapidly and the application of Eq. 12 yields estimates of temperature in shallower parts of the hydrothermal system [9].

Just as in the case of the development of the CCG geothermometer [24], Giggenbach [9] faced the need to develop an indication, based on the concentration of Mg^{2+}, to determine if thermal water had been at equilibrium at depth. This author proposed the use of the triangular diagram shown in Fig. 3, based on the parameters $Na^+/1,000$, $K^+/100$, $(Mg^{2+})^{1/2}$. In this diagram, data points of waters such as those produced by geothermal wells, which have a cationic composition compatible with chemical equilibrium of reactions 9 and 10, fall on the “fully equilibrated waters” curve. In contrast, data points of water with composition compatible with full dissolution of crustal rocks fall in the lower right-hand corner. The region in the diagram belonging to “partially-equilibrated waters” is bounded on the top by the “fully equilibrated waters” curve and on the bottom by a rather arbitrary curve. This lower curve is drawn by plotting data as for the “fully equilibrated waters” but first dividing the concentration of sodium by 4.57. Giggenbach [9] recommends the use of the K-Mg geothermometer for samples that fall in the partially-equilibrated waters area of the diagram, but to exercise caution when they fall near the lower curve.

Table 1 illustrates the application of the CCG [24] and the Na-K-Mg [9] geothermometers, as applied to

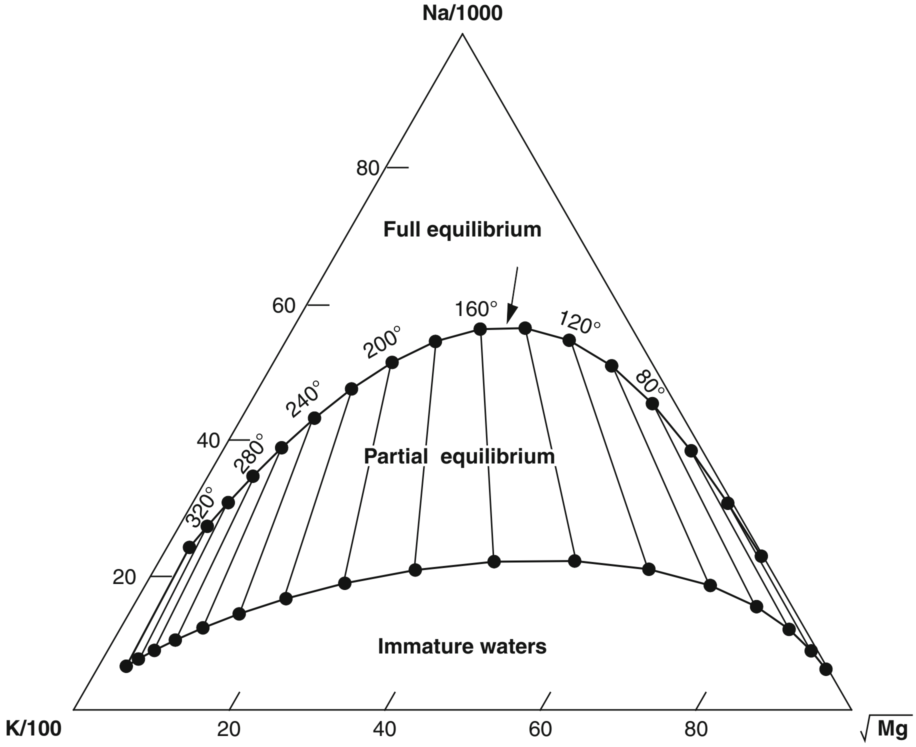

Hydrothermal Systems, Geochemistry of. Figure 3

Triangular diagram for estimation of equilibrium reservoir temperatures by simultaneous application of geothermometric expressions from Eqs. 11 and 12. The “full equilibrium” curve represents the loci of intersections of isotherms drawn by use of Eqs. 11 and 12. Dot-joining lines are isotherms drawn by use of Eq. 12. Figure constructed with information provided by Giggenbach [9]

Hydrothermal Systems, Geochemistry of. Table 1 Application of the CCG [24] and the Na-K-Mg [9] geothermometers to geothermal wells and associated hot springs. Concentrations are in mg/kg and temperatures are in Celsius. Data is from [9]

Origin	Reservoir Temperature	pH	Na	K	Mg	Ca	t CCG	t K-Na	t K-Mg
Geoth. well NG-9, Ngawha, New Zealand	230	7.7	893	79	0.110	3	194	223	204
Jubilee pool, New Zealand	230	7.2	842	72	1.600	9	191	220	147
Geoth. well WK66, Wairakei, New Zealand	240	8.5	995	142	0.040	17	236	262	258
Champagne Pool, New Zealand	240	8.0	1,070	102	0.400	26	200	229	187
Geoth. well BR-11, Broadlands, New Zealand	260	7.4	675	130	0.011	1	266	291	291
Ohaki Pool, New Zealand	260	7.1	860	82	0.100	3	200	229	208
Geoth. well 10, Miravalles, Costa Rica	250	7.8	1,750	216	0.110	59	222	250	254
Sal. Bagaces, Costa Rica	250	8.6	2,063	85	6.600	33	140	170	129
Geoth. well ZQ-3, Zunil, Guatemala	295	8.1	933	231	0.012	15	294	317	327
Zunil Spring	295	7.0	384	32	39	17	189	218	77
Geoth. well from Cerro Prieto, Mexico	280	7.3	5,600	1,260	0.270	333	283	307	337
Spring N29, Cerro Prieto, Mexico	280	7.6	5,120	664	4.600	357	227	254	216
Geoth. well from Tongonan, Philippines	330	7.0	3,580	1,090	0.200	128	320	340	337
Banati Spring, Philippines	330	8.3	1,990	210	0.400	86	208	237	219
Salton Sea well, USA	330	5.2	38,400	13,400	10	22,010	338	357	381
Seawater	4	7.8	10,760	390	1,290	410	132	162	97

samples from geothermal wells and hot springs from a number of hydrothermal systems. For most wells, the CCG yields temperatures quite close to the measured values. When applied to hot springs, the CCG yields temperatures that, in the context of a survey of a geothermal area, could be safely taken as a lower bound for the reservoir temperature. The Na-K-Mg geothermometer yields temperatures close to the measured value but in some cases, it overestimates the temperature of the reservoir. For this reason, some authors [30, 31] prefer to construct the triangular diagram of Giggenbach [9] using Eq. 8 of the CCG instead of Eq. 11 of the Na-K-Mg geothermometer. Cationic geothermometers fail when applied to ocean water, yielding high-temperature values possibly reflecting the interaction of ocean water with basaltic rock in mid-ocean ridges [9]. In cases of hydrothermal systems with an important intrusion of ocean water, care must be taken in the application of cationic geothermometers; their application should be limited to brines produced by deep wells which presumably have been subject to interaction with reservoir rocks at high temperatures for long periods of time.

Most cation geothermometers involve only the major cations (Na^+, K^+, Mg^{2+}, Ca^{2+}) but some are based on lithium equilibrium between the aqueous solution and some mineral assembly [32, 33]. Lithium–magnesium geothermometers yield values close to the measure reservoir temperature when applied to water produced by geothermal and oil wells; however, when applied to hot spring water, the calculated temperatures are frequently too low, presumably due to the re-equilibration at lower temperatures of reactions involving magnesium [26].

Silica Geothermometry

The concentration of silica in hydrothermal fluids is determined by the solubility of quartz [34]. The fact that the solubility of quartz shows strong temperature dependence [34–36] provides the basis for the silica geothermometer [37, 38], which has been applied extensively for the exploration of geothermal resources.

Two basic assumptions underlie the application of the silica geothermometer. The first assumption is that the solubility of quartz in moderately saline hydrothermal fluids is similar enough to its solubility in pure water, so that the latter could be taken as reference. This assumption is quite plausible as long as the salinity is below 2% by weight and temperatures are below 300°C, which is the case for many hydrothermal systems; a correction must be made when salinity or temperature are higher [26].

The second assumption is that the hydrothermal fluid does not gain or lose silica after it has reached equilibrium with quartz in the reservoir. This assumption does not hold in cases when the hydrothermal fluid undergoes a relatively slow rise to the surface. This is the reason why the silica geothermometer applied to hot spring waters does not yield temperatures higher than about 230°C; the reactions of quartz dissolution or precipitation are very fast above this temperature [39, 40]. However, when applied to hydrothermal fluids produced by lined wells that deliver the fluid to the surface much more rapidly and without interaction with the rock, the silica geothermometer is quite useful to estimate the reservoir temperature.

In addition to the above assumptions, when applying the silica geothermometer to hot spring waters, one must make some conjecture as to the processes affecting the sample on its way to the surface. When reaching the point of discharge, the hydrothermal liquid must have reduced its temperature to some value at or below the boiling point. There are basically three mechanisms by which this may be accomplished: mixing with colder waters, loss of heat to the rock by conduction, and adiabatic separation of steam; in most cases, at least two of these mechanisms intervene. When modeling these processes, it is much more convenient to deal with enthalpy (i.e., heat content) rather than temperature because the former is a conservative quantity. Thus, when the hydrothermal liquid loses heat to the rock by conduction, the heat transferred is subtracted from the enthalpy of the liquid. When the hydrothermal liquid mixes with a colder water, the enthalpy (and silica) content of the mixture is simply the sum of the quantities contributed by each of the mixing components. Likewise, when a hydrothermal fluid undergoes adiabatic steam separation at a given temperature, the enthalpy distributes itself between the resulting liquid and steam phases according to the specific enthalpy (i.e., the heat content per unit mass) of each phase:

$$H_{hf} = (1-f)\bar{H}_{t,l} + f\bar{H}_{t,s} \tag{13}$$

where f is the mass fraction of steam, H_{hf} stands for the specific enthalpy of the hydrothermal liquid before undergoing steam separation, and $\bar{H}_{t,l}$ and $\bar{H}_{t,s}$ refer to the specific enthalpies at temperature t of saturated liquid and steam, respectively. Specific enthalpies of saturated steam and liquid are usually taken as those for pure H_2O and could be obtained from steam tables. The silica content of the hydrothermal liquid also distributes itself between the separated phases:

$$[\mathrm{SiO_2}]_{hf} = (1-f)[\mathrm{SiO_2}]_l + f[\mathrm{SiO_2}]_s \tag{14}$$

When the steam separation occurs at temperatures of 260°C or less, the silica concentration in the separated steam could be approximated safely as zero.

These processes could be modeled graphically in a Cartesian plot of silica concentration vs. enthalpy. Fournier and Potter [37] provide a plot of the equilibrium silica concentration in H_2O at the vapor pressure of the solution, as a function of enthalpy, covering the range of liquid water at 20°C to temperatures close to the critical point; Fig. 4, which reproduces a portion of that plot, was constructed with information provided in the cited reference. In such a plot, a point representing the hydrothermal liquid would fall on the quartz solubility curve. A point representing the mixture of the hydrothermal liquid with a cold water component would fall on the tie line joining the points which represent the two mixing components. In order to represent a process of adiabatic steam separation, one would locate the point representing the separated steam, with zero silica concentration and the specific enthalpy of the steam; then one would draw a line joining this point with the point representing the original hydrothermal liquid; by extending this line to the value of the specific enthalpy of the separated (saturated) liquid, one would find the resulting silica concentration and thus the position of the point representing this liquid. As an example, the following process is depicted graphically in Fig. 4: A hydrothermal liquid at 240°C undergoes adiabatic cooling by expansion with single-stage steam separation at 120°C. The separated liquid then mixes (w/w) with 60% meteoric water at 15°C, containing 5 mg/kg of silica, giving rise to a thermal water at about 57°C and a silica concentration of about 224 mg/kg.

As mentioned above, in spite of the potential complexity of the processes affecting the silica content of hot spring fluids the silica geothermometer has been applied extensively for the exploration of geothermal resources. When applied to hydrothermal liquid produced by geothermal wells, the situation is particularly simple. The liquid is brought to the surface rapidly, with negligible loss of heat to the walls and without mixing with other fluids; the only mechanism that intervenes is the adiabatic separation of steam. For these reasons, the silica geothermometer applied to well fluids is a powerful tool for the estimation of the reservoir temperature.

Gas Geothermometry

Reactions that involve gaseous substances that are present and measurable in the hydrothermal fluid may provide the basis for gas geothermometers. These reactions may or may not involve solid (mineral) phases. Examples of reactions which take place in the hydrothermal fluid and do not involve a mineral phase are the so-called Fischer–Tropsch reaction:

$$CH_4 + 2H_2O = CO_2 + 4H_2 \tag{15}$$

and the conversion of nitrogen to ammonia:

$$2NH_3 = N_2 + 3H_2 \tag{16}$$

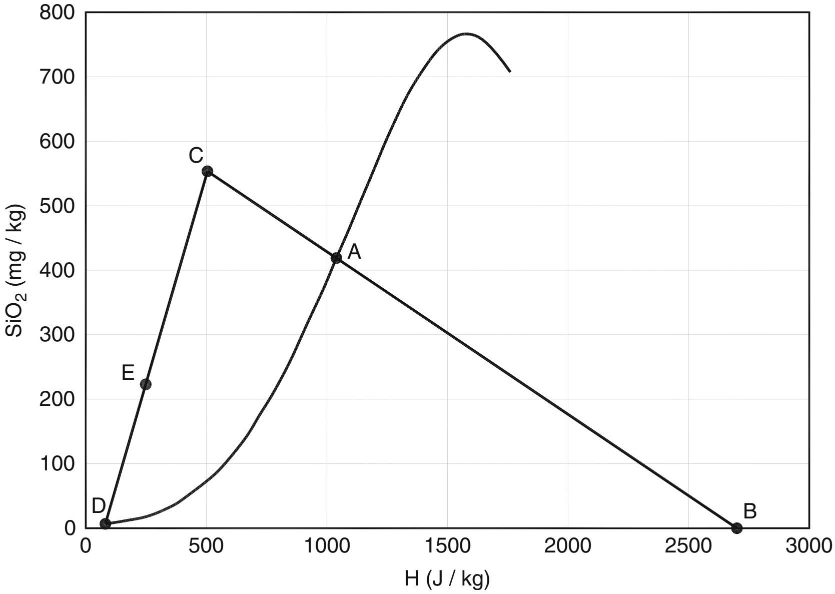

Hydrothermal Systems, Geochemistry of. Figure 4
Graph of equilibrium silica concentration in H2O at the vapor pressure of the solution vs. specific enthalpy. A process of adiabatic cooling of a hydrothermal liquid (point A), followed by mixing with a local meteoric water component (point D), is depicted graphically (see main text). Points (A, B, C, D, E) and compositions (specific enthalpy in J/kg, dissolved silica in mg/kg) are as follows: Original hydrothermal liquid: A (1,037, 418); steam separated adiabatically at 120°C: B (2,706, 0); liquid separated adiabatically at 120°C: C (503.7, 552); cold meteoric water: D (62.99, 5); resulting thermal water: E (239.3, 224)

An example of a gas reaction which involves mineral phases is the oxidation of pyrite to produce magnetite:

$$3FeS_2 + 2H_2 + 4H_2O = Fe_3O_4 + 6H_2S \quad (17)$$

The collection and handling of samples for the analysis of gaseous species in hydrothermal fluids is, in general, more complicated than is the case for species completely dissolved in the liquid phase [41]. Furthermore, the relative proportions of the gaseous species sampled in the hydrothermal fluid may have been altered by a number of untraceable processes that affect the fluid on its transit from the reservoir to the surface. All these circumstances introduce uncertainty in the interpretation of these analyses, as will be discussed below.

The equilibrium proportions of chemical species that participate in a reaction at a given temperature in, say, the steam phase, are known from thermochemical data. It is safe usually to assume that there exists phase equilibrium between liquid and steam phases, so from the knowledge of liquid–steam partition coefficients, one may know also the equilibrium proportions of species in the liquid phase.

The most favorable situation for the interpretation of the gaseous composition of the hydrothermal fluid is one in which the undisturbed liquid phase is sampled directly from the reservoir. This situation is approximated closely when one knows that a geothermal well is fed only by liquid phase. In such situation, one may determine the temperature of equilibration of the chemical reaction (i.e., the reservoir temperature) from the analyses of the fluid and the temperature dependence of the equilibrium constant (Eq. 3).

In most cases, however, a geothermal well receives a mixture of liquid and steam phases from the reservoir. This leads to a situation that is considerably more complex [42] because the mobilities of liquid and steam phases in the porous medium are different; thus, the proportions of liquid and steam phases reaching the well will be somewhat different than the proportions in the undisturbed reservoir. In spite of these drawbacks, in these situations the gas composition of the produced fluid is utilized to estimate the fractions of reservoir steam and liquid that make up the mixture feeding the well [43–45]. The fraction of reservoir steam that results from these calculations, which is referred to as the *reservoir steam fraction* and frequently represented by the letter y, approximate as it may be, is a useful reservoir parameter, particularly when employed to detect variations in the conditions of the reservoir resulting from exploitation.

The reservoir temperature, which is a necessary piece of information for the calculations described in the last paragraph, is measured directly, or estimated by the use of other geothermometers. D'Amore and Truesdell [46] developed a graphical method to calculate *both* the reservoir temperature and the reservoir steam fraction by considering simultaneous equilibrium in two reactions in the gas phase.

Some of the reactions that serve as a basis for the calculation of the reservoir steam fraction, namely, the Fischer–Tropsch reaction (Eq. 15) and the conversion of nitrogen to ammonia (Eq. 16), have been reported NOT to be at equilibrium in hydrothermal systems with reservoir temperatures below 250°C [47, 48], so these calculations must be interpreted with caution for such systems.

If the interpretation of the gas composition of fluids produced by geothermal wells is complicated, the case of natural steam vents is even more so. Indeed, there are several processes that may occur during the rise of the hydrothermal fluid to the surface that may affect its composition. For example, the hydrothermal fluid may lose steam at different stages (and different pressures and temperatures) during its rise; the rising steam–liquid mixture may suffer partial condensation at different stages; also, partial re-equilibration of chemical reactions may occur in transit to the surface. Nevertheless, Arnorsson and Gunnlaugsson [47] developed a number of geothermometers based on the concentration of gaseous species, and applied them to steam vents in Icelandic geothermal fields. For some of these sites, the calculated temperatures compare surprisingly well with temperatures measured in nearby wells, but this may be due to particularly favorable hydrological conditions.

Giggenbach [49] proposes a geothermometer based on the ratio of molar concentrations of argon and hydrogen in the hydrothermal fluid, which is designed to be relatively insensitive to processes of steam separation or partial condensation occurring as the hydrothermal fluid ascends toward the natural steam vents. Since both argon and hydrogen are very insoluble in water, and would separate almost quantitatively from the liquid phase upon separation of even a small mass fraction of steam, they are likely to keep their relative proportions unchanged during the rise of the hydrothermal steam to the surface. This geothermometer is based on the following main assumptions. (a) In liquid-dominated systems, the chemical equilibration of species, including volatile components, occurs in the liquid phase. (b) The redox conditions in a fully equilibrated hydrothermal system are quite invariant and keep the ratio of the fugacities of hydrogen to water at a value of approximately $10^{-2.8}$ at temperatures up to 1,200°C. (c) The argon concentration in the reservoir liquid corresponds to that of air-saturated groundwater. With these assumptions, Giggenbach [49] arrives to the expression:

$$t(^{o}C) = 71\left(\log_{10}\frac{X_{H2}}{X_{Ar}} + 2.5\right) \tag{18}$$

where X_i stands for the molar fraction of species i in the sampled fluid. This geothermometer was tested with appreciable success in samples from New Zealand and elsewhere. One serious drawback with this geothermometer is the fact that even the smallest contamination of the sample with air may lead to very erroneous results. Another problem is the possibility that, during its rise to the surface, the fluid may have lost argon and hydrogen by steam separation, followed by recuperation of hydrogen via chemical re-equilibration, thus leading to an erroneous high ratio of hydrogen to argon, and thus to an overestimation of the reservoir temperature.

It is fair to say that for the exploration of a geothermal site, gas geothermometers should be interpreted with extreme care, and only in conjunction with other techniques such as the cationic or silica geothermometers. This may not be possible in sites where most or all the surface manifestations consist of steam vents and steam-heated waters, in which case the gas geothermometer results should be taken as a rough reference.

Solid Solution Geothermometry

Some minerals tend to form solid solutions through substitution of ions at specific sites in the crystal structure, or by inclusion of ions at interstitial spaces. These ion substitutions or inclusions do not change the crystal structure except for rather minor dimensional distortions. The extent of ion replacement depends on various physical and chemical factors, such as the composition of the surrounding medium, the temperature, and the pressure. In principle, this property of minerals offers the opportunity to identify solid-solution geothermometers when the dominating factor that controls the composition of the solid solution is the temperature.

When drilling a geothermal well in a new area, where there are no nearby wells that provide an indication of the temperature vs. depth profile, a relatively accurate temperature estimation that one could obtain, say from the study of drill cuttings, would be extremely useful. This is so because the information would help decide when to stop drilling and complete construction of the well. At present, engineers need to run costly and time-consuming temperature logs in order to obtain this information. This is an important motivation to develop solid-solution geothermometers.

A geothermometer based on the composition of chlorites has been developed [50–52]. Indeed, linear correlations have been observed of increasing crystallization temperature with increasing aluminum substitution for silicon in the tetrahedral site and with decreasing octahedral site vacancy. In spite of the successful substitution of the original automatic electron microprobe technique with the use of X-Ray Diffractometry [53], the process of sample isolation, analysis, and interpretation is much too complex and time consuming for this geothermometer to be useful in the context described in the preceding paragraph. Nevertheless the geothermometer has been quite useful for the determination of paleotemperatures in a variety of studies.

Geochemical Modeling of Hydrothermal Fluids

In the exploratory stage of development of a hydrothermal resource, the main purpose of geochemical modeling is to determine the temperature and composition of the reservoir fluid, based on the available evidence from surface discharges. This is done by tracing back the processes occurring during the rise to the surface of the hydrothermal fluid. As mentioned above, the reliability of the resulting model will depend on its ability to account for all available evidence, that is, its ability to explain through simple but reasonable processes the origin of all surface discharges, as originating from deep reservoir fluids.

Our ability to model the rise of the hydrothermal fluid depends on our knowledge of the behavior of certain elements and compounds, generally called tracers, upon occurrence of processes of steam–liquid separation and mixing of different fluids.

Stable Isotopes of Hydrogen and Oxygen

Two of those tracers are the stable isotopes of hydrogen and oxygen, deuterium (^2H) and oxygen-18, present in natural waters. Indeed, the species $H_2{}^{18}O$ is present in ocean water in concentrations of the order of 2,000 parts per million. Also, the species HDO, where D stands for deuterium, is present in concentrations of the order of 300 parts per million.

The hydrogen and oxygen isotopic composition of water is measured with a mass spectrometer that determines the ratio of the rare to the common isotopic species (i.e., the ratios HDO/H_2O and $H_2{}^{18}O/H_2O$). Rather than expressing these ratios in absolute terms, they are conveniently expressed in the delta notation (δ) as a per thousand (‰) difference with respect to a water standard. Thus, the sample's deuterium composition, δD, is calculated as follows:

$$\delta D = \frac{R_{\text{sample}} - R_{\text{standard}}}{R_{\text{standard}}} \times 1000 \tag{19}$$

where R stands for the ratio HDO/H_2O. The oxygen-18 composition, $\delta^{18}O$, is calculated in a similar manner.

The standard that has been adopted almost universally is Standard Mean Ocean Water (SMOW), a water sample with oxygen and hydrogen isotope ratios close to the mean isotope ratios of ocean water [54].

When water separates in two phases (by condensation of steam or evaporation of liquid water), its isotopic composition undergoes *fractionation*, that is, the isotopic composition of the resulting phases is different than the isotopic composition of the original phase. At atmospheric temperatures, the resulting liquid phase will be enriched in the heavy isotopes, deuterium and ^{18}O, and the resulting steam phase will be depleted of them.

As part of the hydrological cycle, water from the ocean continuously evaporates. As the resulting mass of water vapor moves into the continental area, it condensates and looses part of its mass as precipitation (rain). In every precipitation event, the remaining atmospheric steam is depleted further of the heavy isotopes. The process continues as the mass of atmospheric steam moves further into the continental area, giving rise to a distribution of isotopic composition of surface waters, also referred to as "meteoric" waters. This isotopic composition of meteoric water may be seen as a natural label. It was first pointed out by Craig [55] that the isotopic compositions of meteoric waters, which had not undergone appreciable evaporation, were such that the deuterium and oxygen-18 concentrations were linearly related by the following expression:

$$\delta \mathrm{D} = 8\delta^{18}\mathrm{O} + 10 \tag{20}$$

After Craig's original observation and with more data, Taylor [56] observed a better fit to the expression:

$$\delta \mathrm{D} = 8\delta^{18}\mathrm{O} + 5 \tag{21}$$

This linear expression is known as the Global Meteoric Water Line (GMWL), and serves as a frame of reference not only for the composition of "fresh" meteoric waters, but also for the isotopic composition of surface waters that have undergone other processes, such as evaporation or isotope exchange with rocks.

There are some natural processes that may alter the isotopic composition of meteoric waters accumulated in the surface or infiltrated in the ground. One of these processes is evaporation. The isotopic composition of a series of surface waters that have originated from the same meteoric water, but which have undergone evaporation to different degrees, would deviate from the GMWL usually along a line of the form

$$\delta \mathrm{D} = y\delta^{18}\mathrm{O} + x \tag{22}$$

where the slope y would have a value between 4 and 6. The residual waters after evaporation would have higher concentrations of the heavy isotopes and therefore would deviate "to the right" of the GMWL in a δD vs. $\delta^{18}O$ Cartesian plot (see Fig. 5).

Craig [57] observed that thermal waters had a deuterium concentration similar to that of local meteoric waters, but had larger concentrations of oxygen-18, a phenomenon that has been termed the "^{18}O shift." This was ascribed to isotope exchange between water and rock, in such a manner that the comparatively small degree of hydrogen exchange leaves the deuterium content of the water virtually unchanged, but its oxygen-18 content is substantially increased. These observations led to the concept that the main component of thermal waters is, by far, meteoric water that has infiltrated the ground to great depth.

Craig made his observations on what was at the time a comprehensive set of data from known thermal sites. However, as data from more thermal areas has accumulated, it has provided grounds to postulate the existence of a deep water component from partial magmatic origin, called "andesitic water," which in hydrothermal systems found in convective plate boundaries mixes with local meteoric water to form the reservoir fluid tapped by geothermal wells [58, 59] (See Fig. 5). According to this alternative proposition, most of the isotopic exchange with the rock occurs at depths greater than those which are normally reached by drilling, presumably in the site where the "primary neutralization" of magma fluids occurs (see "Introduction"), and the result of this neutralization is the formation of andesitic water. At the very high temperatures at which this process occurs (close to magma temperatures), it is expected that the proportion of deuterium (and of oxygen-18) in the andesitic water be completely determined by the isotopic composition of the rock or magma phases. It has been suggested that this composition should fall in the ranges of +5‰ to +10‰ for δ^{18}O and −30‰ to −10‰ for δD [59–61]. It is further postulated that part of this andesitic water would ascend and mix with more meteoric water to form the hydrothermal or reservoir fluid which is reached by drilling in geothermal fields.

As explained in section on "Introduction," in the natural state of a hydrothermal system, the reservoir fluid ascends to the surface through a variety of processes and gives rise to thermal springs, steam vents, and other features typical of thermal areas. In the absence of drilled wells, these are the only sources of information on the chemical and isotopic characteristics of the reservoir fluid. It is the task of geochemistry to infer the temperature and

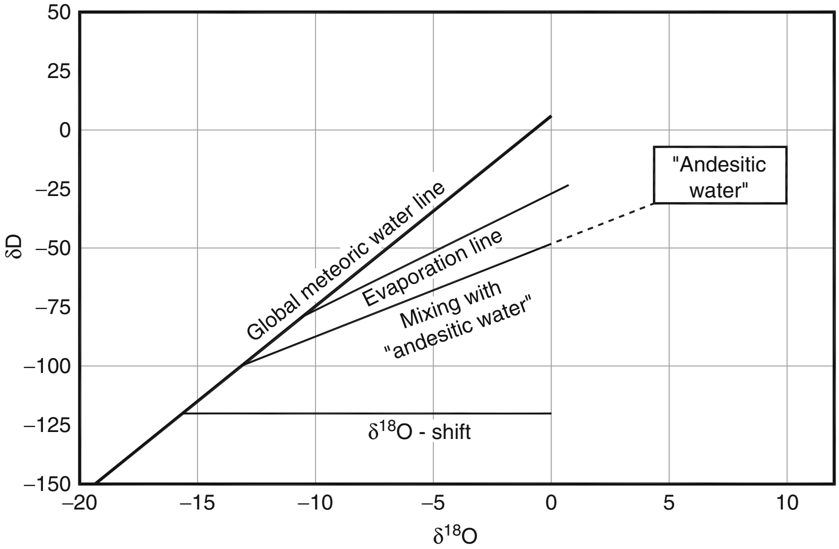

Hydrothermal Systems, Geochemistry of. Figure 5
δD vs. δ^{18}O diagram showing the position of meteoric waters (Global Meteoric Water Line) and the positions of meteoric waters subjected to evaporation, oxygen-exchange with the rock, and mixing with a deep magmatic component (andesitic water)

composition of the reservoir fluid from the available evidence.

As explained in relation to the application of the silica geothermometer (Section on "Silica Geothermometer"), with the consideration of parameters that are conserved in the fluid (silica, enthalpy, chloride ion), it is possible to model the processes affecting the rising fluid on its transit to the surface. Under the reasonable hypothesis that no further isotopic exchange occurs between the fluid and the rock during this transit, the deuterium and oxygen-18 contents of the fluid constitute two more conservative parameters.

When liquid water boils, the resulting liquid and steam phases will in general not have identical isotopic compositions. The parameter that describes the equilibrium distribution of isotopes between the two resulting phases (i.e., the isotopic *fractionation*) is the fractionation factor, α. For a given isotope, the fractionation factor is given by:

$$\alpha = \frac{R_{\text{liquid}}}{R_{\text{steam}}} \tag{23}$$

where R stands for the ratio HDO/H_2O in the case of deuterium, and for the ratio $H_2{}^{18}O/H_2O$ in the case of oxygen-18. For these two isotopes, Truesdell et al. [14] have given a compendium of values of α at temperatures from 0°C to 374°C. The fractionation factor is related to the isotopic compositions of the resulting liquid and steam phases by the following expression:

$$\alpha = \frac{1000 + \delta_{\text{liquid}}}{1000 + \delta_{\text{steam}}} \tag{24}$$

On its rise to the surface, the reservoir liquid may cool by adiabatic boiling, with the steam and liquid remaining in physical contact (and isotopic equilibrium) until the two phases are physically separated at a given temperature. This process shall be called *single-step adiabatic steam separation*. The term adiabatic means that no heat is transferred from or to any surrounding solid (rock) phases. The conservation of enthalpy demands that the mass fraction, y, of generated steam be given by:

$$y = \frac{H_{\text{ol}} - H_{\text{sl}}}{H_{\text{ss}} - H_{\text{sl}}} \tag{25}$$

where H_{ol} represents the specific enthalpy of the original liquid, and H_{sl} and H_{ss} represent the specific enthalpy of liquid water and steam at the separation temperature, respectively.

The conservation of mass for deuterium (or oxygen-18) leads to the following expressions relating the isotopic compositions of the original liquid and the resulting liquid and steam phases:

$$\delta_{\text{ol}} + 1000 = (\alpha + y(1 - \alpha))(\delta_{\text{ss}} + 1000) \tag{26}$$

and

$$\delta_{\text{sl}} + 1000 = \alpha(\delta_{\text{ss}} + 1000) \tag{27}$$

where α represents the value of the fractionation factor at the temperature of separation.

In a real situation, the ascending fluid may suffer more than one event of steam–liquid separation at decreasing temperatures. In fact, one could conceive of a process in which the generated steam separates immediately and continuously from the remaining liquid as soon as it is formed. This process shall be termed *continuous adiabatic steam separation* and, together with the *single-step adiabatic steam separation* described above, constitute the two extreme possible mechanisms of adiabatic boiling of the reservoir fluid on its way to the surface. Both mechanisms lead to an increase in deuterium and oxygen-18 contents of the boiling liquid, but the extent of enrichment is different from one case to the other. An intermediate mechanism that may be called *multiple-stage steam separation* leads, correspondingly, to intermediate enrichments.

The rising reservoir fluid may cool by adiabatic boiling or by mixing with cooler meteoric waters. It may also boil and then mix with meteoric waters, or mix first and then boil, depending on the particular hydrological situation. Truesdell et al. [14] were able to explain the variety of isotopic and chemical compositions of thermal spring waters in Yellowstone National Park, United States, as resulting from a single reservoir liquid at 360°C and particular deuterium and chloride ion contents.

Other Useful Tracers

Other useful tracers are atomic, molecular, or ionic species that exhibit very low chemical reactivity under the conditions prevailing in geothermal reservoirs and upper strata of hydrothermal systems. Some of these tracers partition very favorably (almost exclusively) in the liquid phase, such as chloride ion; some partition very favorably in the steam phase, such as the noble gases, and some distribute themselves in the two phases, but in a manner that can be calculated quantitatively from known partition coefficients (such as the cases of deuterium and oxygen-18). The particular case of silica was discussed in section on "Silica Geothermometer."

When a relatively high flow of the hydrothermal fluid has passed through some natural conduit to the surface, or through a geothermal well, for a sufficiently long time, the radial distribution of temperature around that conduit or well has reached a steady state. Under these conditions, the transfer of heat between the fluid and the rock could be considered negligible, and the enthalpy of the fluid remains constant (see the appendix of reference [14], for a quantitative discussion on this subject). Under these circumstances the enthalpy is another useful "tracer," or conserved parameter, that could be quite useful in modeling the processes affecting the fluid on its rise to the surface [62]. In preceding paragraphs, when referring to adiabatic processes, we have implicitly assumed conditions that support the conservation of the enthalpy of the fluid.

The combined use of tracers and conserved parameters has made possible the determination of conditions at depth in hydrothermal systems [13–16, 63].

Future Directions

There are, of course, many scientific questions remaining to be answered regarding the geochemistry of hydrothermal systems, among them the details of the contribution of magmatic fluids to the formation of the hydrothermal brine. From a technological perspective, however, one would expect more future activity in the interplay between geochemistry and reservoir engineering in studies regarding the sustainability of hydrothermal systems under exploitation.

The next type of geothermal resources to be exploited for electric power generation on a large scale will probably be the so-called Enhanced (or Engineered) Geothermal Systems (EGS). These consist of volumes of hot, impermeable rock, located at reachable depths, which contain substantial amounts of heat. Their development as an exploitable reservoir consists of creating a network of fractures, so as to allow the injection of a working fluid (water) at some point and its extraction through wells located at other points, in such a way that the working fluid extracts the heat from the rock. Important practical issues will arise as a result of the interaction of the working fluid with the rock, which will lead to the dissolution of some minerals and the formation of others, with concomitant changes in porosity and permeability. Geochemistry is expected to play an important role in dealing with these issues.

Bibliography

Primary Literature

1. von Knebel W (1906) Studien in den Thermengebieten Islands. Naturwissenschaftliche Rundschau
2. Thorkelsson T (1910) The hot springs of Iceland. Det kongelige danske Videnskabernes Seleskabs Skrifter
3. Ingersoll LR, Zobel OJ (1913) Mathematical theory of heat conduction. Ginn, Waltham
4. Einarsson T (1942) Ueber das Wesen der heissen Quellen Islands. Soc Sci Islandica 42:91
5. White DE (1957) Magmatic, connate and metamorphic waters. Geol Soc Am Bull 69:1659–1682
6. Ellis AJ, Wilson SH (1960) The geochemistry of alkali metal ions in the Wairakei hydrothermal system. N Z J Geol Geophys 3:593–617
7. Ellis AJ, Mahon WAJ (1977) Chemistry and geothermal systems. Academic, New York, p 392
8. White DE (1967) Some principles of geyser activity, mainly from Steamboat Springs, Nevada. Am J Sci 265:641–684
9. Giggenbach WF (1988) Geothermal solute equilibria. Derivation of Na-K-Mg- Ca geoindicators. Geochim Cosmochim Acta 52:2749–2765
10. Giggenbach WF, Le Guern F (1976) The chemistry of magmatic gases from Erta'Ale Ethiopia. Geochim Cosmochim Acta 40:25–30
11. Giggenbach WF (1987) Redox processes governing the chemistry of fumarolic gas discharges from White Island, New Zealand. Appl Geochem 2:143–161
12. Giggenbach WF (1990) Water and gas chemistry of Lake Nyos and its bearing on the eruptive process. J Volcanol Geoth Res 42:337–362
13. Truesdell AH, Fournier RO (1977) Conditions in the deeper parts of the hot spring systems of Yellowstone National Park, Wyoming, US Geological Survey Open-file report No. 76-428. US Geological Survey, Reston
14. Truesdell AH, Nathenson M, Rye RO (1977) The effects of subsurface boiling and dilution on the isotopic compositions of Yellowstone thermal waters. J Geophys Res 82:3694–3704
15. Giggenbach WF (1978) The isotopic composition of waters from the El Tatio geothermal field. Northern Chile. Geochim Cosmochim Acta 42:979–988

16. Nieva D, Verma MP, Santoyo E, Portugal E, Campos A (1997) Geochemical exploration of the Chipilapa geothermal field, El Salvador. Geothermics 26:589–612
17. Mercado (1975) Movement of geothermal fluids and temperature distribution in the Cerro Prieto geothermal field, Baja California, Mexico. In: United Nations Symposium on the Development and Use of Geothermal Resources, San Francisco, 1975, vol 1. U. S. Government Printing Office, Washington, pp 487–494
18. Ellis AJ, Mahon WAJ (1967) Natural hydrothermal systems and experimental hot water/rock interactions (Part II). Geochim Cosmochim Acta 31:519–538
19. Fournier RO, Truesdell AH (1973) An empirical Na-K-Ca geothermometer for natural waters. Geochim Cosmochim Acta 37:1255–1275
20. Truesdell AH (1975) Geochemical techniques in exploration. In: National Energy Authority (ed) Proc. 2nd. UN Symp. on the development and use of geothermal resources, San Francisco, 1975, vol 1. National Energy Authority, Reykjavik, pp 53–86
21. Arnorsson S, Gunnlaugsson E, Svavarsson H (1983) The chemistry of geothermal waters in Iceland III. Chemical geothermometry in geothermal investigations. Geochim Cosmochim Acta 42:567–577
22. Fournier RO (1979) A revised equation for the Na/K geothermometer. Geoth Res Counc Trans 3:221–224
23. Giggenbach WF, Gonfiantini R, Jangi BL, Truesdell AH (1983) Isotopic and chemical composition of Parbati Valley geothermal discharges, NW-Himalaya, India. Geothermics 12:199–222
24. Nieva D, Nieva R (1987) Developments in geothermal energy in Mexico – Part Twelve. A cationic composition geothermometer for prospecting of geothermal resources. Heat Recovery Syst CHP 7:243–258
25. Bowers TS, Jackson KI, Helgeson HC (1984) Equilibrium activity diagrams. Springer, Berlin
26. Fournier RO (1991) Water geothermometers applied to geothermal energy. In: D'Amore F (ed) Application of geochemistry in geothermal reservoir development, Series of technical guides on the use of geothermal energy. UNITAR/UNDP, New York, p 37
27. Paces T (1975) A systematic deviation from Na-K-Ca geothermometer below 75°C and above 10^{-4} atm P_{CO2}. Geochim Cosmochim Acta 39:541–544
28. Fouillac C, Michard G (1977) Sodium, potassium, calcium relationships in hot springs of Massif Central. In: Pacquet H, Tardy Y (eds) Proc. 2nd. Intl. Symp. on Water-Rock Interaction, Strasbourg, 17–25 August 1977, vol 3. Université Louis Pasteur, Strasbourg, pp 109–116
29. Fournier RO, Potter RW (1979) Magnesium correction to the Na-K-Ca chemical geothermometer. Geochim Cosmochim Acta 43:1543–1550
30. Truesdell AH, Nakanishi S (2005) Chemistry of neutral and acid production fluids from the Onikobe geothermal field, Miyagi prefecture, Honshu, Japan. In: IAEA (ed) Use of isotope techniques to trace the origin of acidic fluids in geothermal systems, Technical document 1448. IAEA, Vienna, p 197
31. Baca Gómez A, Segovia N, Martínez Miranda V, Armienta MA, Barragán Reyes RM, Iturbe García JL, López Muñoz BE, Seidel JL (2006) Physical, chemical, bacteriological and radioisotopic parameters from springs and wells around Jocotitlán volcano, Mexico. Int J Environ Pollut 26:266–283
32. Kharaka YK, Mariner RH (1989) Chemical geothermometers and their application to formation waters from sedimentary basins. In: Naeser ND, McCollon TH (eds) Thermal history of sedimentary basins. Springer, New York, pp 99–117
33. Fouillac C, Michard G (1981) Sodium/lithium ratios in water applied to geothermometry of geothermal reservoirs. Geothermics 10:55–70
34. Fournier RO, Rowe JJ (1966) Estimation of underground temperatures from the silica content of water from hot springs and wet-steam wells. Am J Sci 264:685–697
35. Kennedy GC (1950) A portion of the system silica-water. Econ Geol 45:629–653
36. Morey GW, Fournier RO, Rowe JJ (1962) The solubility of quartz in water in the temperature interval 25 °C to 30 °C. Geochim Cosmochim Acta 26:1029–1043
37. Fournier RO, Potter RW (1982) A revised and expanded silica (quartz) geothermometer. Geoth Res Counc Bull 11:3–12
38. Truesdell AH, Fournier RO (1977) Procedure for estimating the temperature of a hot-water component in a mixed water by using a plot of dissolved silica versus enthalpy. USGS J Res 5:49–52
39. Fournier RO (1973) Silica in thermal waters: laboratory and field investigations. In: Ingerson E (ed) Proceedings: International Symposium on Hydrogeochemistry and Biogeochemistry, Tokyo, 7–9 September 1970, vol 1. Clarke, Washington, DC, pp 122–139
40. Rimstidt JD, Barnes HL (1980) The kinetics of silica-water reaction. Geochim Cosmochim Acta 44:1683–1699
41. Giggenbach WF, Goguel RL (1989) Collection and analysis of geothermal and volcanic water and gas samples, Report No. CD 2387. DSIR, Petone, p 53
42. Nieva D, Quijano León JL (1991) Applications of geochemistry to the study of geothermal resources in Mexico: case study of Los Azufres field. In: D'Amore F (ed) Application of geochemistry in geothermal reservoir development, Series of technical guides on the use of geothermal energy. UNITAR/UNDP, New York, pp 299–316
43. Giggenbach WF (1980) Geothermal gas equilibria. Geochim Cosmochim Acta 44:2021–2032
44. D'Amore F, Celati R (1983) Methodology for calculating steam quality in geothermal reservoirs. Geothermics 12:129–140
45. Nieva D, Fausto J, González J, Garibaldi F (1982) Afluencia de vapor a la zona de alimentación de pozos de Cerro Prieto I. In: Fourth Symp. on the Cerro Prieto Field, Baja California, Mexico, vol 1, p 145
46. D'Amore F, Truesdell AH (1985) Calculation of geothermal reservoir temperatures and steam fraction from gas compositions. Geoth Res Counc Trans 9(1):305–310
47. Arnorsson S, Gunnlaugsson E (1985) New gas geothermometers for geothermal exploration – calibration and application. Geochim Cosmochim Acta 49:1307–1325

48. Taran Y (1986) Gas geothermometers for hydrothermal systems. Geochem Int 20:111–126
49. Giggenbach WF (1991) Chemical techniques in geothermal exploration. In: D'Amore F (ed) Application of geochemistry in geothermal reservoir development, Series of technical guides on the use of geothermal energy. UNITAR/UNDP, New York, p 119
50. Cathelineau M, Nieva D (1985) A chlorite solid solution geothermometer. The Los Azufres (Mexico) geothermal system. Contrib Mineral Petrol 91:235–244
51. Cathelineau M (1988) Cation site occupancy in chlorites and illites as a function of temperature. Clay Miner 23:471–485
52. Kranidiotis P, MacLean WH (1987) Systematics of chlorite alteration at the Phelps Dodge massive sulfide deposits, Matagami, Quebec. Econ Geol 82:1898–1911
53. Battaglia S (1999) Applying X-ray geothermometer diffraction to a chlorite. Clays Clay Miner 47:54–63
54. Craig H (1961) Standard for reporting concentrations of deuterium and oxygen-18 in natural waters. Science 133:1833
55. Craig H (1961) Isotopic variations in meteoric waters. Science 133:1702–1703
56. Taylor HP (1974) The application of oxygen and hydrogen isotope studies to problems of hydrothermal alteration and ore deposition. Econ Geol 69:843–883
57. Craig H (1963) The isotopic geochemistry of water and carbon in geothermal areas. In: Tongiorgi E (ed) Nuclear geology on geothermal areas: Spoleto 1963. Consiglio Nazionale della Richerche, Pisa, pp 17–53
58. Giggenbach WF (1989) The chemical and isotopic position of Ohaaki field within the Taupo Volcanic Zone. In: Proc. 11th New Zealand Geothermal Workshop, Aukland, 1989, pp 81–88
59. Giggenbach WF (1991) Isotopic composition of geothermal water and steam discharges. In: D'Amore F (ed) Application of geochemistry in geothermal reservoir development, Series of technical guides on the use of geothermal energy. UNITAR/UNDP, New York, pp 253–273
60. Sakai H, Matsubaya O (1977) Stable isotope studies of Japanese geothermal systems. Geothermics 5:97–124
61. Taran YA, Pokrovsky BG, Esikov AD (1988) Deuterium and oxygen-18 in fumarolic steam and amphiboles from some Kamchatka volcanoes: "Andesitic" waters. IAVCEI, Commission on the Chemistry of Volcanic Gases Newsletter No. 1, pp 15–18
62. Fournier RO (1979) Geochemical and hydrologic considerations and the use of enthalpy-chloride diagrams in the prediction of underground conditions in hot- spring systems. J Volcanol Geoth Res 5:1–16
63. Giggenbach WF, Stewart MK (1982) Processes controlling the isotopic composition of steam and water discharges from steam vents and steam- heated pools in geothermal areas. Geothermics 11:71–80

Books and Reviews

D'Amore F (ed) (1991) Application of geochemistry in geothermal reservoir development. Series of technical guides on the use of geothermal energy. UNITAR/UNDP, New York

Henley RW, Truesdell AH, Barton PB Jr (eds) (1984) Fluid-mineral equilibria in hydrothermal systems. Reviews in Economic Geology, vol I

IAEA (1983) Guidebook on nuclear techniques in hydrology. International Atomic Energy Agency, Technical Report Series No. 91, Vienna

Valley JW, Taylor HP Jr, O'Neil JR (1986) Stable isotopes in high temperature geological processes. Reviews in Mineralogy, vol 16